AN INVESTIGATION OF NON-LINEAR SYSTEM PERFORMANCE ON THE PARAMETER PLANE

CHARLES A. PELLEGRINI

Library
U. S. Naval Postgraduate School
Monterey, California

Libra
U. S.
Mont

Libra
U. S.
Mon

AN INVESTIGATION OF NONLINEAR SYSTEM PERFORMANCE ON THE PARAMETER PLANE

by

Charles A. Pellegrini
Lieutenant, United States Navy
B.S., Purdue University, 1961

Submitted in partial fulfillment
for the degree of

MASTER OF SCIENCE IN ENGINEERING ELECTRONICS

from the

UNITED STATES NAVAL POSTGRADUATE SCHOOL
May 1966

ABSTRACT

Control systems containing two nonlinear elements are separated into three broad classes which are dependent upon the location of an initial signal excitation with respect to the two nonlinear elements. The nonlinear elements are considered as the α and β variables of the parameter plane which defines the region containing the roots of the system characteristic equation. A "dynamic describing function" curve, which determines the locus of the M or operating point for initial condition input signals, is plotted on the parameter plane. Additionally, the transient response is graphically determined for conditions of second order dominance. The theoretical results are compared with actual analog computer simulation.

DUDLEY KNOX LIBRARY
NAVAL POSTGRADUATE SCHOOL
MONTEREY CA 93943-5101

ACKNOWLEDGEMENTS

The author wishes to thank Dr. G. J. Thaler of the United States Naval Postgraduate School for his guidance and many helpful ideas during this thesis project.

A sincere thanks is extended to Dr. D. D. Šiljak, visiting professor at the University of Santa Clara from the University of Belgrade, Yugoslavia, for his helpful discussions which clarified many concepts in this thesis.

TABLE OF CONTENTS

CHAPTER		PAGE
I.	Introduction	1
II.	Application of the Parameter Plane to the Two Nonlinearities Problem	6
III.	Two Nonlinear Elements with Identical Signal Excitation	14
IV.	Two Nonlinear Elements Related to a Common Signal by a Linear Differential Equation	25
V.	Two Nonlinear Elements Related to a Common Signal by a Nonlinear Differential Equation	67
VI.	Conclusions	78
VII.	Bibliography	80
Appendix A.	Graphical Method for Determining the Transient Response	81
Appendix B.	Digital Computer Program for Plotting Constant Zeta-Sigma-Omega Curves	95

LIST OF TABLES

TABLE		PAGE
1	Comparison of Limit Cycle Performance Between Dynamic Describing Function Curve and Analog Computer	53
2	Data for Calculating Transient Response from Zeta-Omega Curves	84
3	Data for Calculating Transient Response from Sigma-Omega Curves	88

LIST OF FIGURES

FIGURE		PAGE
1	General Classification of Control Systems with Two Nonlinear Elements	4
3-1	Block Diagram of Third Order System with Two Nonlinear Elements	15
3-2	Dynamic Describing Function Curves on Zeta-Omega Curves	16
3-3	Dynamic Describing Function Curves on Sigma-Omega Curves	17
3-4	Analog Computer Simulation	19
3-5	Calculated and Analog Computer Transient Response for A = 11 Volts, Curve 1	21
3-6	Calculated and Analog Computer Transient Response for A = 11 Volts, Curve 2	22
3-7	Calculated and Analog Computer Transient Response for A = 11 Volts, Curve 3	23
4-1	Block Diagram of Fourth Order System with Two Nonlinear Elements	26
4-2	Dynamic Describing Function Curve on Zeta-Omega Curves	27
4-3	Dynamic Describing Function Curve on Sigma-Omega Curves	28
4-4	ω -A Grid for Figures 4-2 and 4-3	29
4-5	Analog Computer Simulation	31
4-6	Calculated Transient Response for A = 9 Volts	33
4-7	Analog Computer Transient Response for A = 9 Volts	34
4-8	Calculated Transient Response for A = 6 Volts	35
4-9	Analog Computer Transient Response for A = 6 Volts	36
4-10	Calculated Transient Response for A = 3 Volts	37
4-11	Analog Computer Transient Response for A = 3 Volts	38

4-12	Dynamic Describing Function Curve on Zeta-Omega Curves	39
4-13	Dynamic Describing Function Curve on Sigma-Omega Curves	40
4-14	ω - A Grid for Figures 4-12 and 4-13	41
4-15	Calculated Transient Response for A = 16 Volts	43
4-16	Analog Computer Transient Response for A = 16 Volts	44
4-17	Calculated Transient Response for A = 12 Volts	45
4-18	Analog Computer Transient Response for A = 12 Volts	46
4-19	Calculated Transient Response for A = 8 Volts	47
4-20	Analog Computer Transient Response for A = 8 Volts	48
4-21	Block Diagram of Modified System	50
4-22	Family of Dynamic Describing Function Curves on Zeta-Omega Curves	51
4-23	Family of Dynamic Describing Function Curves on Sigma-Omega Curves	52
4-24	Calculated and Analog Computer Transient Response for A = 5 Volts	55
4-25	Calculated and Analog Computer Transient Response for A = 5 Volts	56
4-26	Calculated and Analog Computer Transient Response for A = 5 Volts	57
4-27	Calculated and Analog Computer Transient Response for A = 5 Volts	58
4-28	Dynamic Root Locus Plot for Figure 4-2	60
4-29	Dynamic Root Locus Plot for Figure 4-12	61
4-30	Dynamic Root Locus Plot for Figure 4-22, Curve A	62
4-31	Dynamic Root Locus Plot for Figure 4-22, Curve B	63
4-32	Dynamic Root Locus Plot for Figure 4-22, Curve C	64
4-33	Dynamic Root Locus Plot for Figure 4-22, Curve D	65

5-1	Block Diagram of Typical Example for Case 3	68
5-2	Block Diagram of Test Example	72
5-3	Parameter Plane Diagram for Figure 5-2, K = .15	74
5-4	Parameter Plane Diagram for Figure 5-2, K = .25	75
A-1	A vs ζ^2 .	82
A-2	A vs ω_n	83
A-3	A vs t A = 3 Volts	85
A-4	ω vs t	86
A-5	A vs t	87
A-6	A vs σ	89
A-7	A vs ω	90
A-8	A vs t A = 3 Volts	91
A-9	ω vs t	92
A-10	A vs t	93

CHAPTER I

INTRODUCTION

The significant feature of nonlinear control problems is that no two problems are identical -- each one has a unique solution. At best one can discuss classes of nonlinear problems where the nonlinear elements appear in the error channel, the feedback loop, or in combinations in the error channel and the feedback channel. In keeping with this quasi-class criterion, control systems containing two amplitude-sensitive nonlinearities which are related with respect to a common signal excitation will be covered in this thesis.

Control systems containing single nonlinear elements have been accurately analyzed. Šiljak [5] has used the parameter plane technique for the analysis and synthesis of single nonlinear problems with excellent results. In Wilson's thesis [8] the limit cycles of feedback control problems were determined by Mitrovic's method and checked by the root locus plot, Nyquist diagram, and analog simulation with high correlation. Another technique which has been used to predict the transient performance to within five to ten percent accuracy for a step input signal is MacAllister's method [2] of calculating a "gain phase" function for the nonlinearity based on a damped cosinusoidal input signal. An obvious brute force method of solving the nonlinear problem is to use linear piecewise approximations of the nonlinearity and program the digital computer to handle the iterative calculations. Almost any degree of accuracy can be obtained to get the transient response by digital computer solution of the system's differential equation.

For systems containing two nonlinearities the determination of system performance has been somewhat less successful due to the increased complexity of the problem. One of the most significant contributions is Šiljak's paper [5] on the use of the parameter plane for establishing the stability region and limit cycles of nonlinear control systems with respect to the system's parameters and initial conditions. The parameter plane technique will be used in this thesis for determining stability and limit cycles and, in addition, as a tool for calculating the transient response under conditions of second order dominance. An unpublished paper by Yockey and Thaler [9] obtains the transient response of a nonlinear system containing two saturation elements in a multiloop feedback path. Excellent correlation with analog computer simulation was obtained in determining the transient response of their system. The concept of a "dynamic describing" function introduced in this last paper will also be used in this thesis.

While many nonlinear problems can be solved using a digital computer or by simulation on an analog computer, a control designer would like to know a priori what will happen to a system when certain parameters in a nonlinear control problem are varied. One design philosophy currently used in control engineering is the perturbation technique where small changes in system parameters are made and the system response calculated on the digital computer. After several and sometimes many alterations to the system parameters the desired response is obtained. While this method is obviously very accurate in the final analysis, considerable time is wasted in the design phase. Furthermore, turning the dials of an analog computer or submitting new data to a digital computer to

obtain a desired response will not answer the fundamental questions of "why" or "how" will the system perform.

In this thesis precise answers for nonlinear control systems will not be sought. Rather, the stability regions, the limit cycle frequency, and the form of the transient response will be predicted for two classes of nonlinear systems and discussed for a third class.

On the basis of the work done by Šiljak [5] it appears that two nonlinear elements can be conveniently classified with respect to an initial signal excitation into three general cases.

Case 1. Identical signal excitation to both nonlinear elements.

In Figure 1a the signal denoted by X is the same input signal to nonlinear elements N_1 and N_2. The transfer functions denoted by G(s) are assumed to provide sufficient low frequency filtering for the control system. This example is considered the simplest case.

Case 2. Input signal excitation to nonlinear elements related by a linear differential equation.

This case is shown in Figure 1b where the input signals to N_1 and N_2 are respectively $X\,G_{-1}(s)$ and X. The input signal to N_1 is a function of frequency and amplitude while the input signal to N_2 is a function of amplitude only. The additional frequency sensitivity of this system complicates the problem.

Case 3. Input signal excitation to nonlinear elements related by a nonlinear differential equation.

The most difficult case appears in Figure 1c where the signal input to N_1 is X and the input signal to N_2 is $X\{N_1\}\{G_2(S)\}$ where the brackets are intended to represent some transform relationship rather

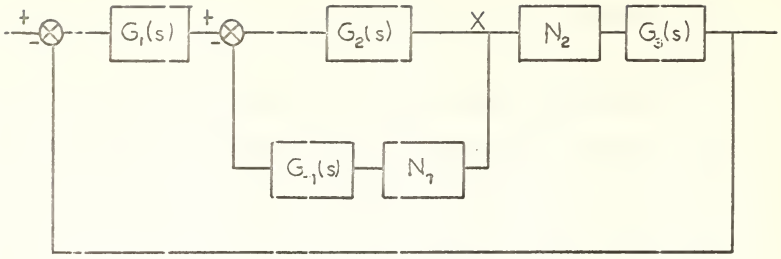

a. Case 1.

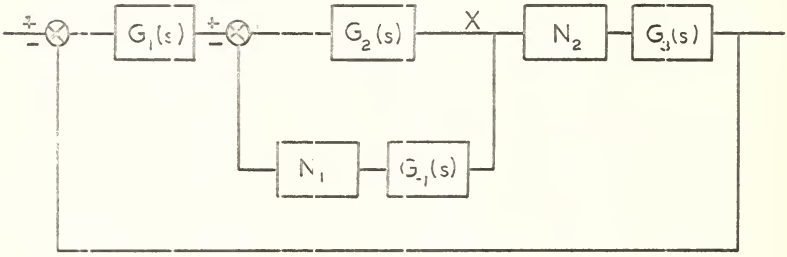

b. Case 2.

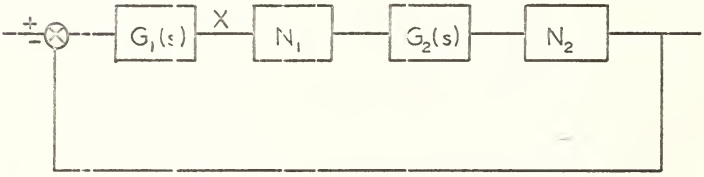

c. Case 3.

Figure 1. General Classification of Control Systems with Two Nonlinear Elements.

than interpreting the three quantities in a strict multiplicative sense.

These three cases will be covered, the first two experimentally and the last case theoretically.

CHAPTER II

APPLICATION OF THE PARAMETER PLANE TO THE TWO NONLINEARITIES PROBLEM

The method used to determine system performance in this thesis is based on the superposition of a dynamic describing function curve on the parameter plane curves for a control system containing two amplitude sensitive nonlinearities. This chapter reviews the theory behind this analytical technique.

2-1 The parameter plane technique

In the previously mentioned reference by Šiljak it has been shown that the sum of the terms of the characteristic equation can be represented as a sum, i.e.,

$$f(s) = \sum_{k=0}^{r} a_k s^k \qquad (2\text{-}1)$$

where the a_k are the linear coefficients of the characteristic equation. By letting $s = -\zeta\omega_n + j\omega_n\sqrt{1-\zeta^2}$ equation (2-1) can be expanded in terms of Chebyshev polynomials of the second kind which are functions of ζ, the damping ratio.

The coefficients of the characteristic equation can be expressed as

$$a_k = \alpha b_k + \beta c_k + d_k \qquad (2\text{-}2)$$

where alpha and beta are any variable system parameters. This feature of the parameter plane technique gives the analyst or designer of control systems two degrees of freedom as opposed to the single parameter techniques such as root locus, Bode diagram, or Nyquist plot. Since an amplitude sensitive nonlinearity can be considered as a variable gain

element whose value varies between zero and one, it is convenient to let alpha and beta become the variable nonlinear elements when the characteristic coefficients are expressible in the form of equation (2-2).

Although the two parameters alpha and beta can be solved for algebraically from equation (2-1), it is more convenient to plot a net of curves in terms of ζ and ω_n, ζ and ω, or $\zeta\omega_n$, and ω, depending upon what particular system characteristics are under consideration. In the following discussion the utility of the different nets of curves will be discussed.

2-1-1 Zeta - omega curves

Because of the recursive nature of the Chebyshev polynomials it is convenient to plot a net of curves for the variables alpha and beta in terms of ζ, the damping ratio, and ω_n, the undamped natural frequency. A computer program which will plot this net of curves appears in Nutting's thesis [3]. Since engineers are used to the concept of the numeric, ζ, the utility of such a set of curves is obvious. The controls engineer can tell at a glance what effect a change in one or both of the system variables will have on system stability by the location of the M or operating point with respect to the $\zeta = 0$ curve. In addition to determining the relative stability, the presence or absence of possible limit cycles can be established. Additionally, if second order dominance is justified an indication of the transient response can be determined since the complex roots are obtained directly from the graph by reading the values of ζ and ω_n at the operating point. Any real roots may be approximated by drawing tangents to the $\zeta = 1$ curve.

The previous discussion considered a static case or a linear system.

For nonlinear systems where alpha and beta are the two nonlinear elements, a dynamic operating condition exists since the nonlinearities are not only sensitive to the input signal amplitude but also to frequency. To cover this nonlinear situation, describing function theory will be discussed in a later section.

Since describing function theory depends upon the oscillating frequency, ω , it is necessary to modify the constant ω_n curves to constant ω curves by the relationship $\omega = \omega_n\sqrt{1-\zeta^2}$. The recursive relationships developed using Chebyshev polynomials are not amenable to this direct substitution. However, a set of constant ω curves can be obtained from the binomial coefficient expansion described in the next section. Hence, it is possible to obtain a net of ζ-ω curves which may be used directly with describing function theory.

2-1-2 Sigma - omega curves

The concept of constant zeta curves or constant omega curves is accepted in engineering circles. But the utility of constant sigma or $\zeta\omega_n$ curves is not generally recognized since there has been no real need for them. Perhaps, the most difficult idea behind constant sigma curves is that engineers have no intuitive feeling for this variable. However, the reference curve for the sigma curves is the sigma = 0 curve which is identical to the zeta = 0 curve. The usefulness of the constant sigma curves will become apparent when the transient response of a system is desired. In those cases where second order dominance is justified, which is usually the case for well-designed control systems, the value of sigma determines the rate of exponential signal decay in the stable region.

Recently, Siljak has shown that the individual terms comprising the characteristic equation, i.e., $f(s) = \sum_{k=0}^{n} a_k s^k$ can be expanded in terms of binomial coefficients. Consider the rectangular coordinate relationship

$$s^k = X_k + jY_k \tag{2-3}$$

where $X_k = X_k(\sigma, \omega)$ and $Y_k = Y_k(\sigma, \omega)$. The first order term of equation (2-3) can be expressed as $s = X_1 + jY_1$, or $s = \sigma + j\omega$. If the latter equation is substituted into equation (2-3) the following pair of recursion formulas are obtained by induction:

$$\begin{aligned} X_{k+1} - 2X_1X_k + (X_1^2 + Y_1^2)\ X_{k-1} &= 0 \\ Y_{k+1} - 2X_1Y_k + (X_1^2 + Y_1^2)\ Y_{k-1} &= 0 \end{aligned} \tag{2-4}$$

subject to the following initial conditions

$$\begin{aligned} X_0 &= 1 & Y_0 &= 0 \\ X_1 &= \sigma & Y_1 &= \omega \end{aligned} \tag{2-5}$$

Each of the k+1 terms in equations (2-4) is a binomial coefficient which satisfies the following pair of equations

$$\begin{aligned} \sum_{k=0}^{n} a_k X_k &= 0 \\ \sum_{k=0}^{n} a_k Y_k &= 0 \end{aligned} \tag{2-6}$$

The first equation in (2-6) represents the summation of the real terms and the second equation the summation of imaginary terms. Alpha and beta of the linear coefficient $a_k = b_k\alpha + c_k\beta + d_k$ are now implicit functions of sigma and omega, i.e., $\alpha = \alpha(\sigma, \omega)$ and $\beta = \beta(\sigma, \omega)$. The following pair of transform equations developed in Šiljak's original paper [5] still holds:

$$\begin{aligned} B_1\alpha + C_1\beta + D_1 &= 0 \\ B_2\alpha + C_2\beta + D_2 &= 0 \end{aligned} \tag{2-7}$$

where the capitalized variables are implicit functions of sigma and omega and are equal to the summation of the corresponding lower case lettered terms of the generalized coefficient $a_k = b_k \alpha + c_k \beta + d_k$. From Cramer's rule alpha and beta can be solved for from equations 2-7:

$$\alpha = \frac{C_1 D_2 - C_2 D_1}{B_1 C_2 - B_2 C_1}$$

$$\beta = \frac{B_2 D_1 - B_1 D_2}{B_1 C_2 - B_2 C_1} \qquad (2\text{-}8)$$

Equations (2-8) are readily programmed on the digital computer with the aid of recursion formulas (2-4). A computer program which plots a net of sigma - omega curves for the parameters alpha and beta appears in Appendix B. As long as the coordinate axes dimensions for alpha and beta remain constant the constant omega curves of this section can be superimposed on the constant zeta curves of the previous section to obtain a net of constant ζ-ω curves. These two nets of curves, namely, ζ-ω and σ-ω, will be used in subsequent discussions. Since ζ is the more generally understood term, it will be used more frequently than sigma.

2-2 Describing function technique

In the analysis of nonlinear systems it is necessary to make certain linear approximations concerning the nonlinear elements to obtain some practical idea of system performance. One of these linearization methods is the describing function in which a sinusoidal signal of the form $A \sin \omega t$ is applied to the nonlinearity. If the input - output characteristic of the nonlinear element is known, the output can be expanded in a Fourier series. The ratio of the fundamental component of the Fourier

expansion to the peak amplitude of the sinusoidal input signal is defined as the describing function, or more explicitly the gain-phase characteristic of the nonlinear element.

2-2-1 Inherent shortcomings

The assumption of a single sinusoidal input signal of constant amplitude occurs in a nonlinear system only under oscillatory conditions, i.e., $\zeta = 0$. Furthermore, the assumption of a single frequency component in the describing function derivation is valid only if sufficient low frequency filtering is available in the control system to limit the harmonics of the limit cycle to negligible values. For a second order system this assumption would normally not be valid, but for higher order systems the accuracy of the describing function technique would normally improve. In practice the describing function gives the best results for third order systems or higher under limit cycle conditions.

Since the nonlinear element is a function of the input signal, A, and the oscillating frequency, ω, the only region on the parameter plane where the describing function is justified occurs when $\omega = \omega_n$ on the $\zeta = 0$ or $\sigma = 0$ curve. But the operating point, $M(\alpha, \beta)$ or $M(N_1, N_2)$ where the alpha - beta parameters become the nonlinear variables N_1 and N_2, moves in the parameter plane due to the dependence of the nonlinearity on A, ζ, and ω_n. Consequently, it is necessary to modify the constant ω_n curves to constant ω curves by the relationship $\omega = \omega_n\sqrt{1-\zeta^2}$. In the previous section a recursion formula using binomial coefficients was indicated to obtain constant ω curves which can be used with the variables ζ or σ.

For two nonlinearities where one or both are a function of frequency, the loci of the describing functions will be constant ω lines for varying signal input. The intersections of the common radian frequencies between the parameter plane curves and the describing function curves will determine the values of the alpha - beta variables for a particular initial condition input. A series of these points connected by a smooth curve is called a "dynamic describing" function curve in the aforementioned paper by Yockey and Thaler. In summary this means that for a specified initial condition the operating or M(α , β) point should lie on the dynamic describing function locus.

The superposition of the dynamic describing function locus atop the parameter curves places in evidence the roots of the characteristic equation at each instant of time. The motion of the M(α , β) point is due to the changed values of the nonlinear elements. This important information can be used to obtain the transient response of the system under second order dominancy conditions, i.e., where one pair of complex poles is dominant. A brief discussion of the theory and an example using ζ - ω curves and σ - ω curves is worked in Appendix A.

2-2-2 Application of the "dynamic describing function" locus

In view of the previous discussion a mathematical justification for the describing function locus for two nonlinearities, which are related in one of the three ways indicated in the introduction, will not be attemped. Rather, the problem will be looked at from an engineering viewpoint. Other system variables such as phase shift, real root effect, and complex roots of higher order systems may alter physical

reasoning as the dynamic describing function locus gets further away from either the $\zeta = 0$ or the $\sigma = 0$ curves. However, these effects are not apparent intuitively, let alone mathematically. Using this semi-empirical approach, the amplitude of the reference signal excitation, A, will be considered as the peak amplitude of a sinusoidal signal at one instant of time.

CHAPTER III

TWO NONLINEAR ELEMENTS WITH IDENTICAL SIGNAL EXCITATION

The first case of two nonlinear elements related by a common signal excitation is considered in this chapter. A third order system containing two amplitude sensitive elements is chosen as the working model. Based on the previous discussion in Chapter II on the parameter plane technique and the describing function method, the system performance is predicted and compared with analog simulation.

3-1 The working model

The experimental system is shown in Figure 3-1. The uncompensated plant with the nonlinear elements is inherently unstable, and is stabilized by tachometer feedback. With the insertion of the nonlinear elements, N_1 and N_2, the prediction of system performance is complicated. The two dead zone elements have a common signal excitation, A, which is assumed to be some initial condition voltage. The dead zone width denoted by $\pm E_d$ does not have to be identical for both elements.

The characteristic equation for this system is

$$s^3 + 10s^2 + (10N_1 + 10N_2)s + 100\,N_1 = 0 . \qquad (3\text{-}1)$$

Using the parameter plane technique it is convenient to let $\alpha = N_1$ and $\beta = N_2$. Equation (3-1) becomes

$$s^3 + 10s^2 + (10\alpha + 10\beta)s + 100\alpha = 0 \qquad (3\text{-}2)$$

A set of zeta-omega and sigma-omega curves can be plotted for this system using digital computer programs. In addition the instantaneous values of N_1 and N_2 can be found for different amplitudes of input signals and various dead zone widths. From reference [7] the describing function for

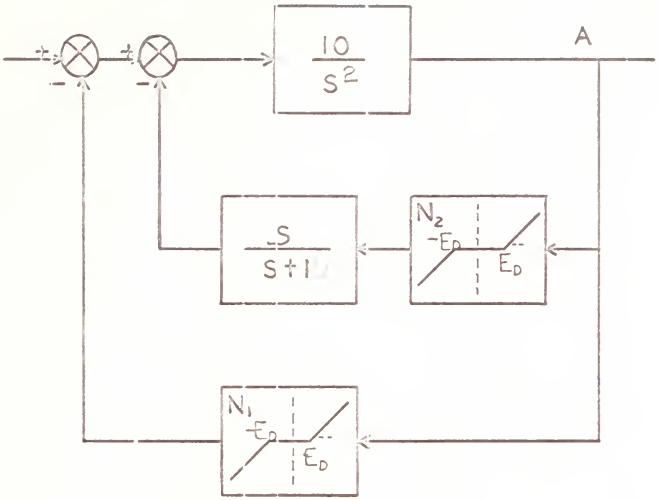

Figure 3-1. Block Diagram of Third Order System with Two Nonlinear Elements.

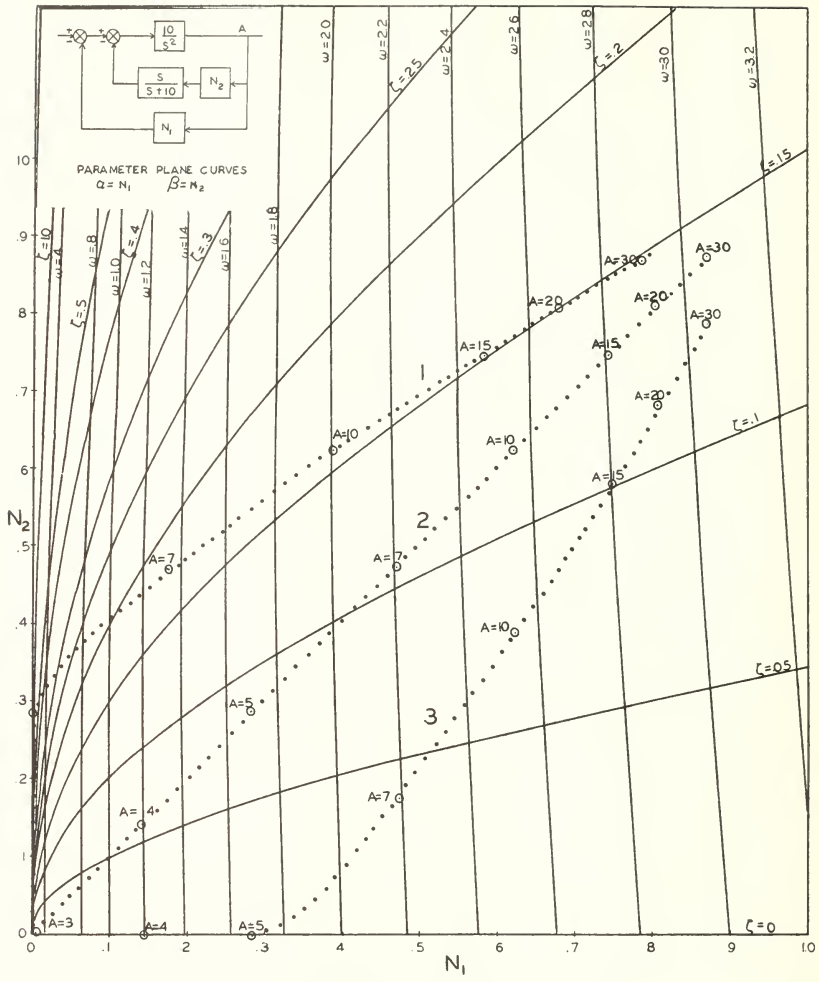

Figure 3-2. Dynamic Describing Function Curves on Zeta-Omega Curves.

	N_1 - Dead Zone	N_2 - Dead Zone
1	$E_d = \pm$ 5 Volts	$E_d = \pm$ 3 Volts
2	$E_d = \pm$ 3 Volts	$E_d = \pm$ 3 Volts
3	$E_d = \pm$ 3 Volts	$E_d = \pm$ 5 Volts

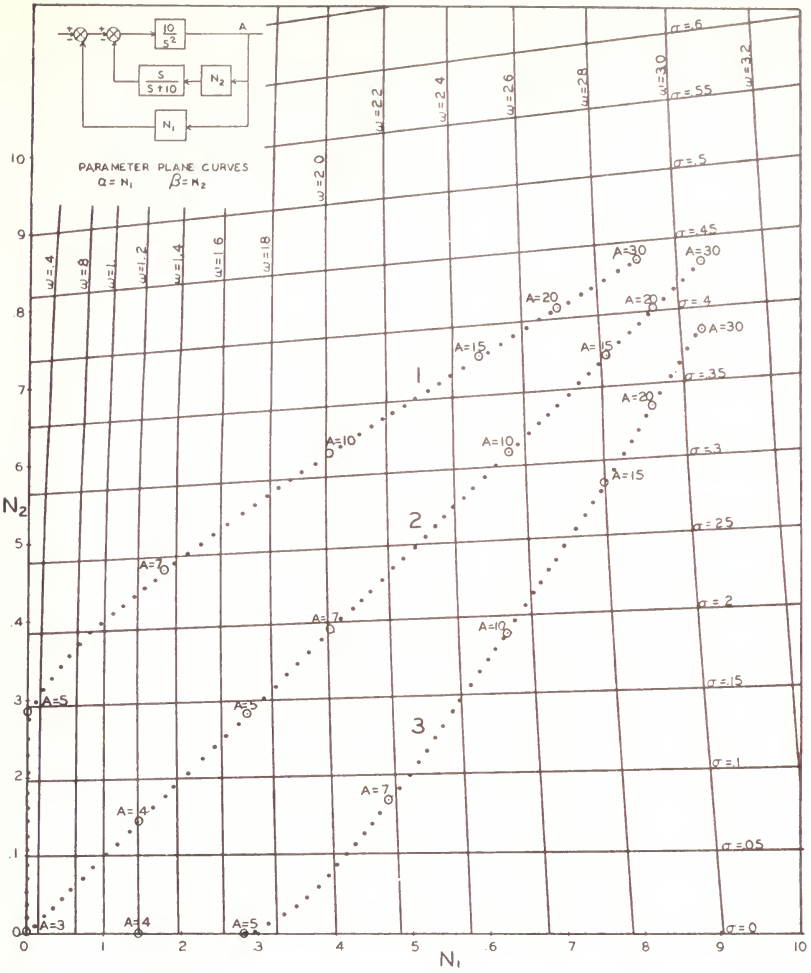

Figure 3-3. Dynamic Describing Function Curve on Sigma-Omega Curves.

	N_1 - Dead Zone	N_2 - Dead Zone
1	$E_d = \pm 5$ Volts	$E_d = \pm 3$ Volts
2	$E_d = \pm 3$ Volts	$E_d = \pm 3$ Volts
3	$E_d = \pm 3$ Volts	$E_d = \pm 5$ Volts

dead zone is

$$G_d = \frac{2}{\pi} \left(\frac{\pi}{2} - \sin^{-1} R - R \sqrt{1-R^2} \right) \qquad (3\text{-}3)$$

where $R = E_d/A$, E_d being one-half the total dead zone width and A the peak amplitude of the signal input. This equation is readily programmed on the computer to obtain the values of N_1 and N_2 for various amplitudes of A and ratios of R. Plotting these parameter values on top of either the zeta-omega or sigma-omega curves determines the systems dynamic describing function.

3-2 Graphical results

Figures 3-2 and 3-3 are the zeta-omega and sigma-omega curves respectively for the system. Physically, the region of interest on both sets of curves is the first quadrant since N_1 and N_2 are passive devices having values lying between zero and one. From the zeta-omega curves, the normal stable region is further confined between the $\zeta = 0$ and the $\zeta = 1$ curve in the first quadrant. As noted on both the zeta-omega and sigma-omega curves, the α or N_1 axis is the $\zeta = 0$ or $\sigma = 0$ curve.

On top of both the zeta-omega and sigma-omega curves are superimposed the describing function loci for three curves: (1) dead zone width of $N_1 = \pm 5$ volts and the dead zone width of $N_1 = \pm 3$ volts, (2) dead zone width of both N_1 and $N_2 = \pm 3$ volts, and (3) dead width of $N_1 = \pm 3$ volts and dead zone width of $N_2 = \pm 5$ volts. Since both nonlinear elements are functions of signal amplitude only, the smooth curves connecting the labelled points also determine the dynamic describing function curve for the three cases.

Dynamic describing function curve 1 reaches the $\zeta = 1$ curve before the nonlinear effects are eliminated. Since ζ is greater than one when the N_2 or β boundary is reached, the system response will be overdamped as modified by the nonlinear element N_2. Curve two should theoretically

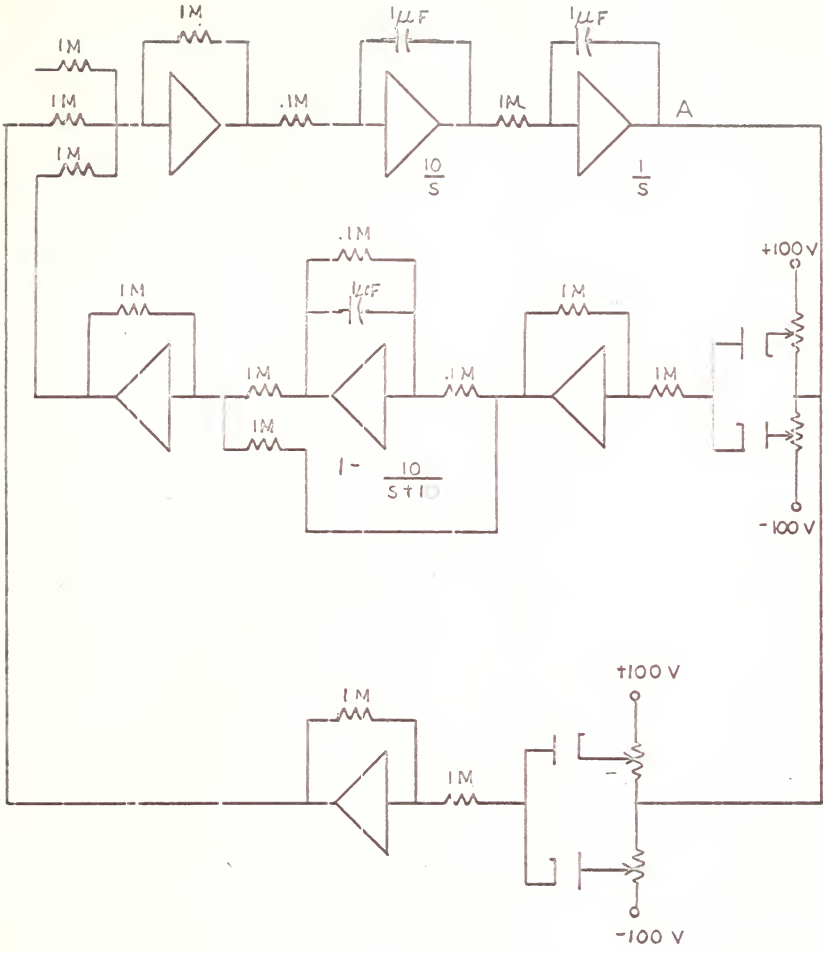

Figure 3-4. Analog Computer Simulation.

end in the nebulous dead zone region which occurs when $N_1 = N_2 = 0$. In the case of curve 3, the $\mathcal{L} = 0$ curve is reached when the envelope of the exciting signal reaches 5 volts. Since smaller amplitudes are indicated below this point, a stable limit cycle is predicted for curve 3.

3-3 Comparison with analog computer

The analog computer setup for this two nonlinear element amplitude sensitive only system appears in Figure 3-4. Initially, the computer was set up for the nonlinear configuration for curve 3 to compare the actual limit cycle performance with the dynamic describing function locus prediction. The results are shown below.

Limit cycle	Amplitude	ω
Theoretical	5.0 volts	1.67
Computer	5.0 volts	1.65

To check the system transient response an initial condition of 11 volts was assumed for each of the dynamic describing function curves in Figures 3-2 and 3-3. The transient response was calculated using the sigma-omega curves as demonstrated in Appendix A. These results appear in Figures 3-5 to 3-7. In the upper right hand corner is the actual brush recording trace of the system response for the indicated initial condition and nonlinear configuration.

The transient response appearing in Figure 3-5 for curve 1 reasonably approximates the analog results until the signal envelope reaches 5 volts. Theoretically, the response should be some slowly decaying waveform because of the high values of $\mathcal{L}$. Practically, the system had an extra overshoot and then a long decaying response. For this unique case part of the shortcoming lies in the graphical technique which is limited to damped oscillatory systems. For curve two the

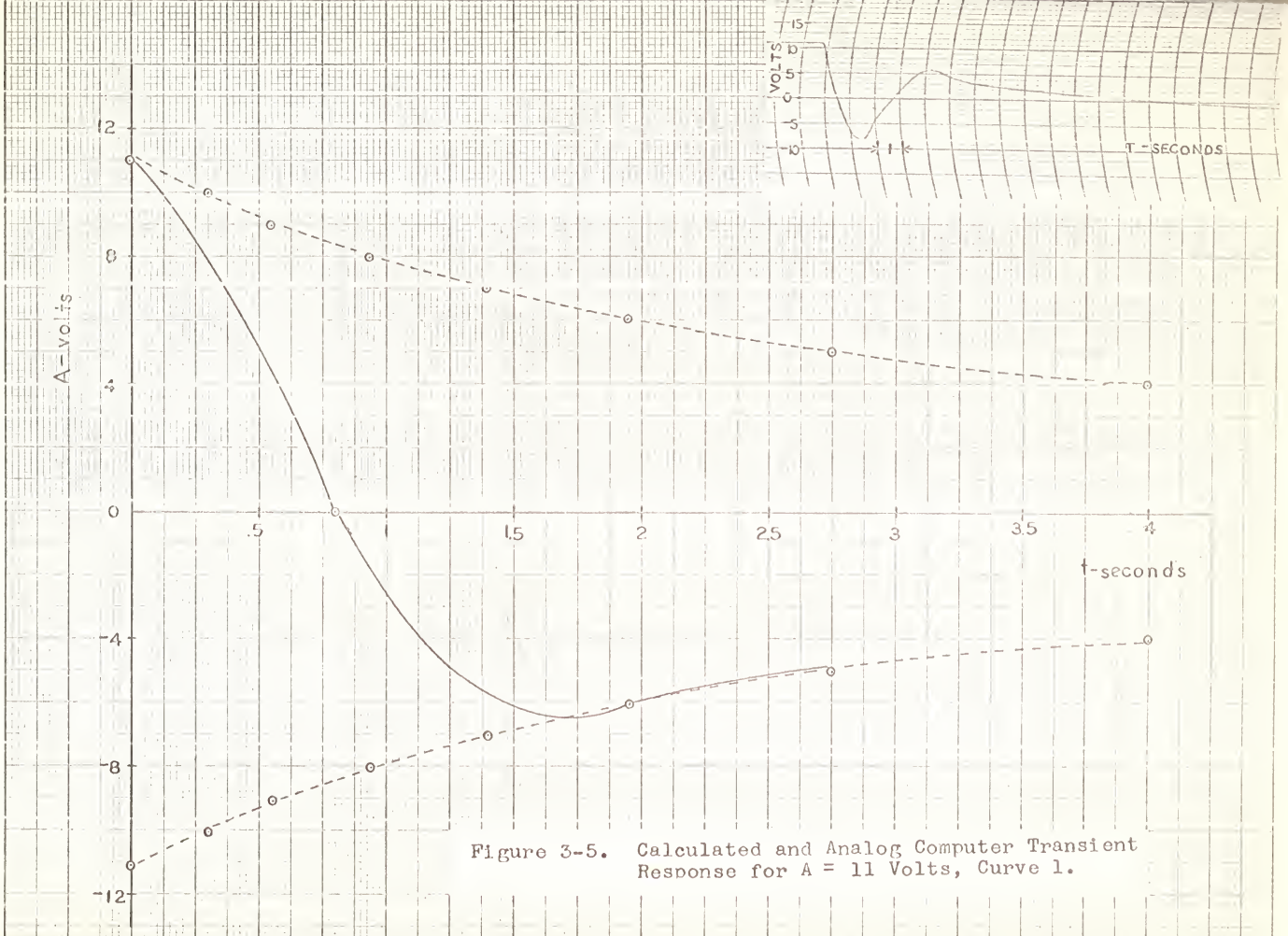

Figure 3-5. Calculated and Analog Computer Transient Response for A = 11 Volts, Curve 1.

KEUFFEL & ESSER CO. MADE IN U.S.A.

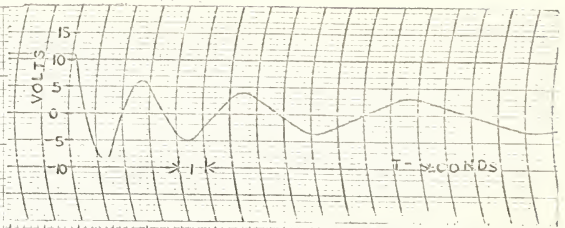

Figure 3-6. Calculated and Analog Computer Transient Response for A = 11 Volts, Curve 2.

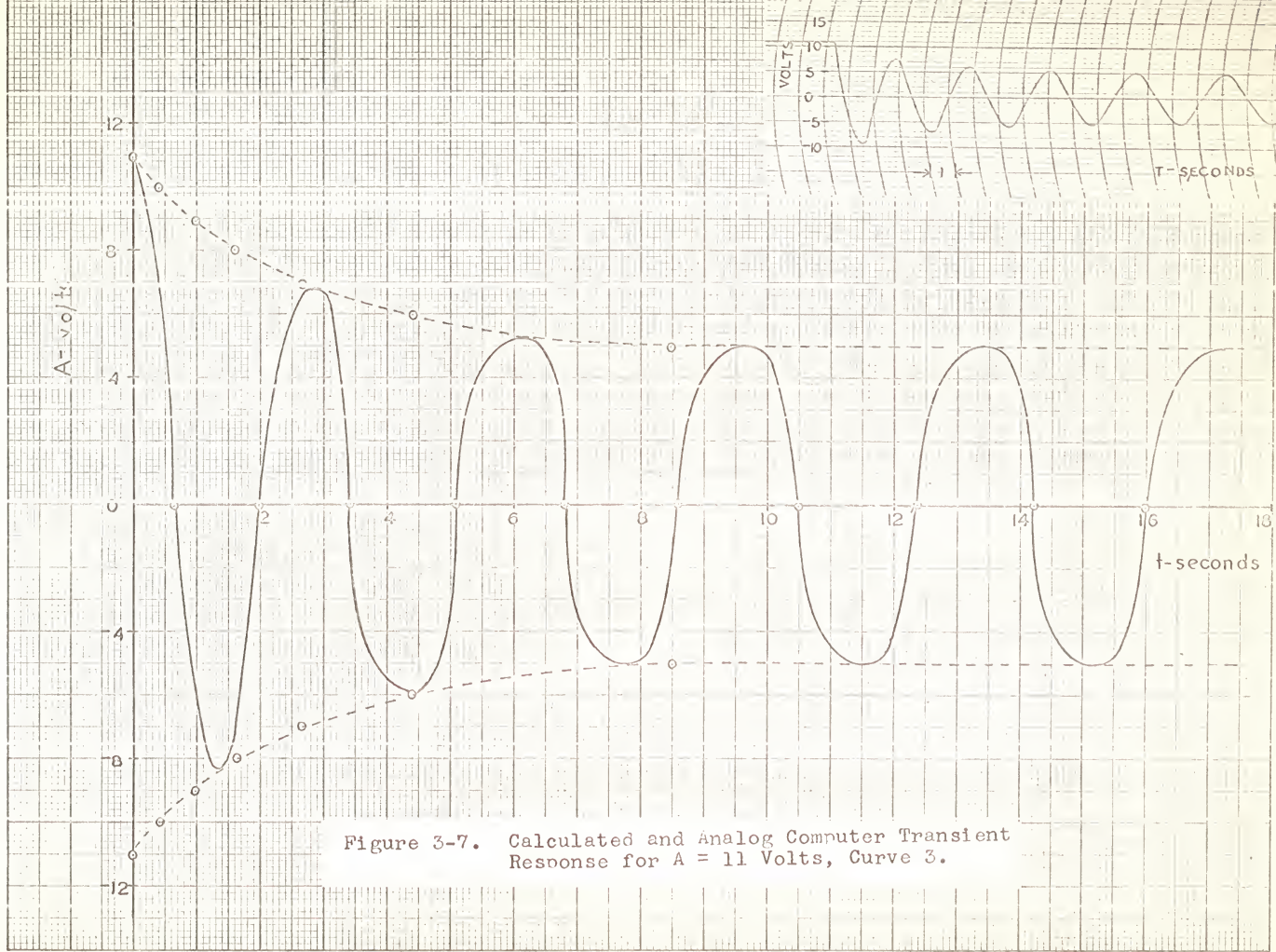

Figure 3-7. Calculated and Analog Computer Transient Response for A = 11 Volts, Curve 3.

transient prediction in Figure 3-6 is improved because the high values of zeta are no longer prominent. During the first five seconds of the transient response the theoretical results closely approximate the analog results. By this time the signal envelope is less than three volts and the system is in the nebulous dead zone region where $N_1 = N_2 = 0$. The analog computer indicates some non-oscillatory waveform after this terminal point is reached. The best correspondence between the theoretical calculations and the analog simulation is shown in the transient response curves appearing in Figure 3-7. Two overshoots are indicated on both the calculated transient response and the actual analog response before the system reaches the stable limit cycle. As indicated earlier the amplitude and frequency of the limit cycle agreed very closely.

3-4 Summary of results

This example indicates that the effect on the variations in system performance due to changes in the nonlinear variables can be predicted to some extent by noting the changing dynamic describing function curves. As already noted excellent prediction of system performance results when the ζ values are low or in the vicinity of the $\zeta = 0$ curve. When the dynamic describing function curve lies in the rapidly changing high zeta or overdamped regions of the parameter plane, it becomes increasingly difficult to anticipate system performance accurately.

CHAPTER IV

TWO NONLINEAR ELEMENTS RELATED TO A COMMON SIGNAL BY A LINEAR DIFFERENTIAL EQUATION

In order to establish the system performance for nonlinear elements related to a common reference signal by a linear differential equation, nonlinearities N_1 and N_2 for case 2 are considered as saturation or dead zone elements. The theoretical describing function curve is calculated for several test cases. A graphical technique which assumes second order dominance was used to calculate the transient responses. The systems were simulated on the analog computer and comparisons were made between the actual and theoretical amplitudes and frequencies of the limit cycles as well as the system transient responses.

4-1 Saturation in the error channel and dead zone in the tachometer feedback channel

Figure 4-1 shows the working model with the dead zone width of N_1 and the saturation level of N_2 set at $\pm$ 1 volt. Using the graphical method outlined in section 2-2-1 a dynamic describing function curve, which appears in Figures 4-2 and 4-3, was determined for this system. As indicated in section 2-2-1 the loci of the describing function curves are superimposed on the zeta-omega and sigma-omega parameter plane curves. The small circles indicate the points of common radian frequency, ω , between the describing function loci and the parameter plane curves. Adjacent to these solution points are indicated the amplitude theoretically required for initial condition, A. The common radian frequency is the constant omega curve passing through the indicated points. The dynamic describing function curve is denoted by

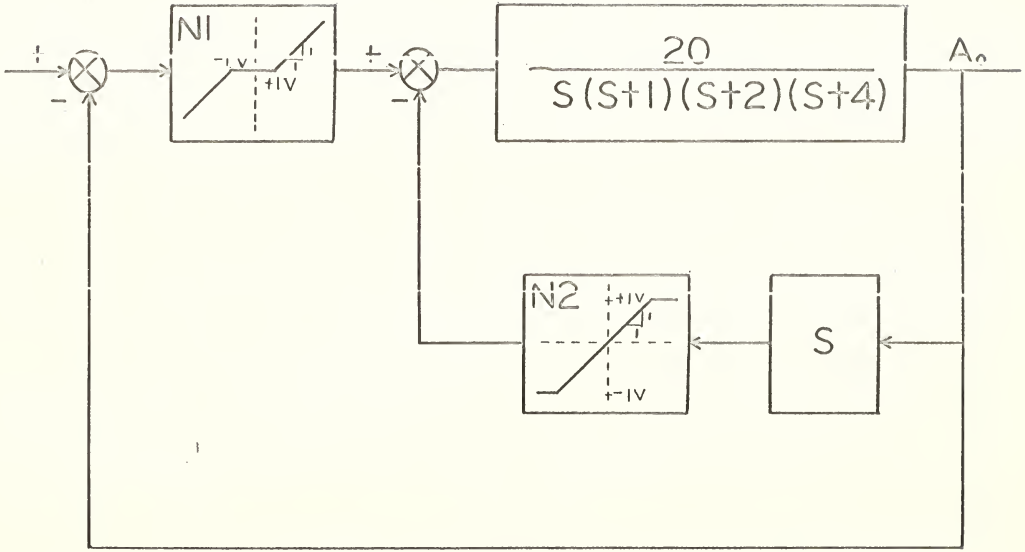

Figure 4-1. Block Diagram of Fourth Order System with Two Nonlinear Elements.

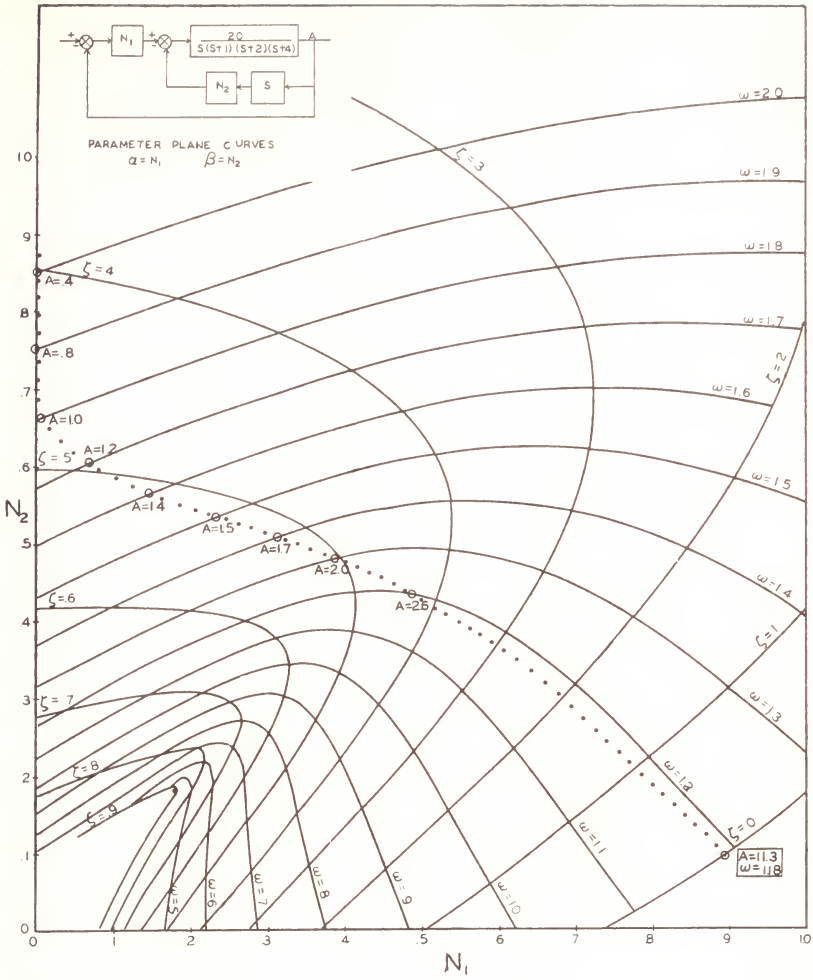

Figure 4-2. Dynamic Describing Function Curve on Zeta-Omega Curves.
N_1 - Dead Zone $E_d = \pm 1$ Volt
N_2 - Saturation $E_{sat} = \pm 1$ Volt

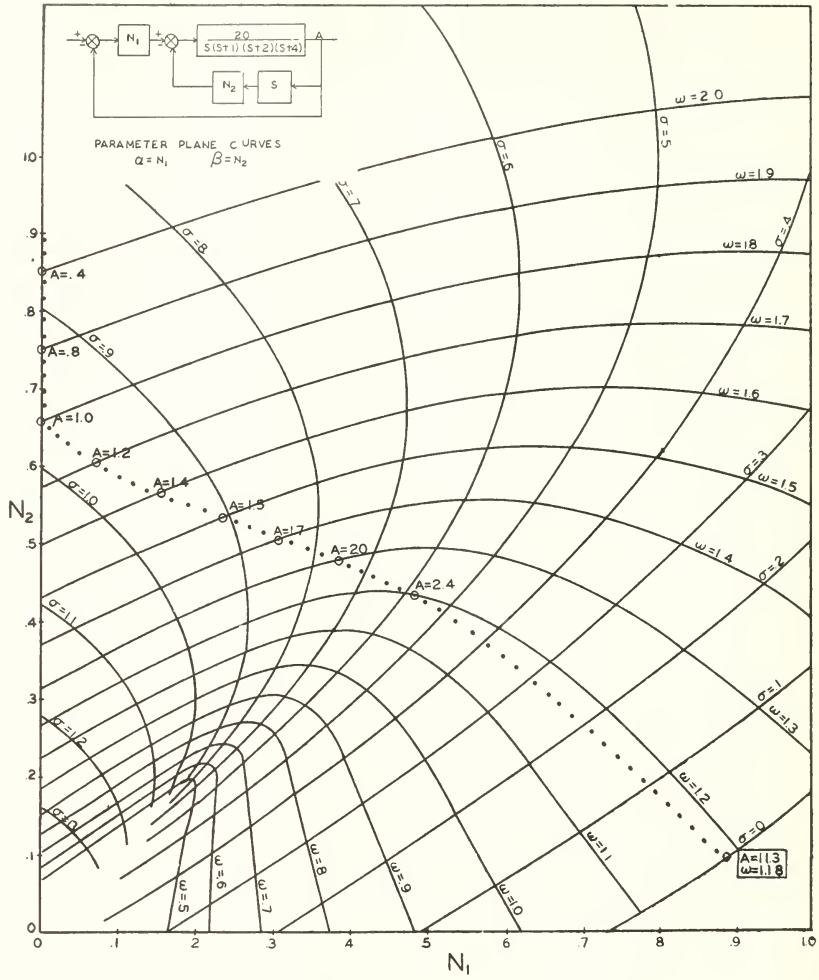

Figure 4-3. Dynamic Describing Function Curve on Sigma-Omega Curves.
N_1 - Dead Zone $E_d = \pm 1$ Volt
N_2 - Saturation $E_{sat} = \pm 1$ Volt

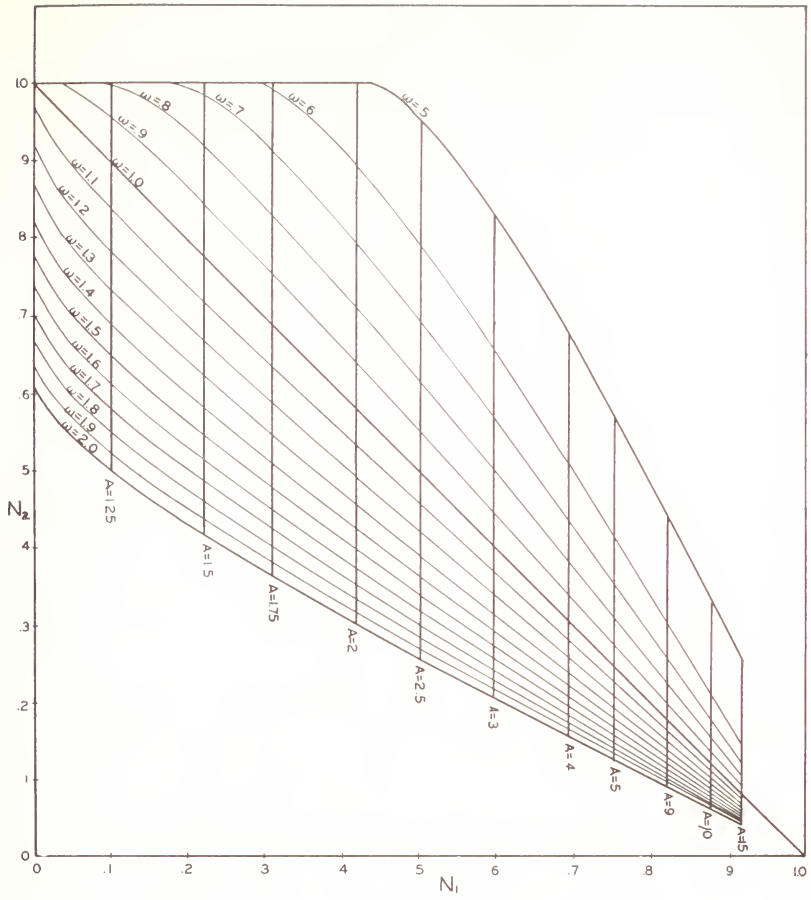

Figure 4-4. ω -A Grid for Figures 4-2 and 4-3.
N_1 - Dead Zone $E_d = \pm 1$ Volt
N_2 - Saturation $E_{sat} = \pm 1$ Volt

the series of heavy dots. Figure 4-4 is the digital computer generated ω -A grid for the describing function loci. If tracing paper were used, this grid could be placed atop the modified parameter plane curves, and the common radian frequency, ω , and initial condition amplitude, A, obtained by inspection. Since the parameter plane curves are for any two amplitude sensitive non-linearities, it is only necessary to obtain a new grid for a different choice of nonlinear elements.

The dynamic describing curve in Figures 4-2 and 4-3 moves progressively leftward, towards decreasing values of N_1 and increasing values of N_2, while the required amplitude of the initial condition, A, decreases until the linear M - point is reached which occurs at $N_1 = 0$ and $N_2 = 1$. At this point the outer feedback loop will have no effect on system response while the inner feedback loop acts as a linear system. Also indicated on the dynamic describing function curve is the amplitude and frequency of the limit cycle which occurs on the $\zeta = 0$ and $\sigma = 0$ curves.

The system was simulated on the analog computer and the output response recorded for various amplitudes of A. Figure 4-5 shows the analog computer setup. The amplitude of the limit cycle was determined by averaging the values of the first oscillation for initial conditions of 13.0 and 13.2 volts. This problem indicated that a finite amount of time was required for the analog computer solution to stabilize due to the energy storage requirements of the transfer functions. The amplitude and radian frequency of the limit cycle are compared below between the graphical method and the computer results. The oscillating frequency is predicted accurately, but the theoretical amplitude

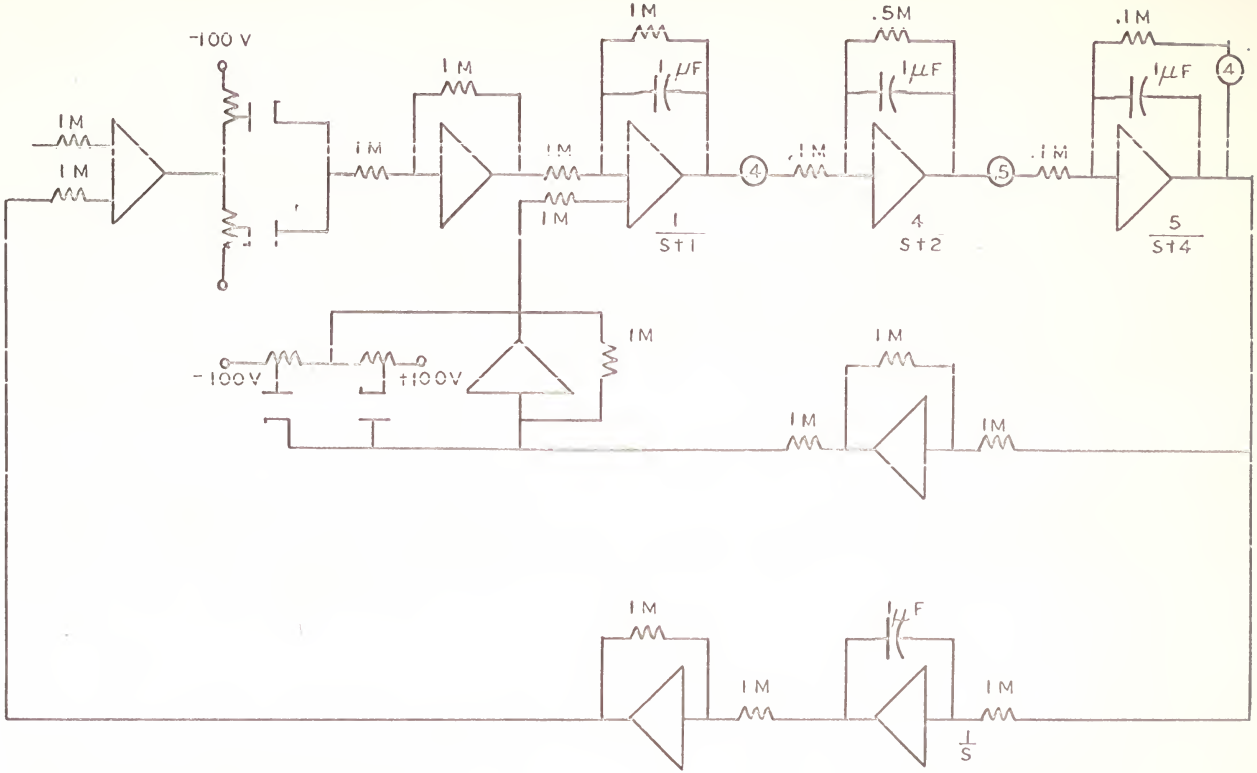

Figure 4-5. Analog Computer Simulation.

is 0.48 volts low.

Limit Cycle	Amplitude	ω_0
Theoretical	11.32 volts	1.18
Computer	11.8 volts	1.18

To obtain a further comparison of the reliability of the dynamic describing function method the transient response was graphically determined. As previously noted this graphical method, developed by Šiljak, assumes second order dominance, meaning that the results are only valid for a system with a dominant pair of complex poles. Hence, at best the results may have only limited validity for a fourth order system over the dynamic describing function curve. An example of this transient response technique using both the zeta-omega and sigma-omega curves appears in Appendix A.

Figures 4-6, 4-8, and 4-10 are the graphically calculated transient responses for A = 9, 6, and 3 volts respectively. The odd-numbered figures 4-7, 4-9, and 4-11 are the corresponding analog computer transient responses. In the three computer cases it should be noted that a finite amount of time is required for the exponential decay to begin after the switch is turned on whereas the graphical solution shows an instantaneous decay. This finite lag time due to imperfect simulation on the analog computer causes the theoretical results to have earlier zero crossings and larger overshoot amplitudes. In addition a real-root effect is noticeable on the analog results shown by the slowly decreasing steady state output which is especially apparent for A = 3 volts. As noted earlier the graphical technique makes no provisions for real-root effects.

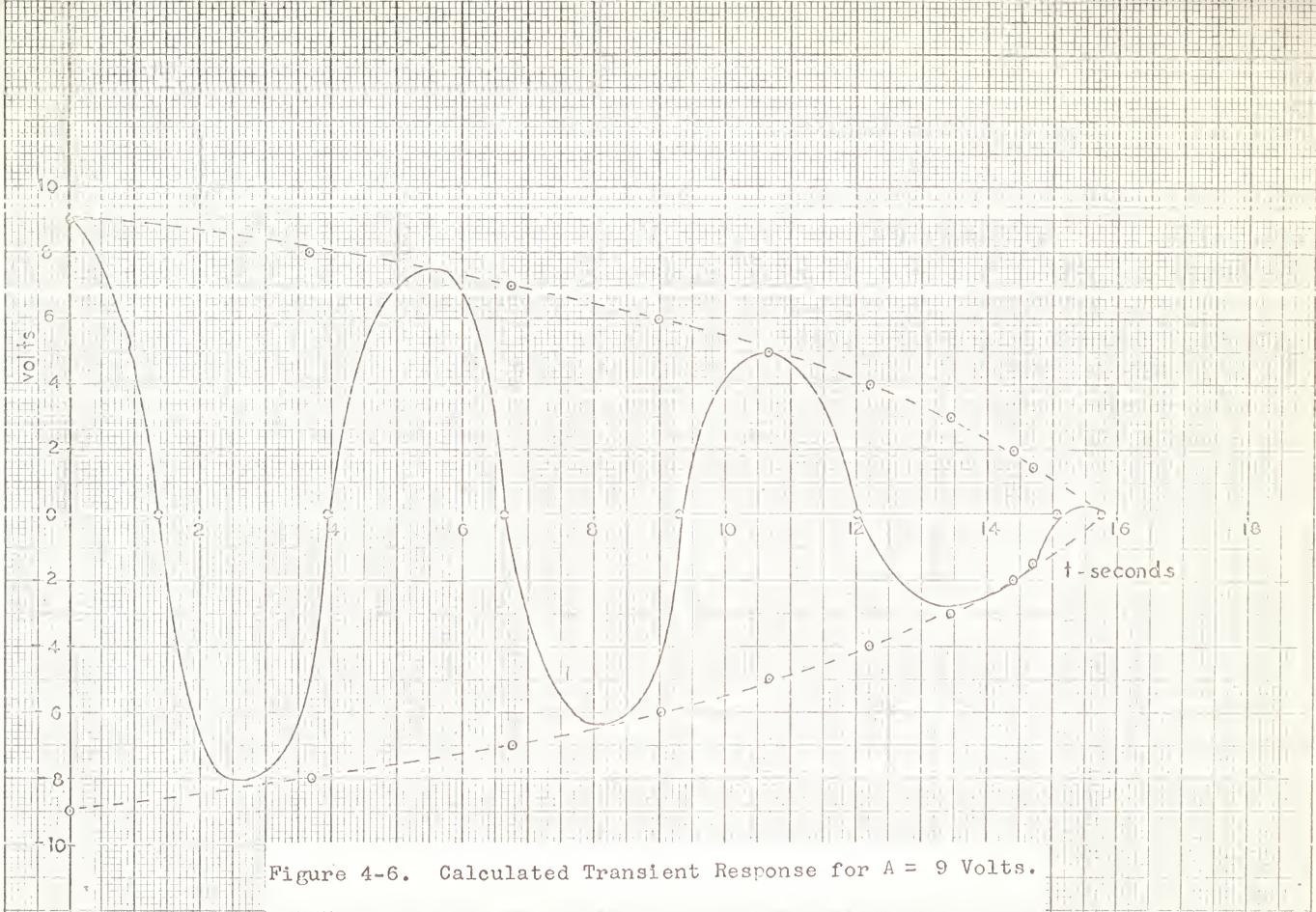

Figure 4-6. Calculated Transient Response for A = 9 Volts.

Figure 4-7. Analog Computer Transient Response for A = 9 Volts.

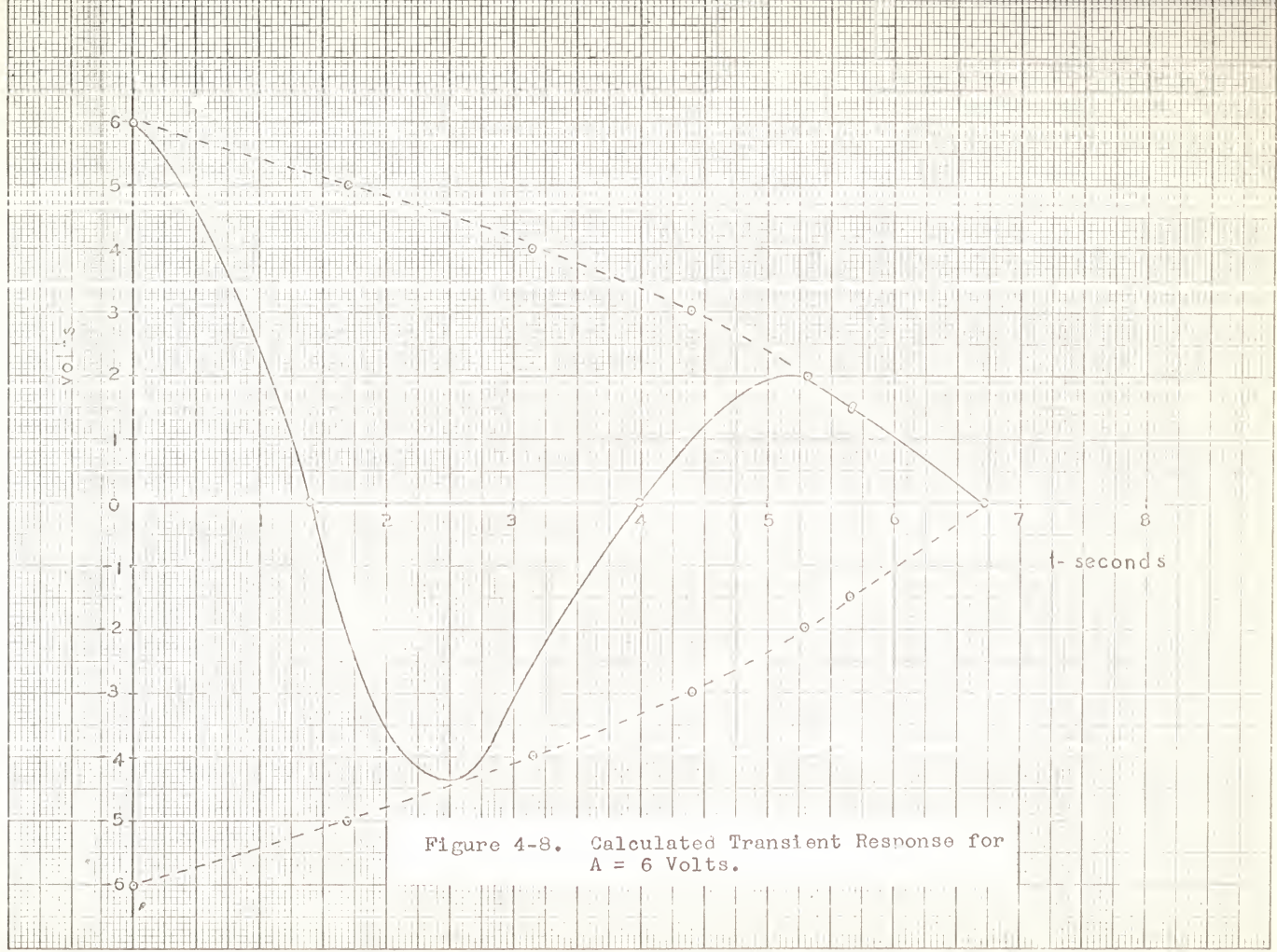

Figure 4-8. Calculated Transient Response for A = 6 Volts.

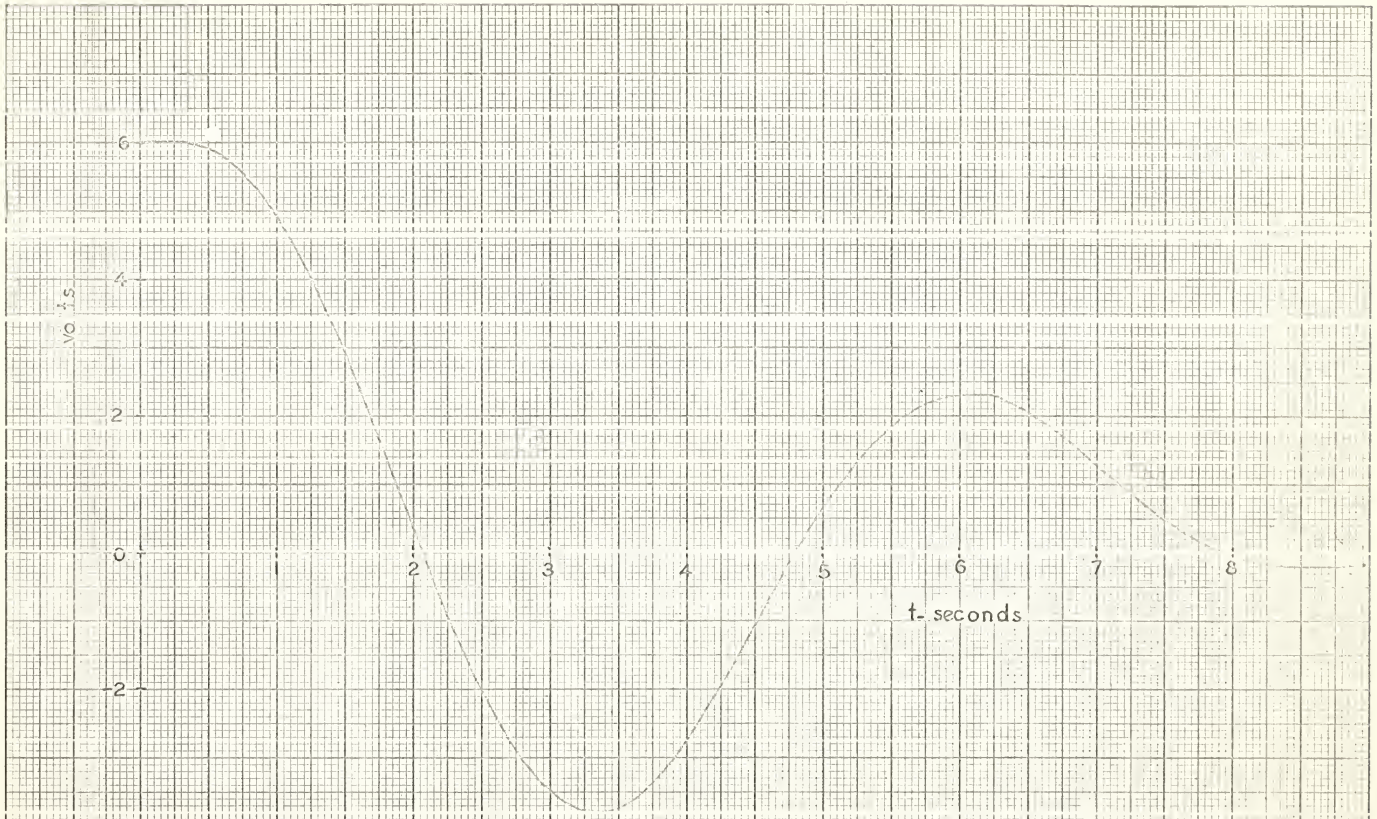

Figure 4-9. Analog Computer Transient Response for A = 6 Volts.

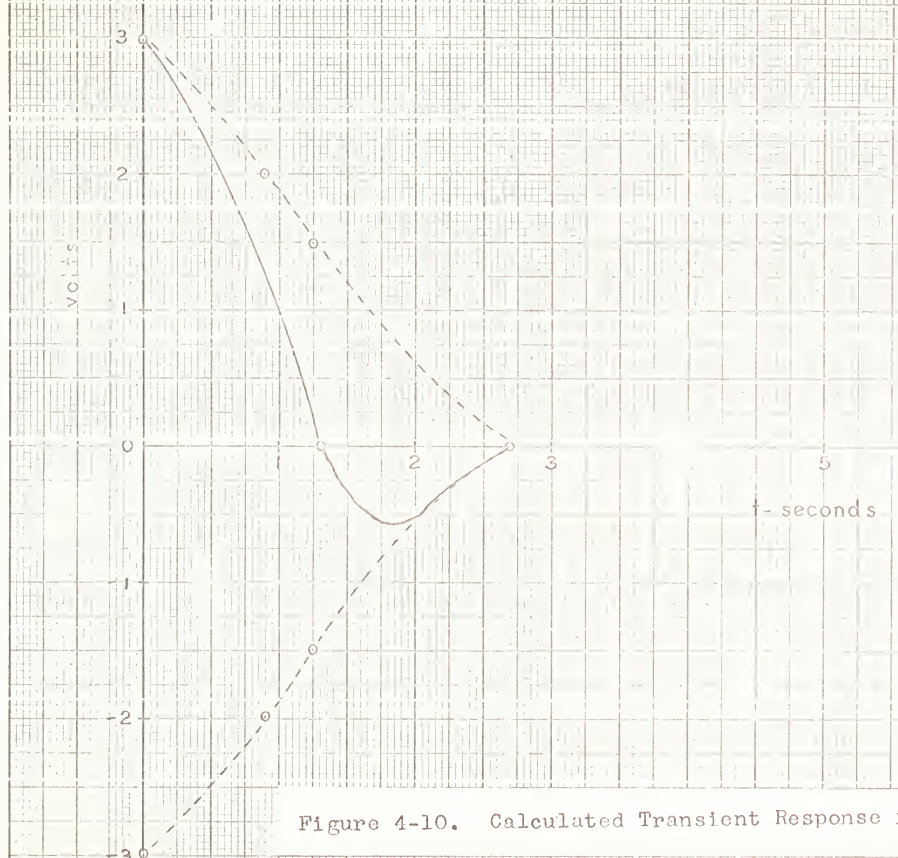

Figure 4-10. Calculated Transient Response for A = 3 Volts.

K&E 7½ X 10 INCHES MADE IN U.S.A.
KEUFFEL & ESSER CO.

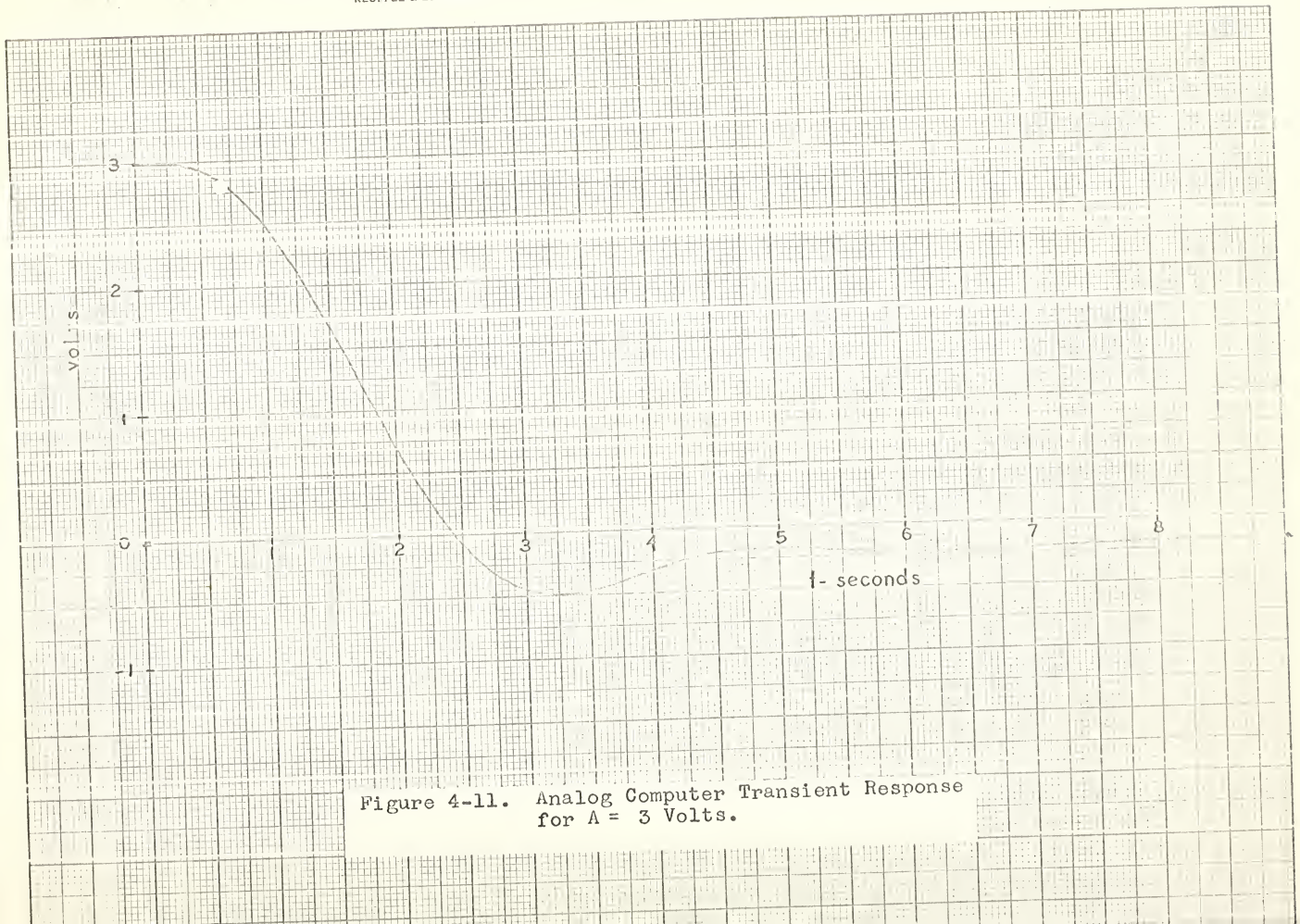

Figure 4-11. Analog Computer Transient Response for A = 3 Volts.

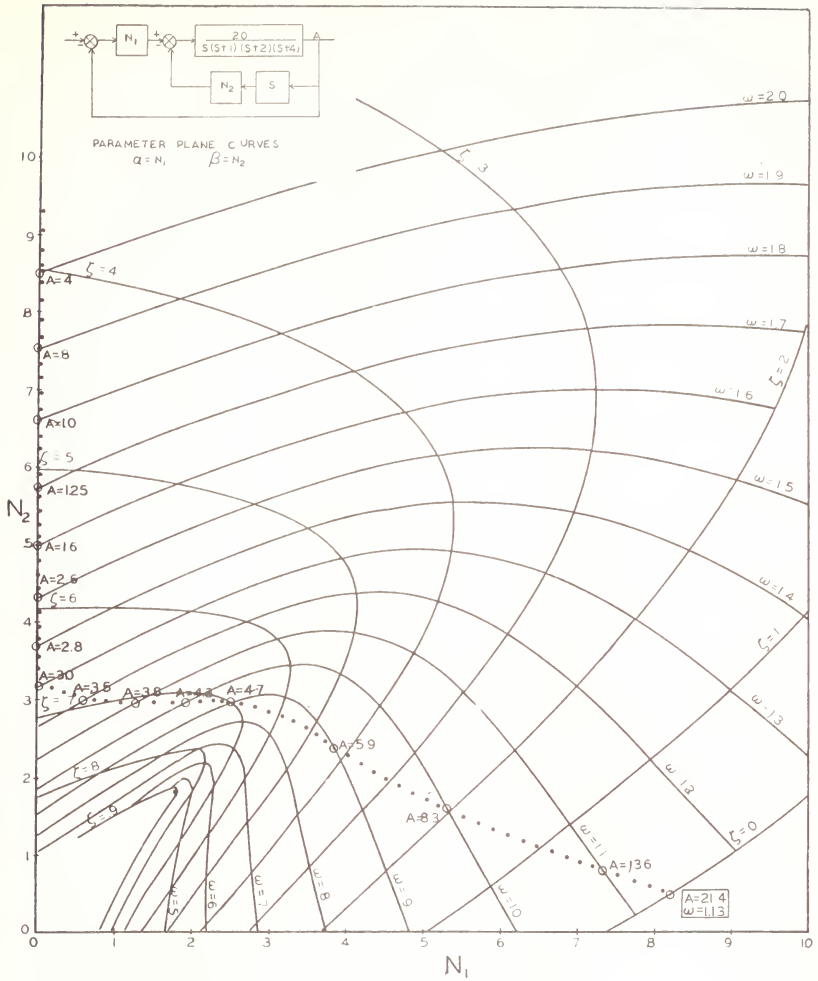

Figure 4-12. Dynamic Describing Function Curve on Zeta-Omega Curves.
N_1 - Dead Zone $E_d = \pm .3$ Volts
N_2 - Saturation $E_{sat} = \pm 1$ Volt

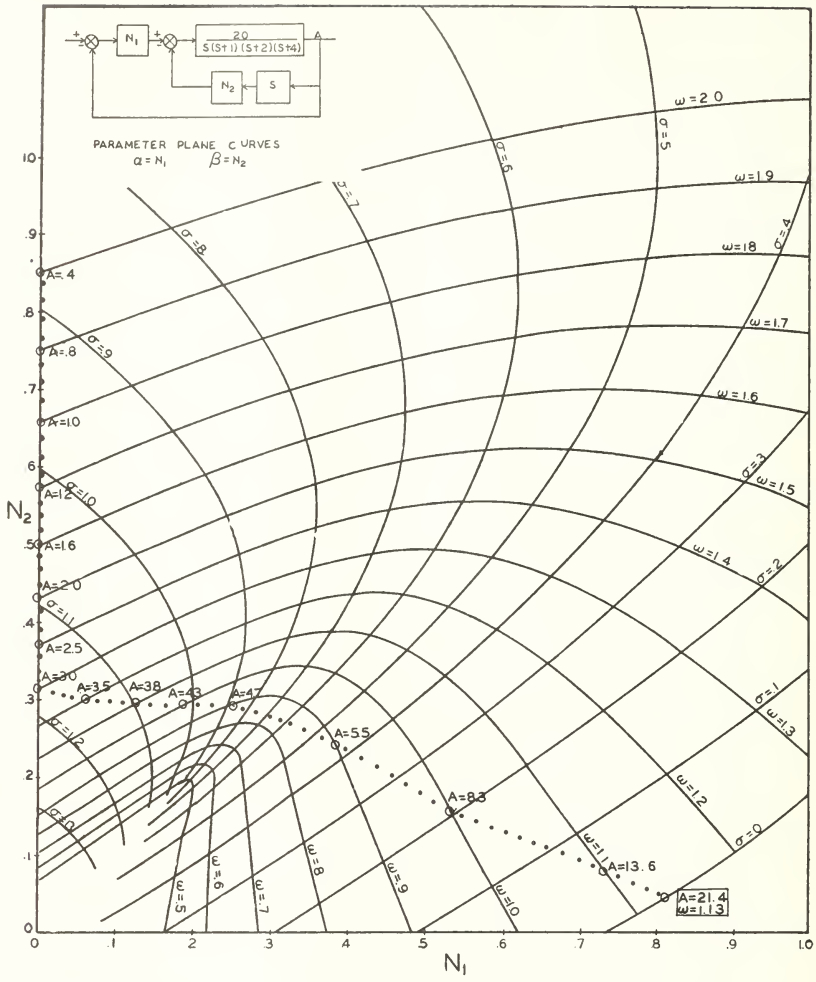

Figure 4-13. Dynamic Describing Function Curve on Sigma-Omega Curves.
N_1 - Dead Zone $E_d = \pm$ 3 Volts
N_2 - Saturation $E_{sat} = \pm$ 1 Volt

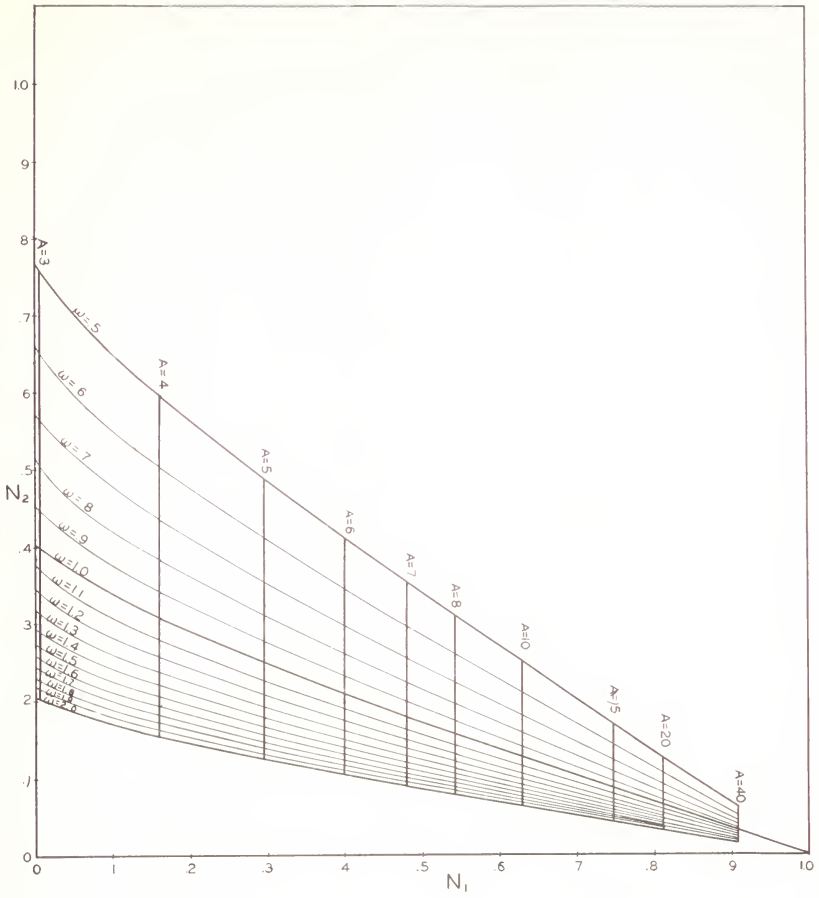

Figure 4-14. ω -A Grid for Figures 4-12 and 4-13.
N_1 - Dead Zone $E_d = \pm$ 3 Volts
N_2 - Saturation $E_{sat} = \pm$ 1 Volt

From this example one would conclude that for this system to expect an exponentially damped response for initial condition signals of less than about 11 volts. For A greater than 11 volts both the dynamic describing function curve and the computer indicate unstable conditions.

4-1-1 Effect of changing one nonlinearity

When the dead zone width was increased to $\pm$ 3 volts, the dynamic describing function curve changed. Figures 4-12 and 4-13 show the modified dynamic describing function curve superimposed on the zeta-omega and sigma-omega parameter plane curves respectively. The ω -A grid for this system appears in Figure 4-14. This latter plot is the only additional labor required since the parameter plane curves do not change for the same two nonlinearities configuration.

As in the previous case the amplitude and frequency of the limit cycle were compared between the dynamic describing function curve and the analog computer.

Limit Cycle	Amplitude	ω
Theoretical	21.4 volts	1.13
Computer	25.5 volts	1.14

In this case the disparity between the amplitudes is about twenty per cent. The reason for this difference is that describing function theory is a first order approximation for the signal amplitude, but it is a second order approximation for the oscillating frequency. Figures 4-15, 4-17, and 4-19 are computed transient responses for A = 16, 12, and 8 volts respectively. The corresponding transient responses for the computer simulation appear in Figures 4-16, 4-18 and 4-20. Once again the real root effect is apparent in the analog computer response.

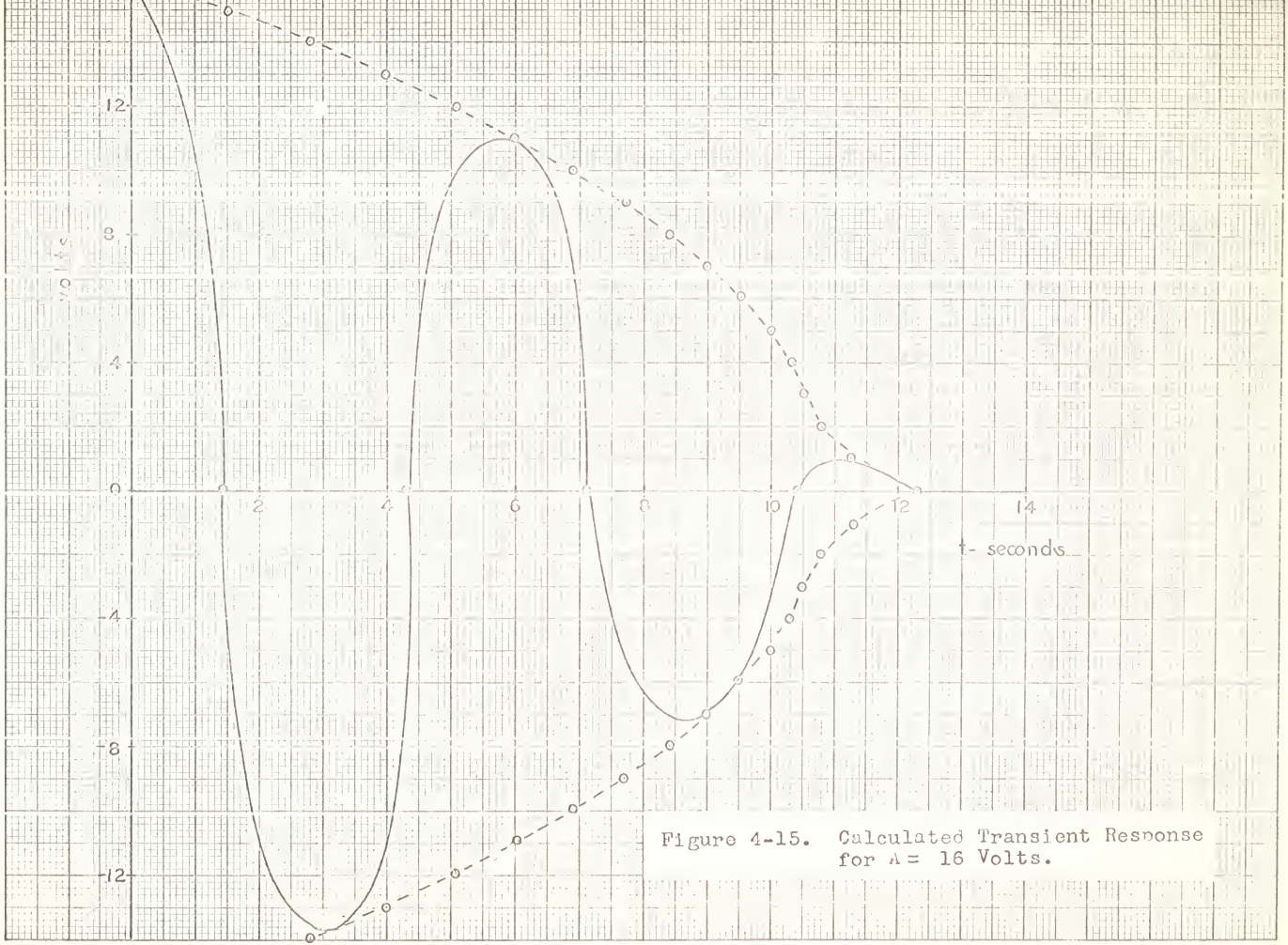

Figure 4-15. Calculated Transient Response for A = 16 Volts.

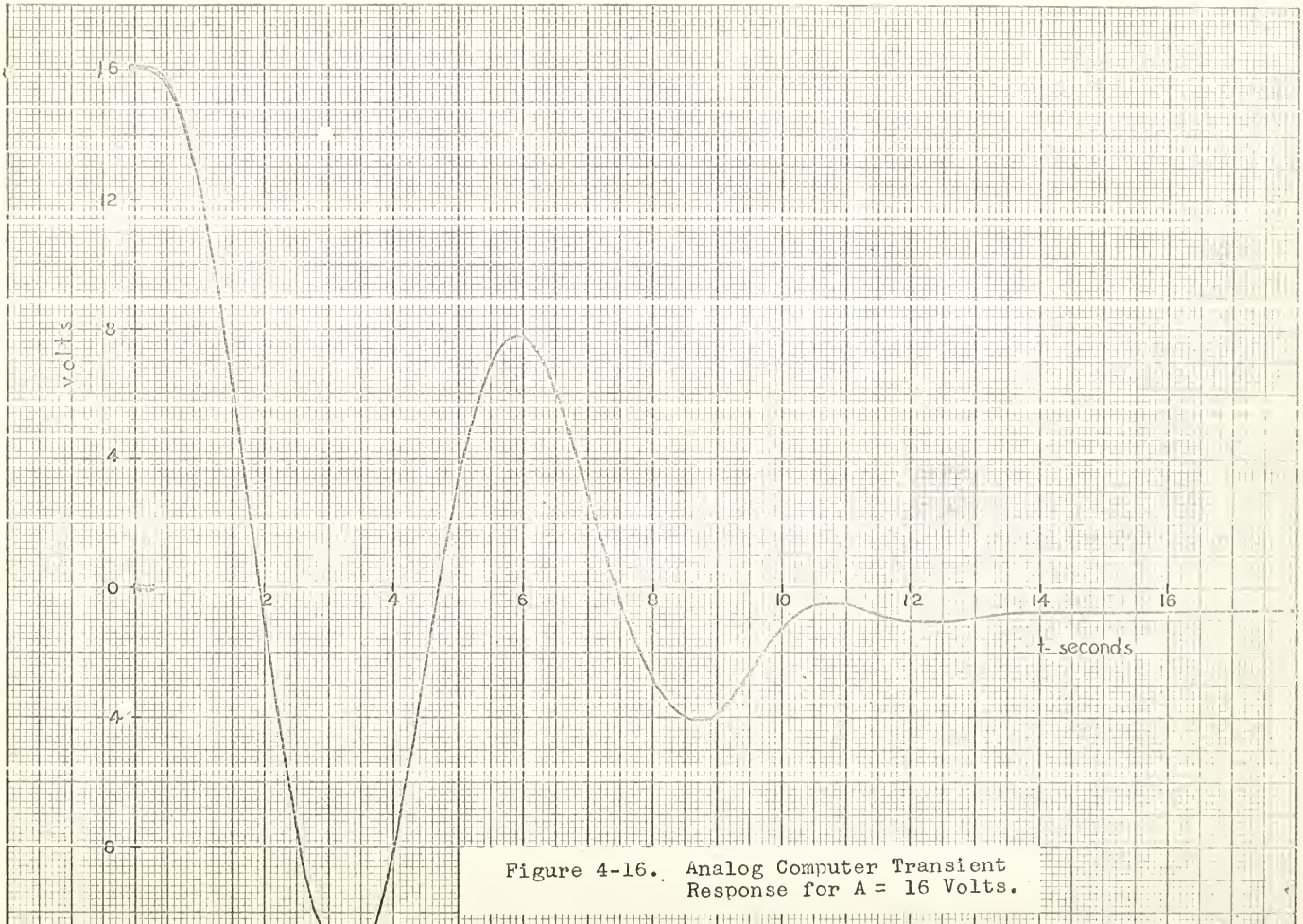

Figure 4-16. Analog Computer Transient Response for A = 16 Volts.

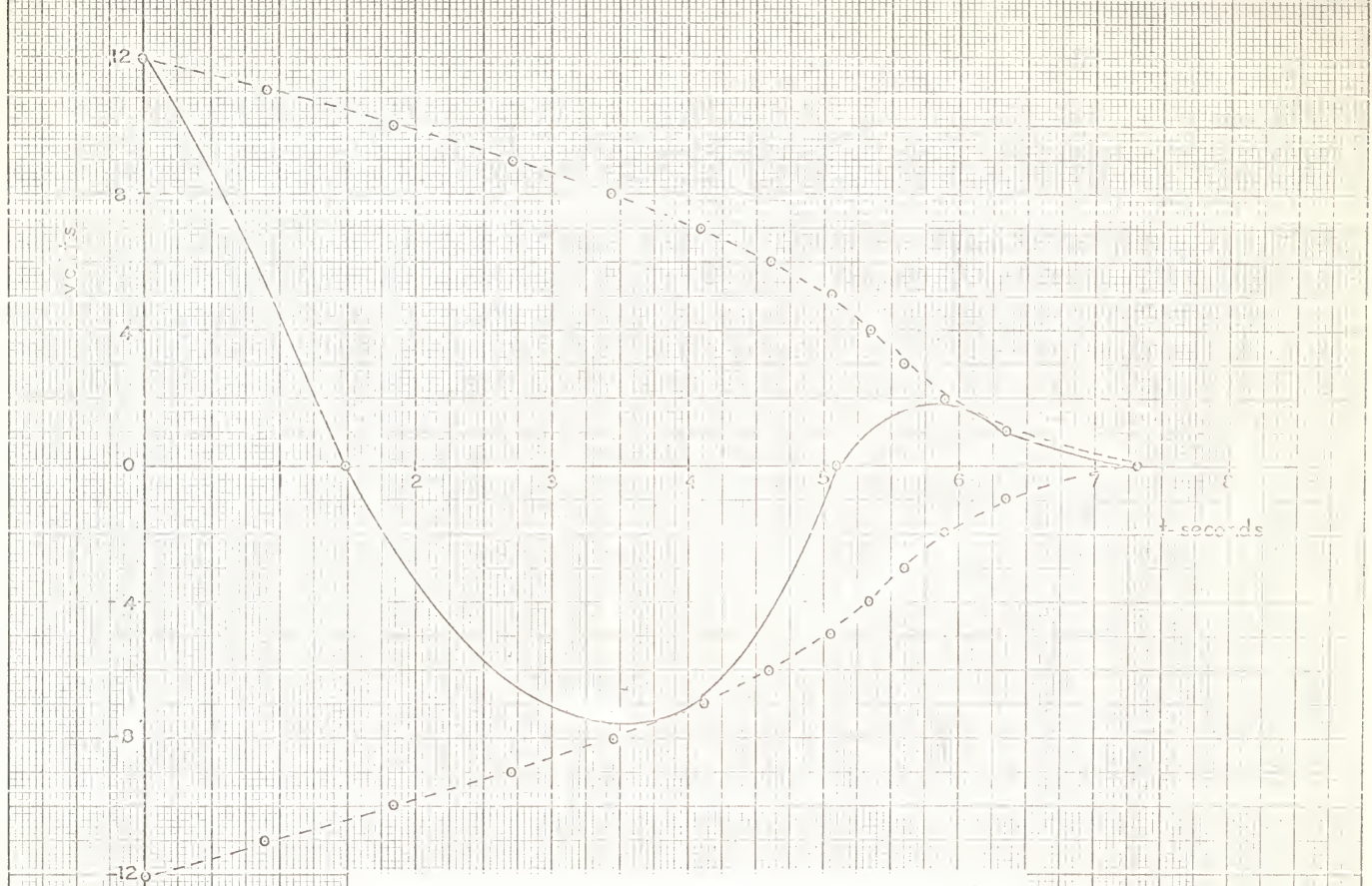

Figure 4-17. Calculated Transient Response for A = 12 Volts.

KEUFFEL & ESSER CO. MADE IN U.S.A.

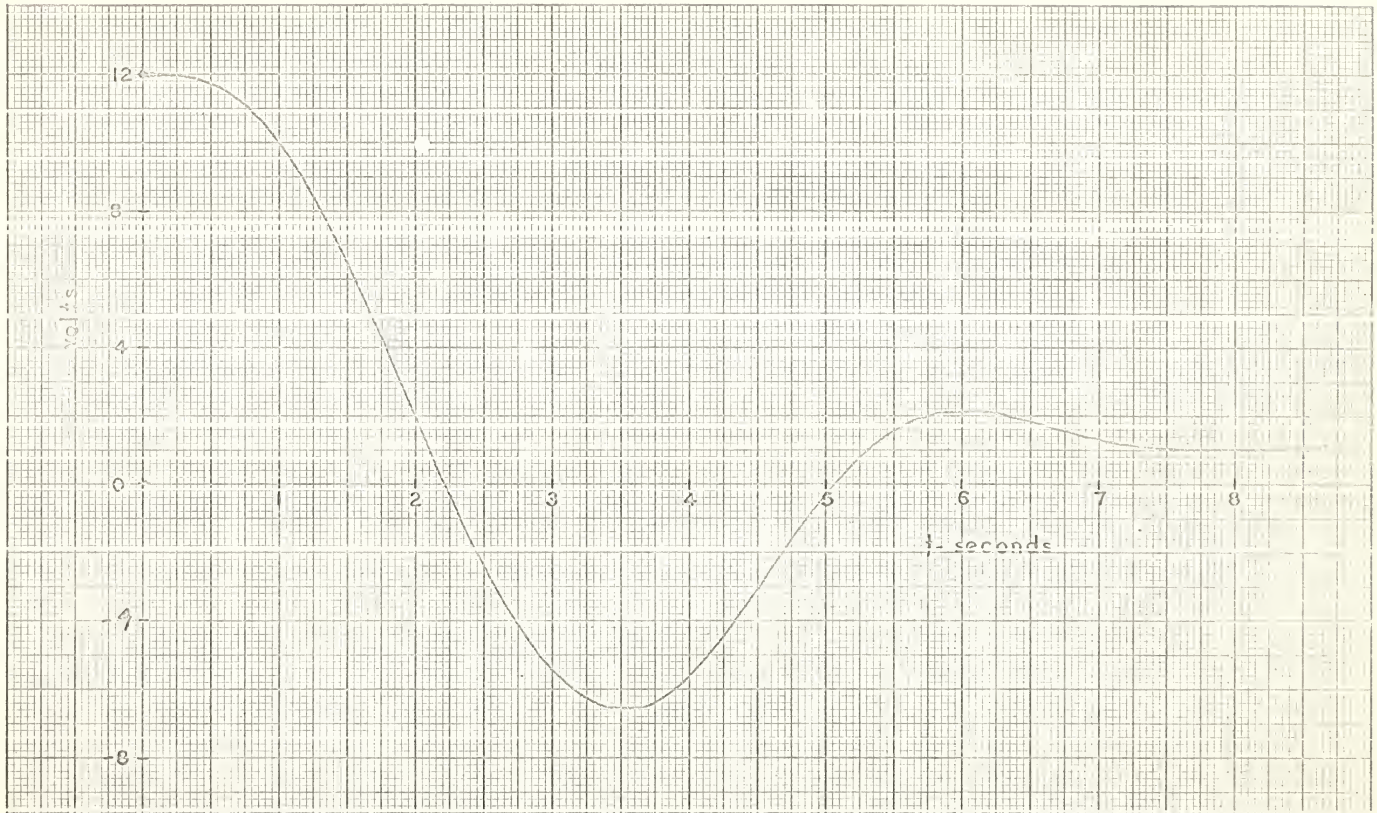

Figure 4-13. Analog Computer Transient Response for A = 12 Volts.

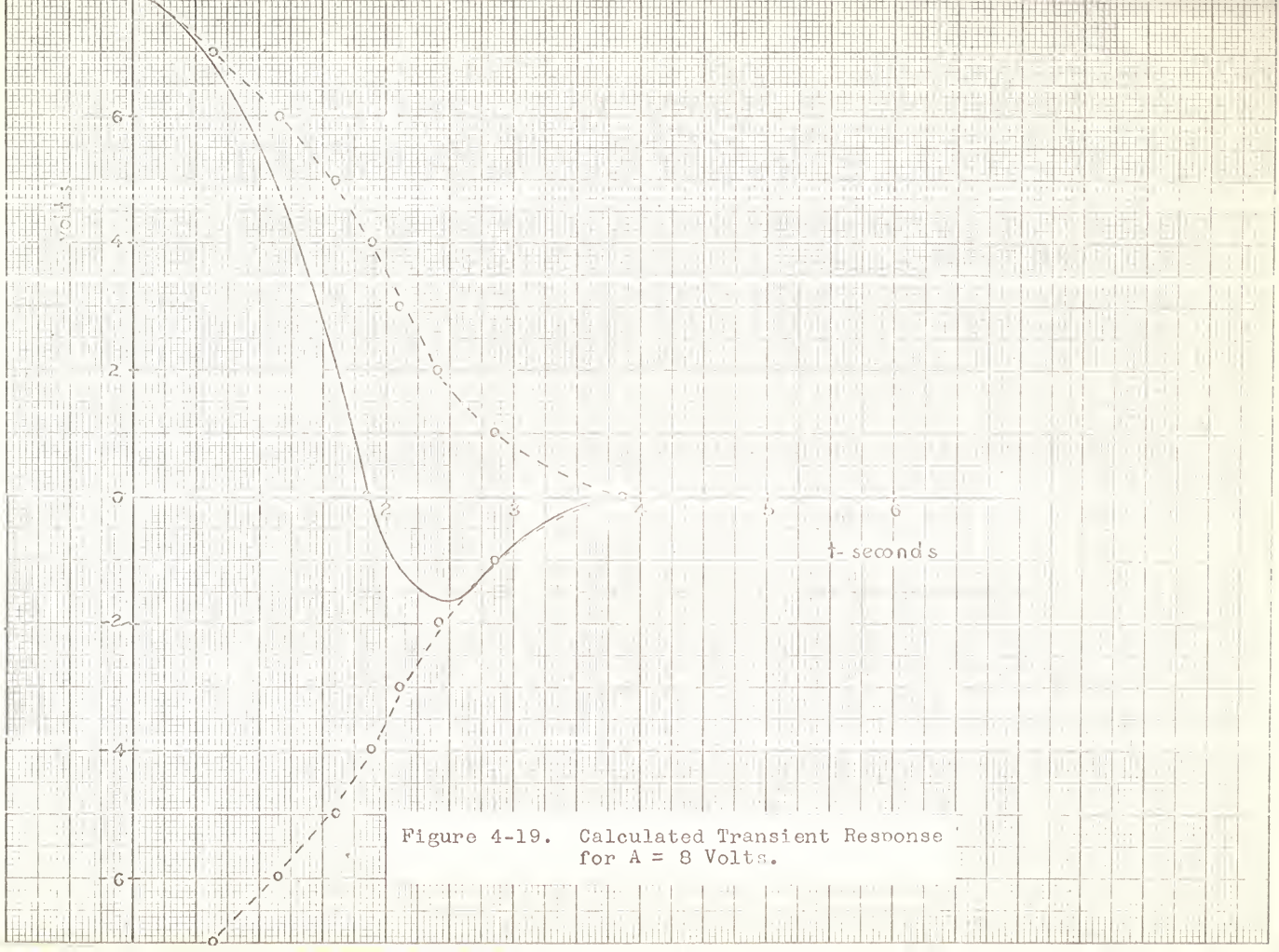

Figure 4-19. Calculated Transient Response for A = 8 Volts.

K&E 10 X 10 TO THE ½ INCH KEUFFEL & ESSER CO. 358-12 MADE IN U.S.A.

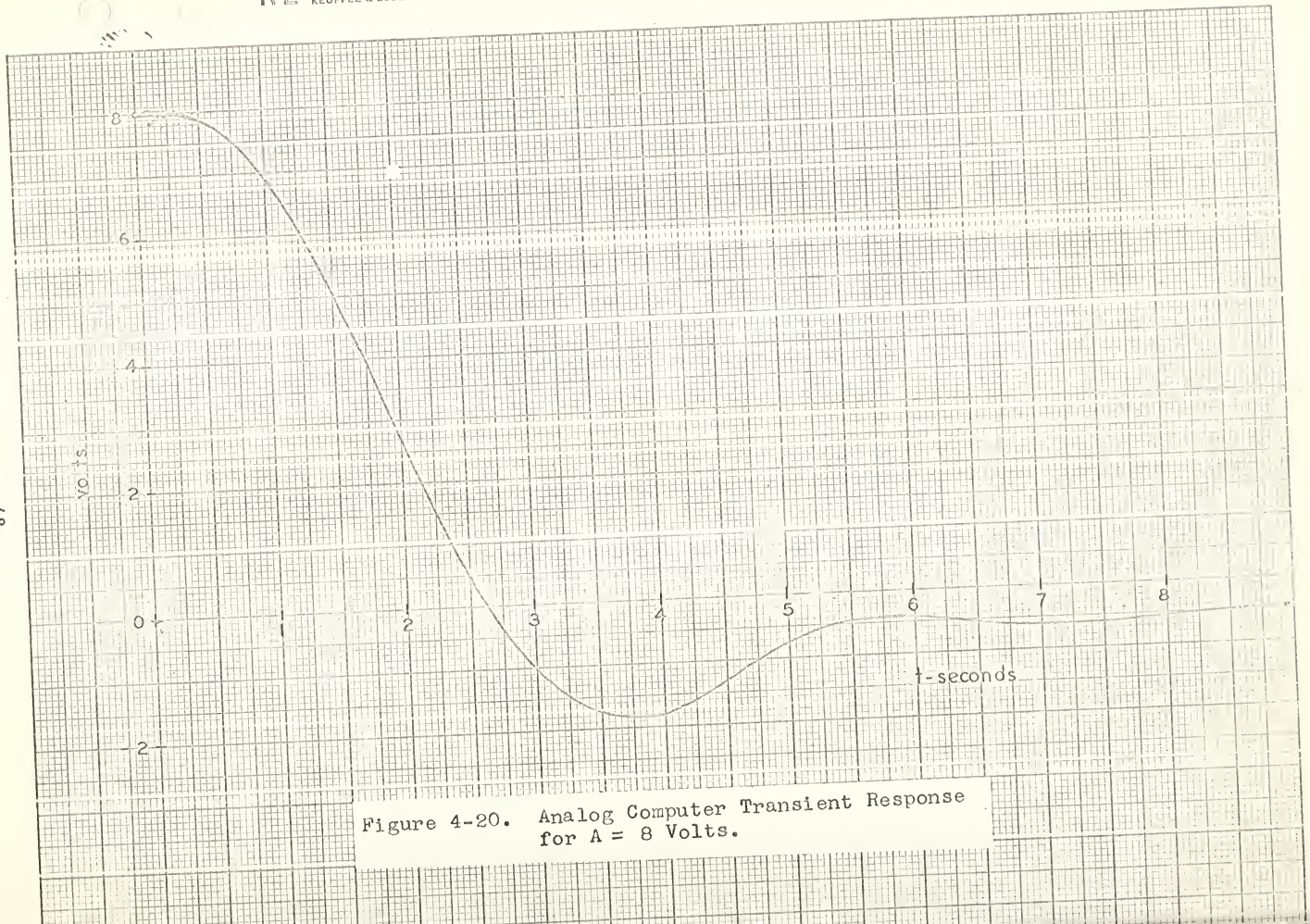

Figure 4-20. Analog Computer Transient Response for A = 8 Volts.

4-2 A family of dynamic describing function curves

The previous two examples have shown that system performance cannot be predicted exactly with the tools at hand, but that information is available on the dynamic describing function curve although the interpretation might be approximate.

Since the parameter plane curves for the working model are for any amplitude sensitive nonlinearities, N_1 and N_2, it was decided to reverse the nonlinear elements - N_1 is now a variable saturation element and N_2 is a $\pm$ 3 volt dead zone element. Figure 4-21 is a block diagram of this example.

By varying the saturation levels, it was anticipated that a series of dynamic describing functions would be obtained that would give some indication which areas of the parameter plane are of the greatest utility in predicting the system performance using the present techniques. A series of dynamic describing function curves were constructed for saturation levels of 1, 2, 3, and 5 volts. This composite plot appears in Figures 4-22 and 4-23.

A few salient features are readily apparent from these plots. First, the amplitude of the initial conditions, A, decreases in a left - to - right manner except for curve A where the initial condition amplitude appears to fluctuate for high values of ζ before settling down. Secondly, all the curves tend towards $N_1 = 1$ and $N_2 = 0$ for smaller initial conditions. This result is expected because for small initial conditions the dead zone element is effectively out of the system while the saturation element becomes linear. Lastly, all the dynamic describing function curves predict a stable limit cycle. That is, when the curves cross the $\zeta = 0$ or $\sigma = 0$ boundary, A becomes smaller as the

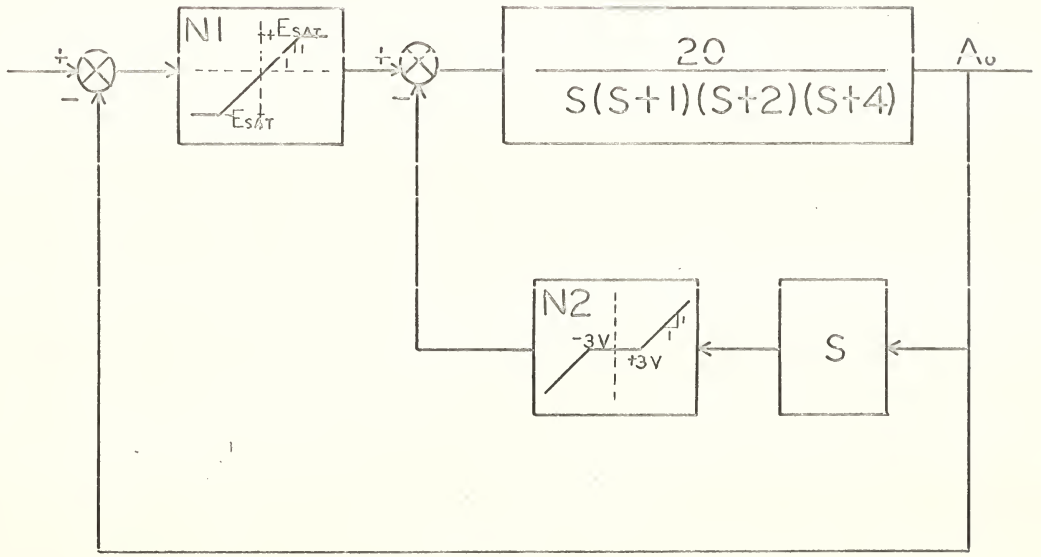

Figure 4-21. Block Diagram of Modified System.

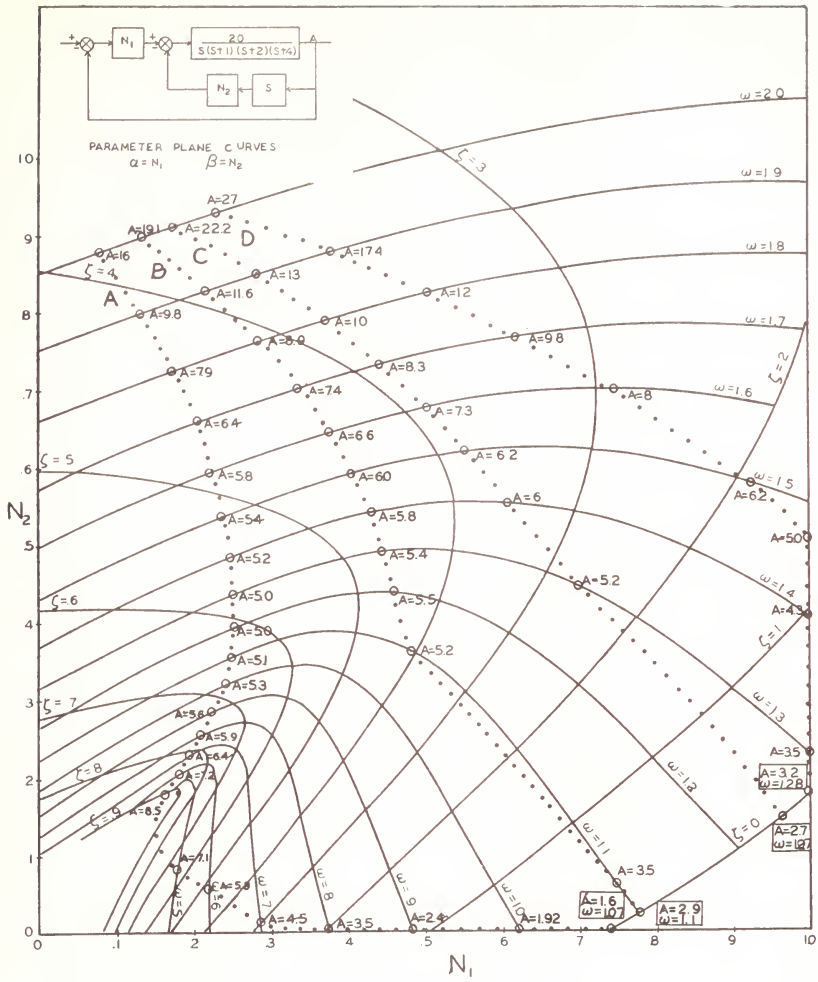

Figure 4-22. Family of Dynamic Describing Function Curves on Zeta-Omega Curves.

N_2 Dead Zone $E_d = \pm 3$ Volts

A - N_1 Saturation $E_{sat} = \pm 1$ Volt

B - N_1 Saturation $E_{sat} = \pm 2$ Volts

C - N_1 Saturation $E_{sat} = \pm 3$ Volts

D - N_1 Saturation $E_{sat} = \pm 5$ Volts

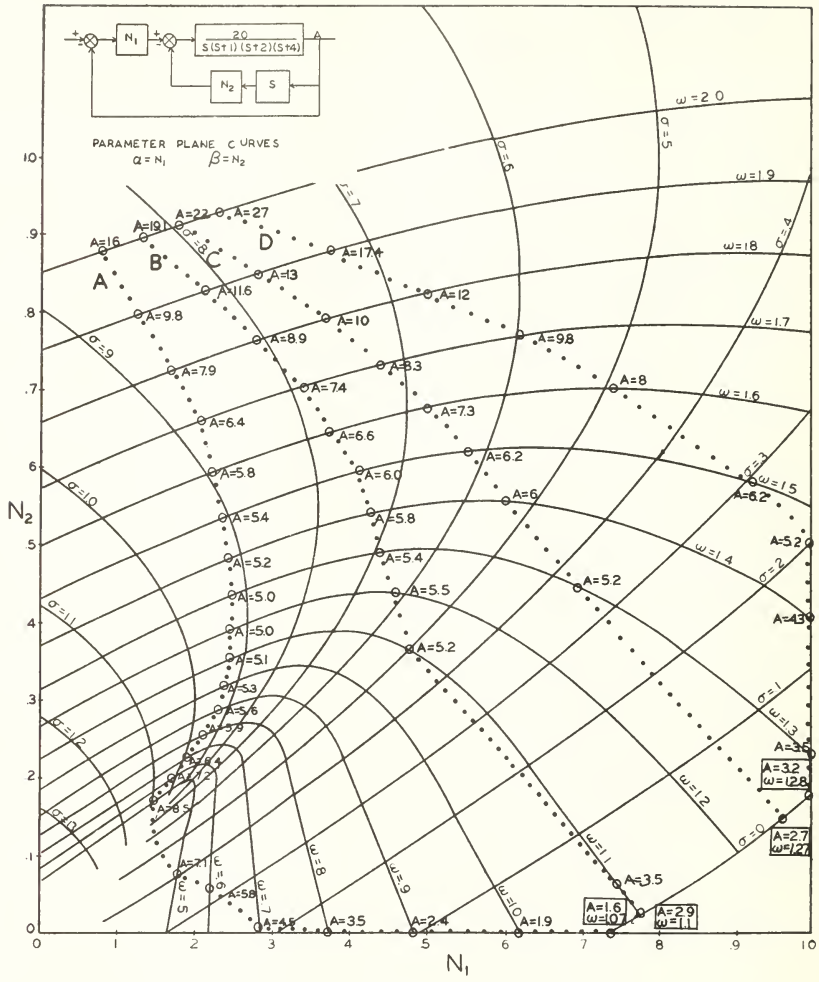

Figure 4-23. Family of Dynamic Describing Function Curves on Sigma-Omega Curves.

N_2 - Dead Zone $E_d = \pm$ 3 Volts

A - N_1 - Saturation $E_{sat} = \pm$ 1 Volt

B - N_1 - Saturation $E_{sat} = \pm$ 2 Volts

C - N_1 - Saturation $E_{sat} = \pm$ 3 Volts

D - N_1 - Saturation $E_{sat} = \pm$ 5 Volts

M-point enters the negative ζ or unstable region. If the amplitudes were increasing, as in the previous test cases, an unstable limit cycle would exist.

In the following table a comparison is made between the dynamic describing function curve prediction and the analog computer simulation of the amplitude and frequency of the limit cycle.

Table 1. Comparison of Limit Cycle Performance Between Dynamic Describing Function Curve and Analog Computer.

Saturation Level	Theoretical		Computer	
For N_1	Amplitude	ω	Amplitude	ω
$\pm$ 1 volt	1.6 volts	1.07	1.0 volt	1.04
$\pm$ 2 volts	2.9 volts	1.1	2.5 volts	1.12
$\pm$ 3 volts	2.7 volts	1.27	3.0 volts	1.25
$\pm$ 5 volts	3.2 volts	1.28	3.0 volts	1.26

As previously noted the amplitude of the initial condition varies in the vicinity of high values of zeta, i.e., ζ = .6 to .9. The reason for this unique behavior is not explainable at this time. Possibly, the technique used in this thesis has reasonable validity for conditions under which the values of zeta do not exceed some level, say ζ = .7. However, is all cases of this example the amplitude of A decreases as the stable limit cycle is approached.

Keeping the previous limitation in mind the transient response was graphically determined for an initial condition of 5 volts. This value was chosen because the four curves behaved the same for this initial condition amplitude; i.e., the amplitude of A decreases as the limit cycle was approached.

In Figures 4-24 to 4-27 are the calculated transient responses and in the upper right hand corner of each plot appears a brush recording trace of the actual computer response. It should be observed that the analog computer simulation also exhibits a stable limit cycle for the four cases.

4-3 Relationship between the dynamic describing function curve and the root locus

The system performance of a nonlinear system depends upon the motion of the characteristic equation roots. In using a graphical technique which assumes second order dominance, real root effects are neglected. Additionally, one would suspect that real roots could not be neglected for a fourth order system since there are regions along the dynamic describing function curves in the previous sections from which tangents can be drawn to the $\zeta = 1$ curve -- indicating the presence of real roots. To determine the values of the characteristic roots at discrete intervals along the dynamic describing function curve, a dynamic root locus plot was made.

4-3-1 Dynamic root locus plot

Each point on the dynamic describing function curve can be identified as an operating or M(α , β) point at one instant of time. The roots of the characteristic could be obtained by inspection for each operating point since zeta, omega, and sigma are known. Another method is to substitute the coordinates of the M(α , β) points, N_1 and N_2, into the general characteristic equation, which is repeated below, and let the digital computer solve for the roots.

$$s^4 + 7s^3 + 14s^2 + (8 + 20N_2)s + 20N_1 = 0 \qquad (4\text{-}1)$$

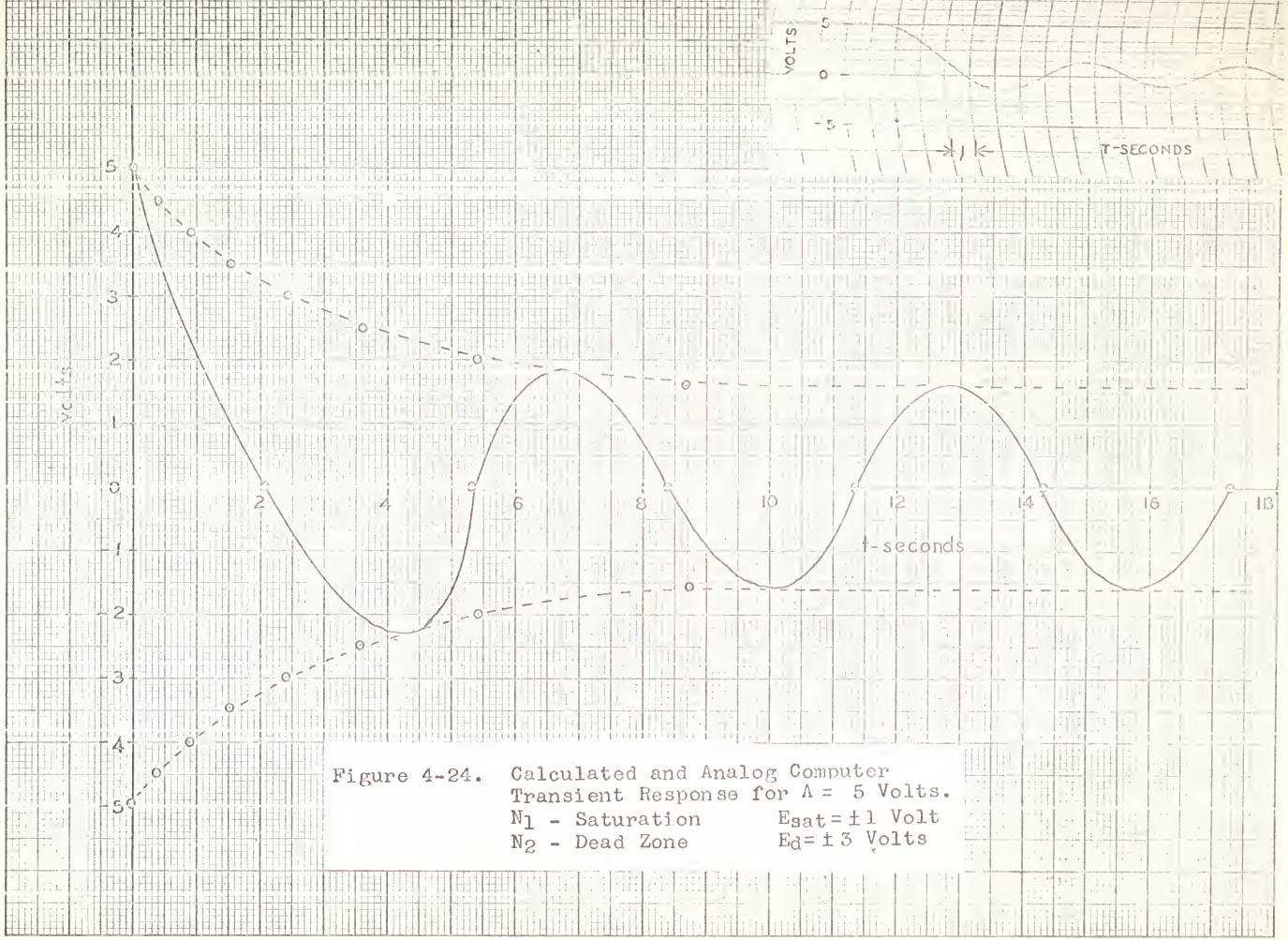

Figure 4-24. Calculated and Analog Computer Transient Response for A = 5 Volts.
N_1 - Saturation $E_{sat} = \pm 1$ Volt
N_2 - Dead Zone $E_d = \pm 3$ Volts

KEUFFEL & ESSER CO. MADE IN U.S.A.

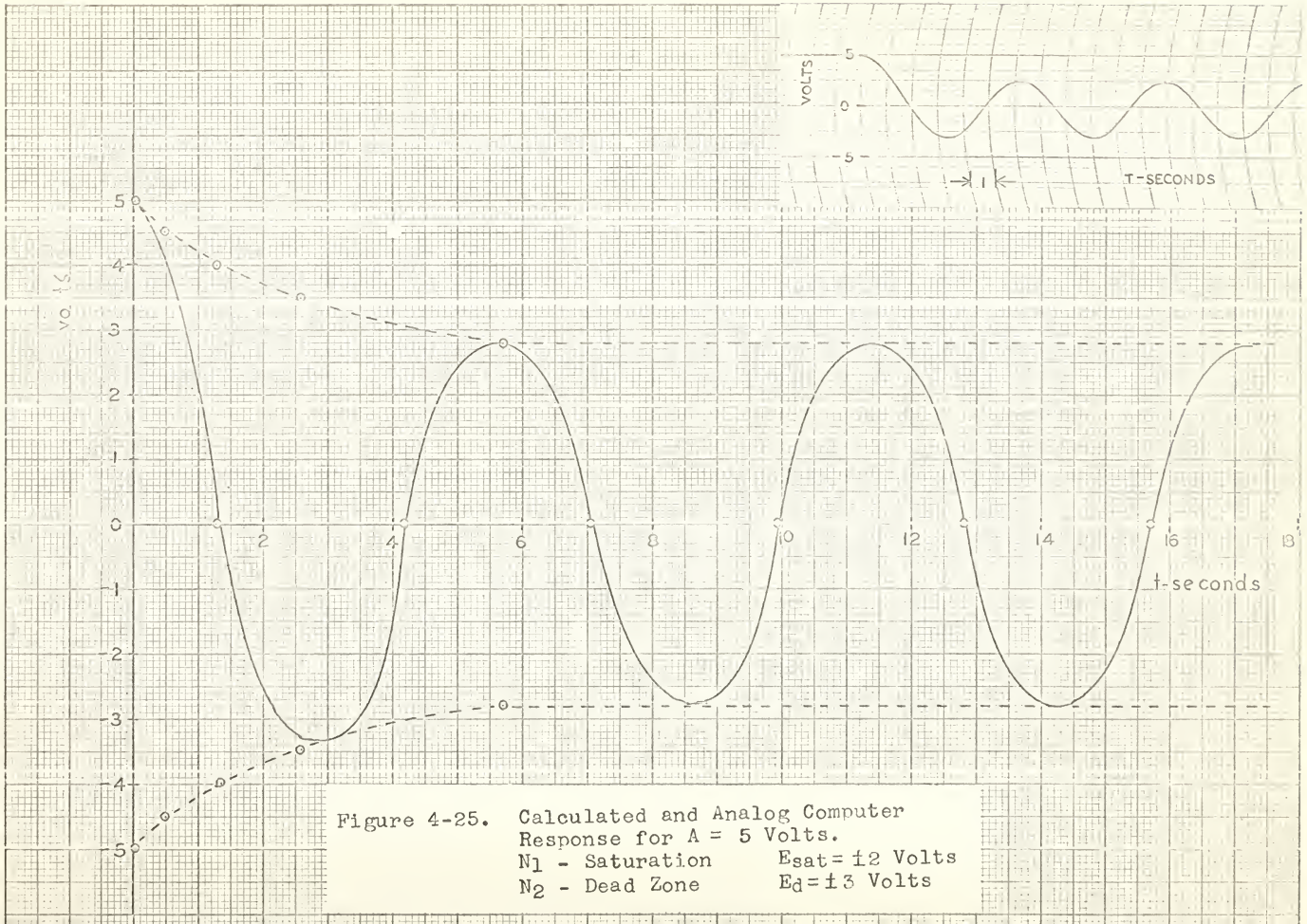

Figure 4-25. Calculated and Analog Computer Response for A = 5 Volts.
N_1 - Saturation $E_{sat} = \pm 2$ Volts
N_2 - Dead Zone $E_d = \pm 3$ Volts

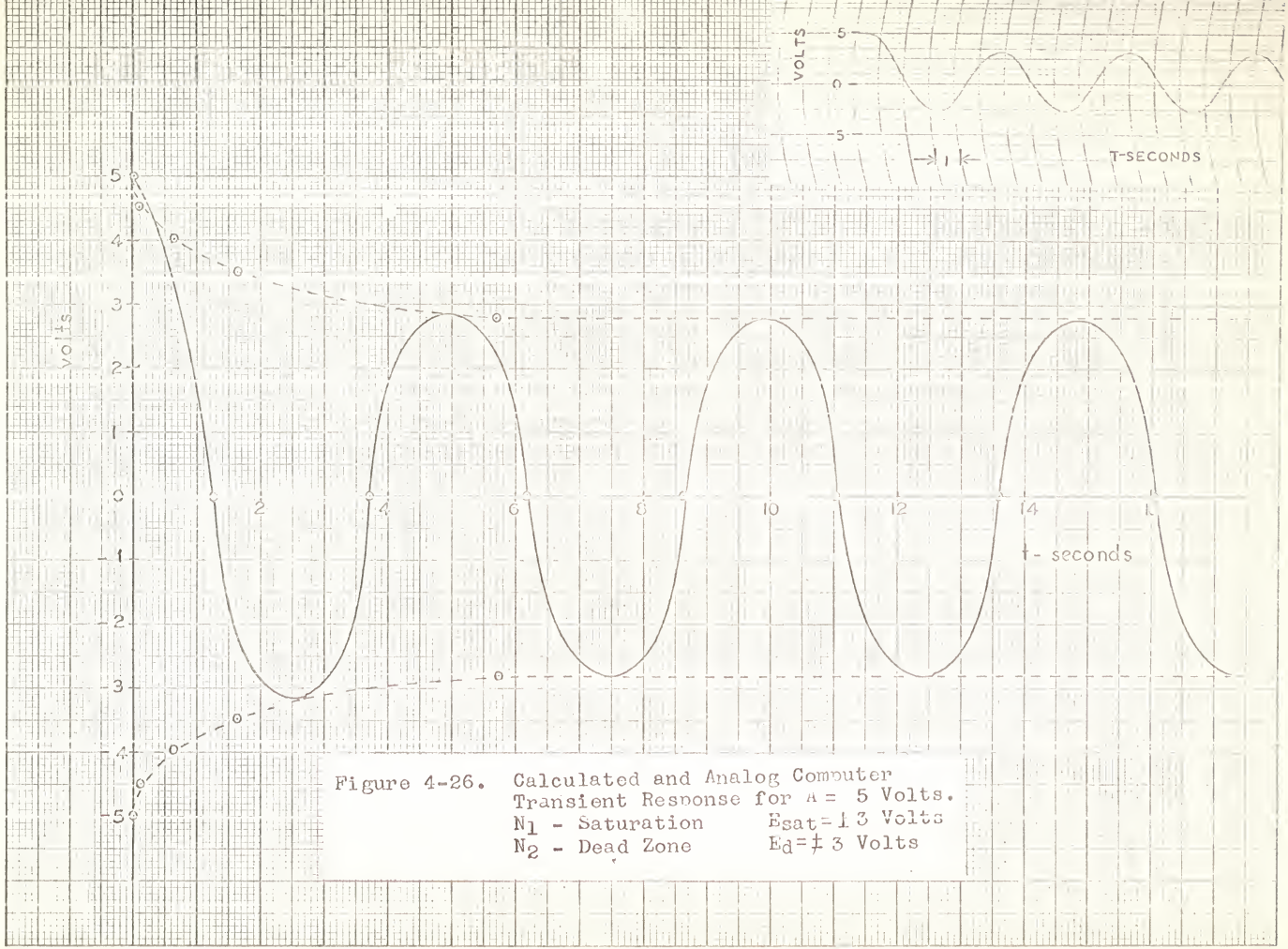

Figure 4-26. Calculated and Analog Computer Transient Response for A = 5 Volts.
N_1 - Saturation $E_{sat} = \pm 3$ Volts
N_2 - Dead Zone $E_d = \pm 3$ Volts

10 X 10 TO THE ½ INCH
KEUFFEL & ESSER CO.
358-12
MADE IN U.S.A.

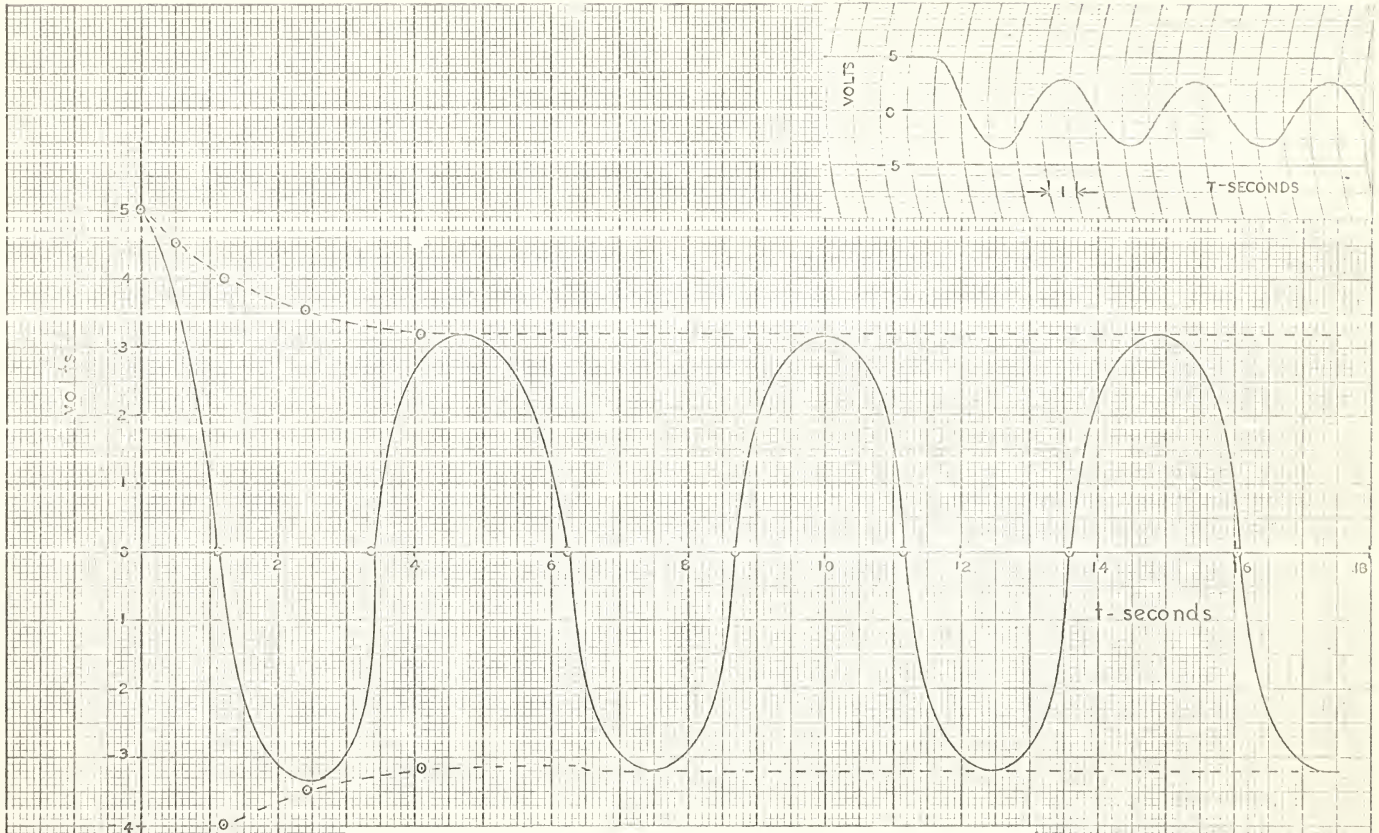

Figure 4-27. Calculated and Analog Computer Transient Response for A = 5 Volts.
N_1 - Saturation $E_{sat} = \pm 5$ Volts
N_2 - Dead Zone $E_d = \pm 3$ Volts

This latter technique was used. When the roots are plotted, we obtain a dynamic root locus plot which determines the system's characteristic roots for each M(α , β) point shown on the dynamic describing function locus. Dynamic root locus plots were made for each of the previously determined dynamic describing function curves from the unstable point to the linear M-point and the intermediate solution points.

4-3-2 Summary of results

Figures 4-28 to 4-33 are the dynamic root locus plots for the indicated examples. Because of the proximity of the plotted points, the identified roots are labelled by A_i, B_i, C_i, and D_i ($i = 1\text{-}4$) which corresponds to the unstable condition, limit cycle, an intermediate value, and the linear M-point respectively. The arrows on the plots denote the direction of decreasing values of A.

In all cases the calculated frequency of the limit cycle points B_i agreed accurately with the dynamic describing function curve prediction. However, as the dominant pair of conjugate roots moved into the left-half plane, the real root effect becomes evident. From these root locus plots the form of the transient solution can be determined at any instant. When two pairs of conjugate complex poles exist, as in the vicinity of points B_i, the form of the output transient solution for an initial condition input is

$$\Theta_0(t) = Ae^{-\zeta\omega_n t}\cos(\omega t + \phi) + Be^{-\sigma_1 t}\cos(\omega t + \phi_1) \qquad (4\text{-}2)$$

If the second term is much smaller than the first, we have essentially second order dominance. When two real roots and a complex pair of conjugate poles exist, as in the vicinity of points C_i, the transient solution

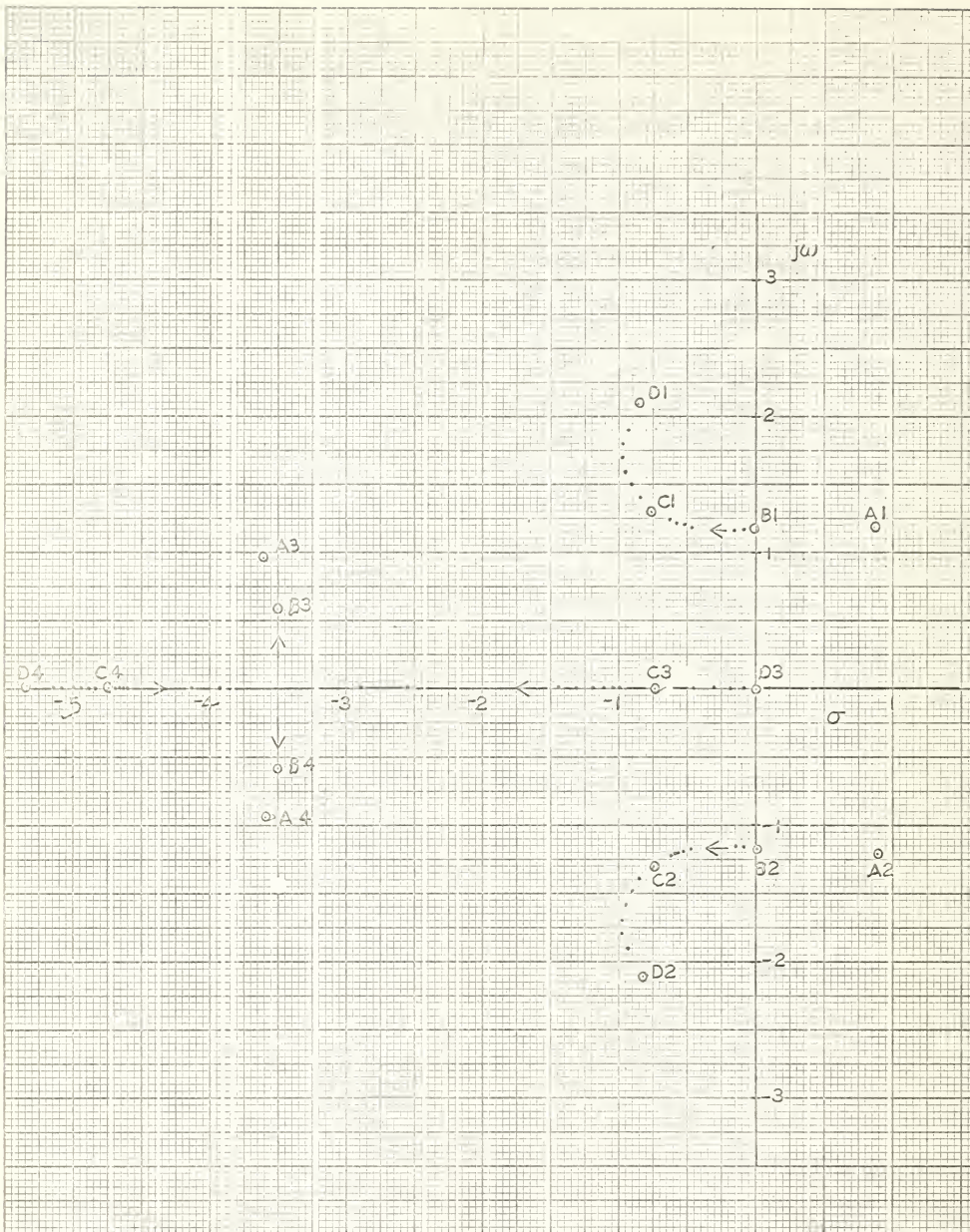

Figure 4-28. Dynamic Root Locus Plot for Figure 4-2.

KEUFFEL & ESSER CO. MADE IN U.S.A.

Figure 4-29. Dynamic Root Locus Plot for Figure 4-12.

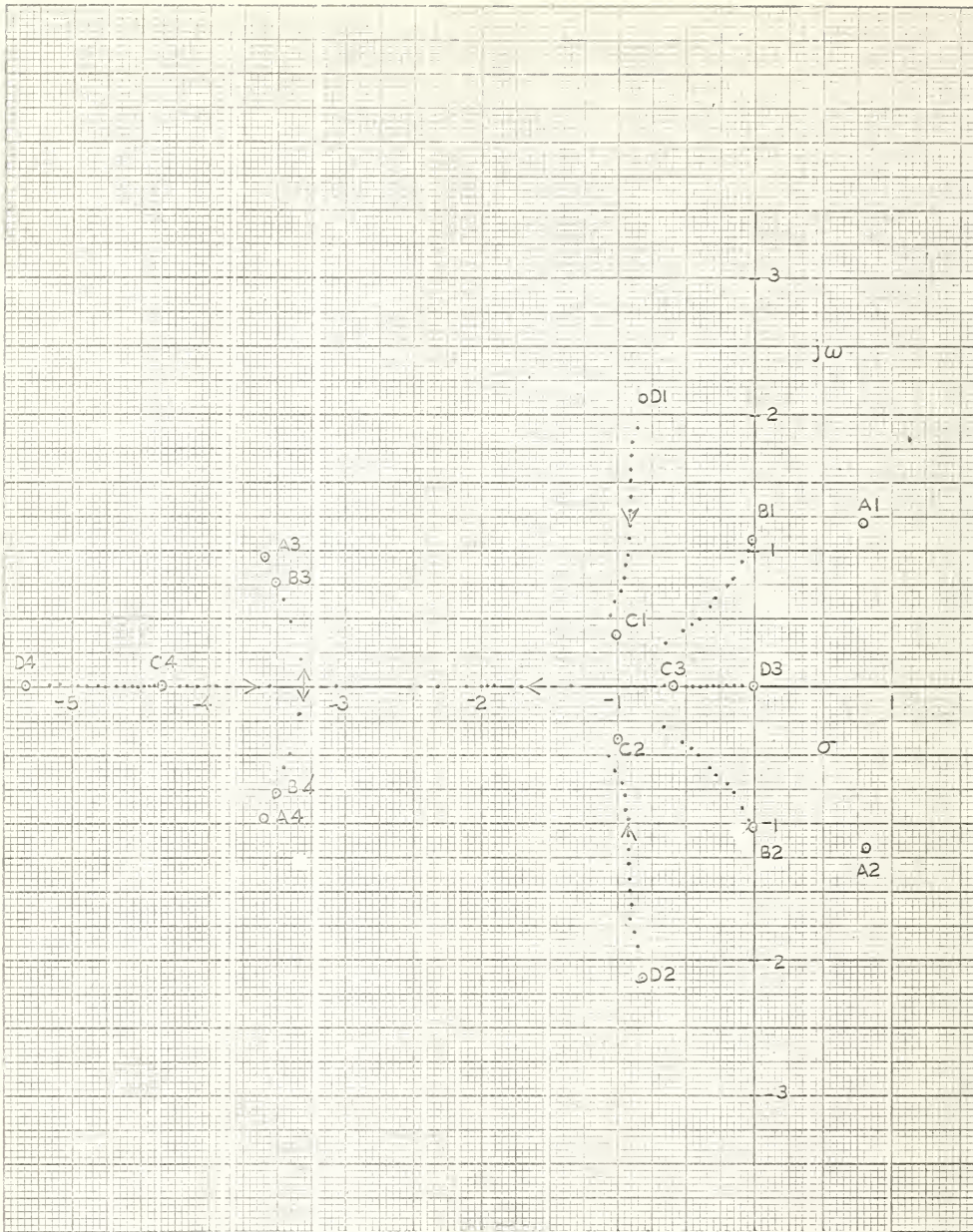

Figure 4-30. Dynamic Foot Locus Plot for Figure 4-22, Curve A.

KEUFFEL & ESSER CO. MADE IN U.S.A.

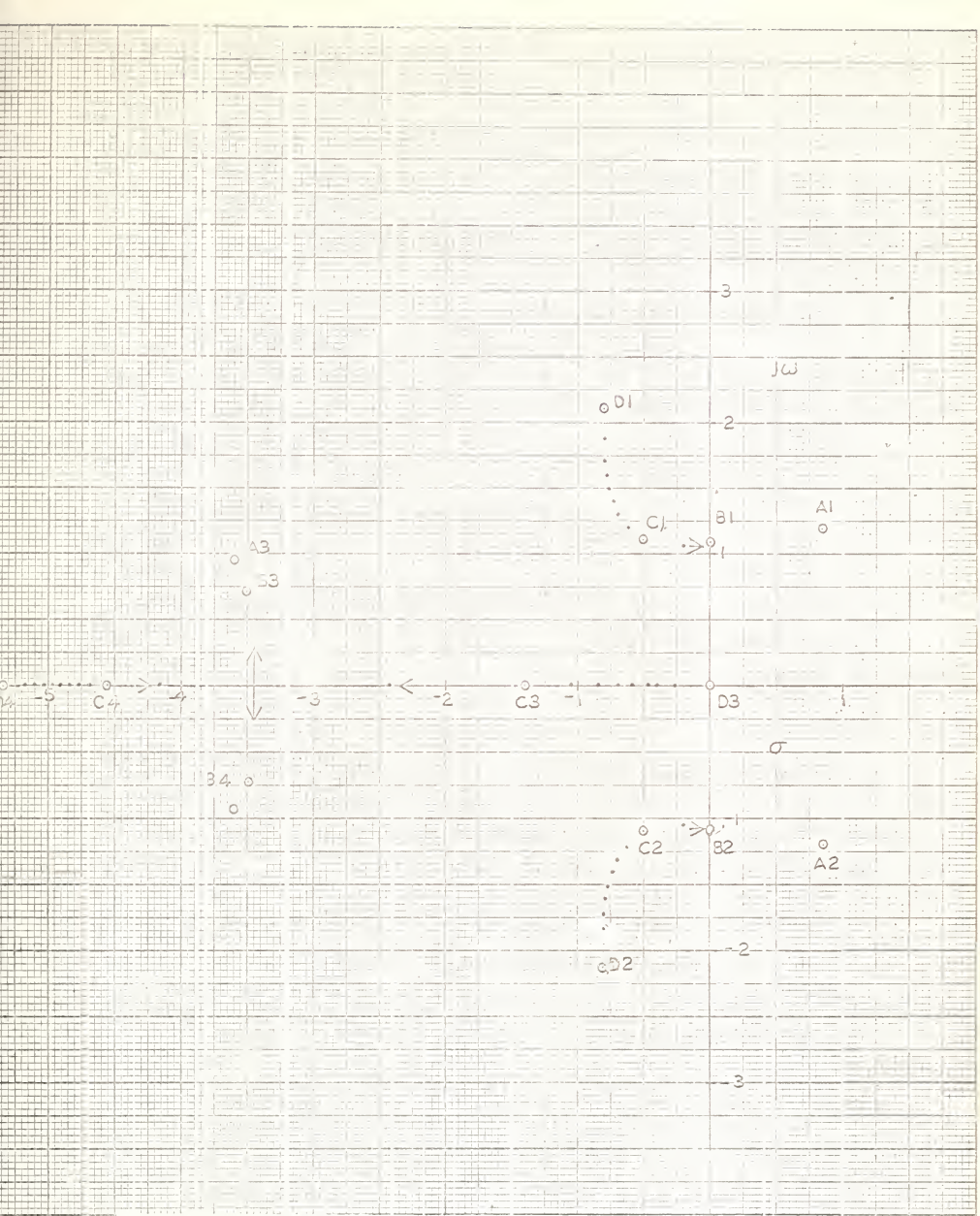

Figure 4-31. Dynamic Root Locus Plot for Figure 4-22, Curve B.

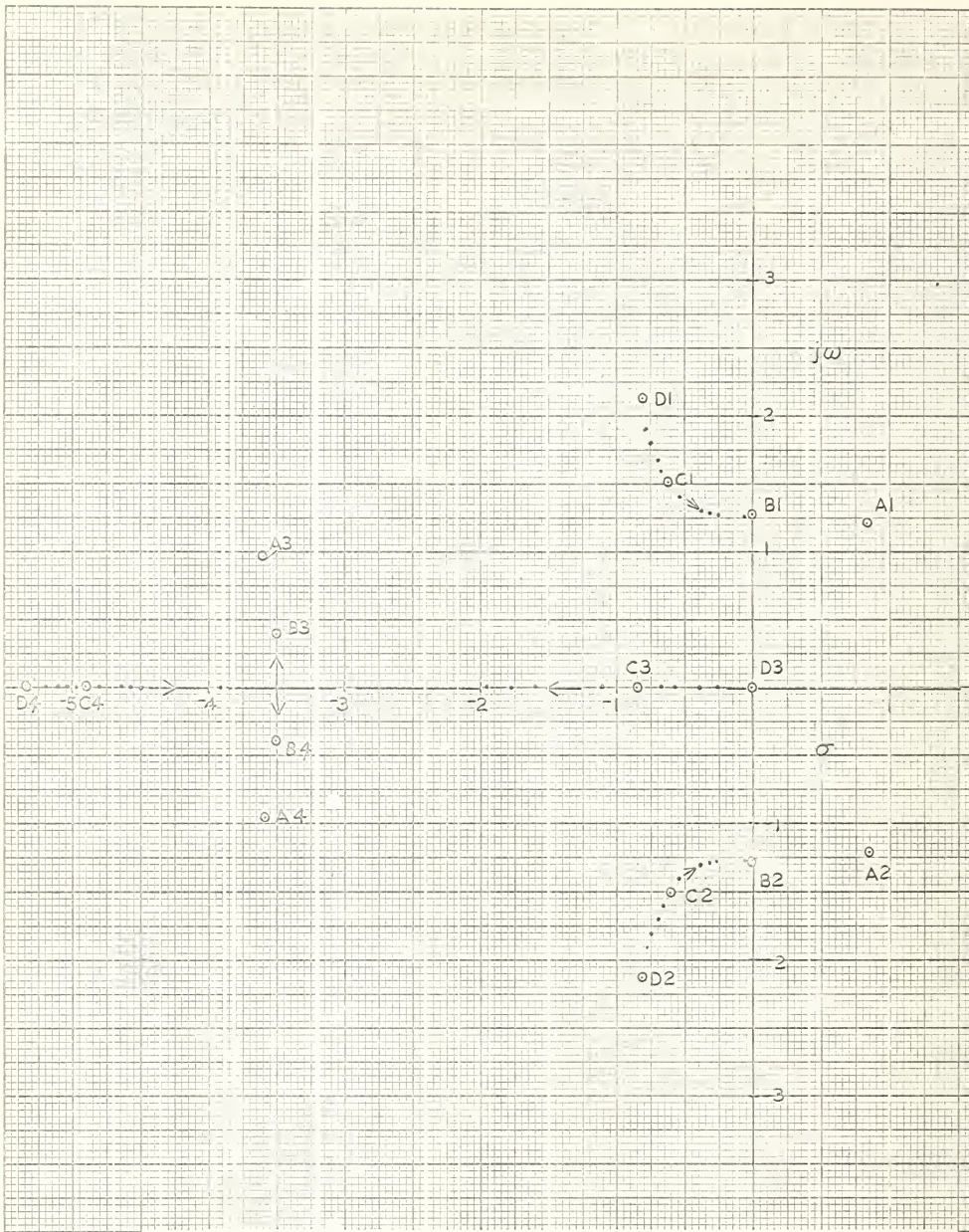

Figure 4-32. Dynamic Root Locus Plot for Figure 4-22, Curve C.

KEUFFEL & ESSER CO. MADE IN U.S.A.

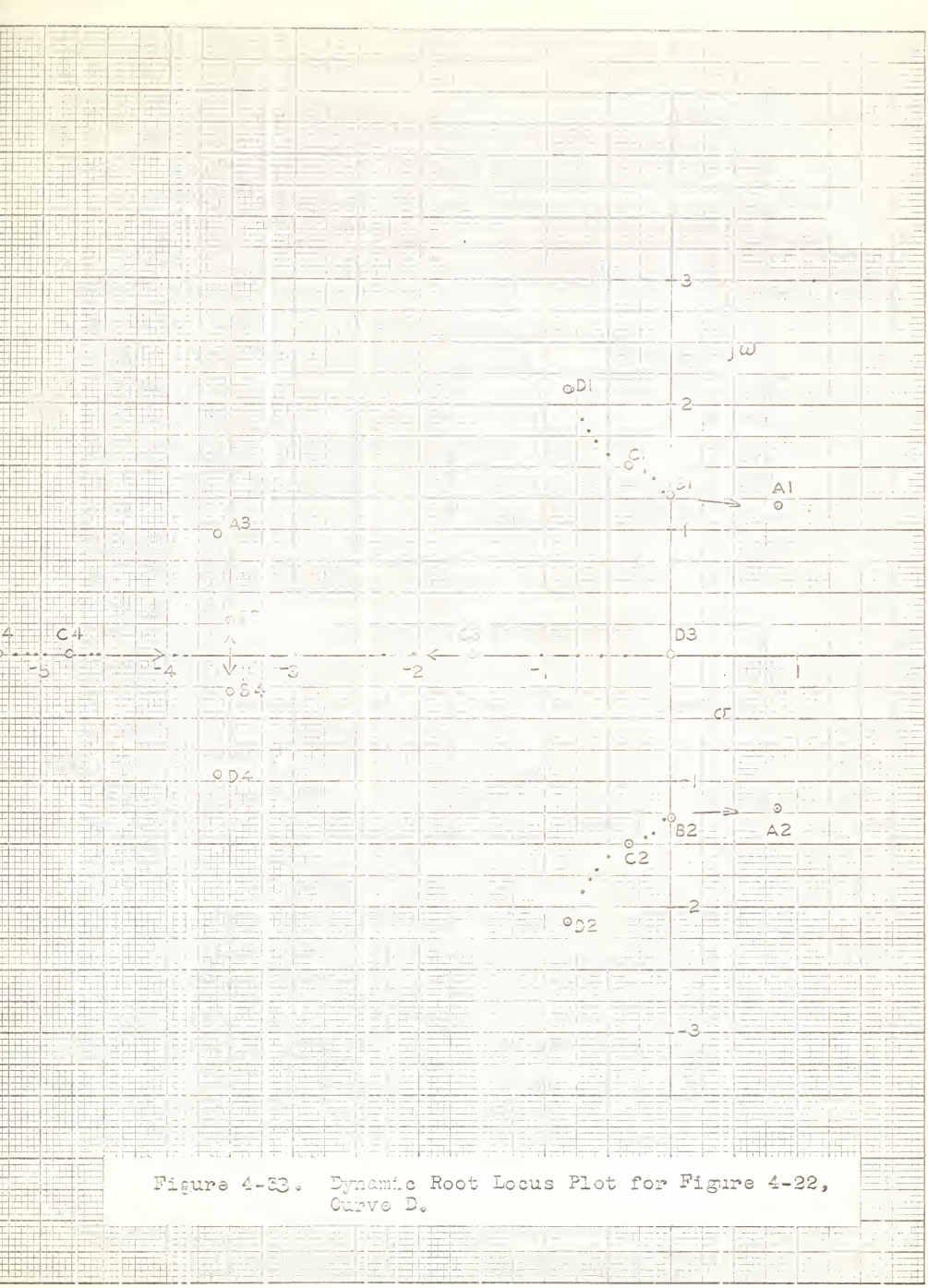

Figure 4-33. Dynamic Root Locus Plot for Figure 4-22, Curve D.

is of the form

$$\theta_0(t) = Ae^{-\zeta\omega_n t}\cos(\omega t + \phi) + Be^{-\sigma_1 t} + De^{-\sigma_2 t} \qquad (4\text{-}3)$$

In this case second order dominance would not be justified unless both real roots, σ_1 and σ_2, were far enough out that their effect is negligible during the transient response. In Figures 4-28 and 4-29 one of the real roots approaches the origin for decreasing values of A which accounts for the real root response from the analog computer. For the other cases in Figures 4-30 to 4-33 the real root effect is not apparent, because the system always approaches a stable limit cycle. The mathematical transient solution could be obtained from the dynamic root locus plot or the dynamic describing function curve by solving a series of differential equations - a tedious and unsatisfactory method.

The reason for the good correspondence between the graphical technique and the analog computer is that several seconds have elapsed before the real root is noticeable. By this time the transient response has decayed to a low value such that only a small, slowly decaying steady state output exists.

CHAPTER V

TWO NONLINEAR ELEMENTS RELATED TO A COMMON SIGNAL BY A NONLINEAR DIFFERENTIAL EQUATION

The third case for relating two nonlinear elements to a common reference signal is more complicated than the previous two cases. A typical example is the single feedback loop system shown in Figure 5-1 where the input signal to N_2 depends upon the characteristics of the nonlinear element, N_1, when both elements are referred to the common signal excitation, A. Both $G_1(s)$ and $G_2(s)$ are assumed to have low frequency filter characteristics so that the requirements for expressing N_1 and N_2 in terms of describing functions are met. This system will first be discussed from a classical viewpoint and lastly related to the parameter plane by a specific example.

5-1 Classical approach

In reference [4] Schiring discusses an approximate method for determining the system stability of nonlinear systems with no theoretical limitations on the number or type of nonlinear elements as long as each element is separated by an adequate low frequency filter. However, when the nonlinear elements number more than two and become functions of both signal amplitude and signal frequency, the amount of trial and error calculation becomes prohibitive so that direct simulation on a computer becomes the only feasible approach to establishing system stability and limit cycles.

If the two nonlinear elements depicted in Figure 5-1 are amplitude-sensitive only, the Bode phase diagram can be used to find the resonant frequency, ω_0. The critical magnitude criterion may be used to

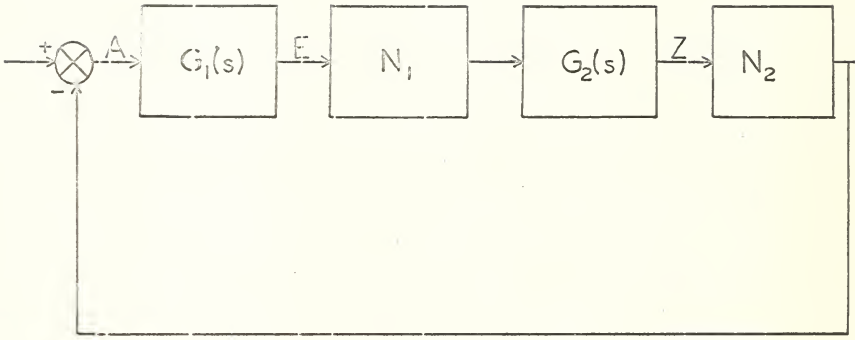

Figure 5-1. Block Diagram of Typical Example for Case 3.

graphically determine the amplitude of the limit cycle i.e.,

$$\left|G_1(j\omega_0)\right| \left|N_1(A)\right| \left|G_2(j\omega_0)\right| = \frac{1}{N_2(A\,N_1\left|G(j\omega_0)\right|)} \qquad (5\text{-}1)$$

Two additional curves above and below this critical amplitude, if it exists, establish the relative stability of the system.

When one or both of the nonlinear elements in this problem have hysteretic or memory-type characteristics, Schiring's method becomes exceedingly tedious because trial and error calculations are required to meet the phase and magnitude relationships. While Shiring's method is time-consuming, it provides accurate results.

5-2 Parameter plane approach

The system analyzed in the preceding section is now analyzed using the parameter plane method which first requires writing the system characteristic equation. As assumed before, N_1 and N_2 are any two general nonlinear elements. The system characteristic equation for Figure 5-1 is

$$1 + G_1(s)N_1G_2(s)N_2 = 0 \qquad (5\text{-}2)$$

The existence of the N_1N_2 product may impose some practical restrictions on the parameter plane method because as noted by Schiring when the product of two describing functions or a composite describing function is used both the amplitude of the input signal and the characteristics of the individual nonlinear elements may limit the accuracy of the results. However, there are no mathematical restrictions on the N_1N_2 product.

When N_1 and N_2 are amplitude-sensitive only, i.e., not functions of

phase, one could let the parameter plane variables take on the values $\alpha = N_1N_2$ and $\beta = K$ the system gain, for example. In this case the system is mathematically reduced to one nonlinear element or a composite describing function where the M - point variations occur in the α or N_1N_2 axis direction.

For the more general case N_1 could be an amplitude-sensitive element and N_2 a memory type or hysteretic element. In this case characteristic equation (5-2) becomes

$$1 + G_1(s)N_1G_2(s)(N_a + jN_b) = 0 \tag{5-3}$$

where $N_2 = N_a + jN_b$ has been expressed in terms of its real and imaginary components. Expanding equation (5-3) results in the expression

$$1 + N_1N_aG_1(s)G_2(s) + jN_1N_bG_1(s)G_2(s) = 0 \tag{5-4}$$

Letting $\alpha = N_1N_a$ and $\beta = N_1N_b$, the general coefficient term, a_k, takes on the form

$$a_k = b_k\alpha + jb_k\beta + d_k \tag{5-5}$$

where the b_k terms are the constant coefficients of the real and imaginary components of the nonlinear elements, and the d_k variables are the constant terms only. Equation (5-5) has been substituted into the general characteristic equation summation, i.e., $f(s) = \sum_{k=0}^{n} a_k sk$ and solved for α and β using Chebyshev functions by Siljak. The following solutions apply:

$$\alpha = -\frac{B_1D_1 + B_2D_2}{B_1^2 + B_2^2}$$

$$\beta = \frac{B_2D_1 - B_1D_2}{B_1^2 + B_2^2} \tag{5-6}$$

where

$$
\begin{aligned}
B_1 &= \sum_{k=0}^{n} (-1)^k b_k \omega_n^k U_{k-1}(\zeta) \\
B_2 &= \sum_{k=0}^{n} (-1)^k b_k \omega_n^k U_k(\zeta) \\
D_1 &= \sum_{k=0}^{n} (-1)^k d_k \omega_n^k U_{k-1}(\zeta) \\
D_2 &= \sum_{k=0}^{n} (-1)^k d_k \omega_n^k U_k(\zeta)
\end{aligned}
\qquad (5\text{-}7)
$$

The $U_k(\zeta)$ terms are Chebyshev functions of the second kind. Equations (5-6) can be readily programmed on the digital computer with the aid of equations (5-7) to obtain curves of constant ζ and ω_n. However, the curves of constant sigma and constant omega derived in section 2-1-2 which use the binomial coefficient expansion will require modification because the implicit assumption of real coefficients is no longer valid.

The $\zeta = 0$ curve obtained from the above relationships can be used to determine the amplitude and frequency of a limit cycle as well as relative stability. Plotting a grid of the variations of N_1N_a and N_1N_b, as functions of A and ω, atop the parameter plane curves will determine the amplitude and frequency of the limit cycle at the common radian frequency intersection on the $\zeta = 0$ curve.

5-3 An example

A specific example, which had been previously worked by Donohue [1], using Schring's method and simulated on the analog computer will now be reworked using the approach outlined in the previous section. Figure 5-2 is a block diagram of the experimental system where N_1 and N_2 are saturation and backlash elements respectively and K is a variable gain. The system characteristic equation is

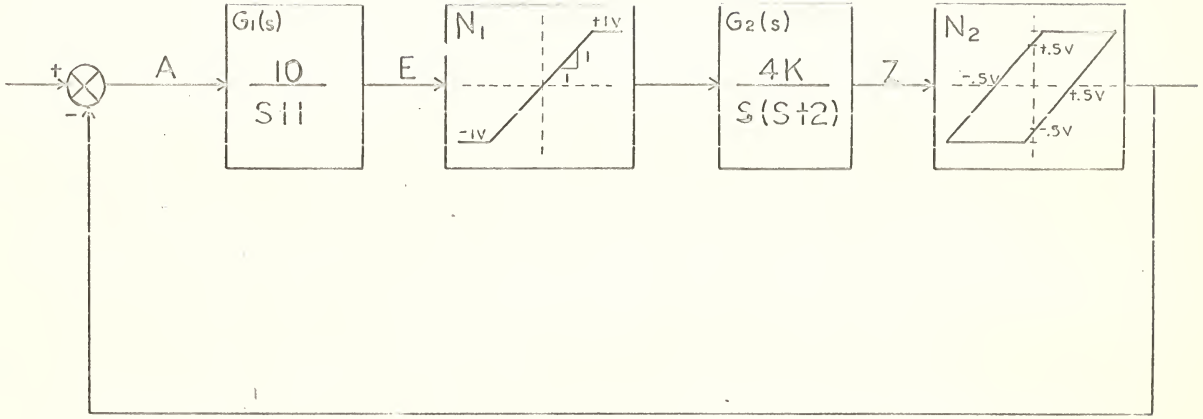

Figure 5-2. Block Diagram of Test Example.

$$s^3 + 3s^2 + 2s + 40K N_1(N_a + jN_b) = 0 \qquad (5\text{-}8)$$

where N_2 has been expressed in terms of its real component, N_a, and imaginary component, N_b. The α variable is selected as N_1N_a and the β variable as N_1N_b.

The variations of N_1N_a versus N_1N_b with respect to signal amplitude, A, and radian frequency, ω , are determined with the aid of describing function theory. Referring to Figure 5-2, the magnitude of the input signal to N_1 is $E = A \left| G_1(j\omega) \right|$ while the magnitude of the input signal to N_2 is $Z = A \left| G_1(j\omega) \right| N_1 \left| G_2(j\omega) \right|$. From the literature, the describing functions for the saturation element, N_1 and the backlash element, N_2, are repeated below.

$$N_1 = \frac{2}{\pi} \left(\sin^{-1} R + R \sqrt{1-R^2} \right) \qquad (5\text{-}9)$$

$$N_2 = Na + jN_b = \frac{2}{\pi} \left(\frac{\pi}{4} + \frac{\Theta}{2} + \frac{\sin 2\Theta}{4} \right) - \frac{j}{\pi} \cos 2\Theta$$

where $R = \frac{1}{E}$ and $\Theta = \sin^{-1} \frac{c}{2}$, c being the value of the projection of the backlash discontinuity on the x-axis. These two equations are readily programmed on the digital computer to obtain a grid of ω -A curves for use with the parameter plane curves. When this net of curves is super-imposed on the parameter plane, the common radian frequency on the $\zeta = 0$ curve will determine the frequency and amplitude of the limit cycle.

The values of K in equation (5-8) were considered in reference [1], namely, K =.15 and K = .25. Figures 5-3 and 5-4 show the $\zeta = 0$ curve for K = .15 and K = .25 respectively. Since the other ζ -curves are not used, they are not shown. The stable region is enclosed by the shaded boundary on the $\zeta = 0$ curve. Along the $\zeta = 0$ curve are indicated the ω values. The lighter lines shown in both plots are the

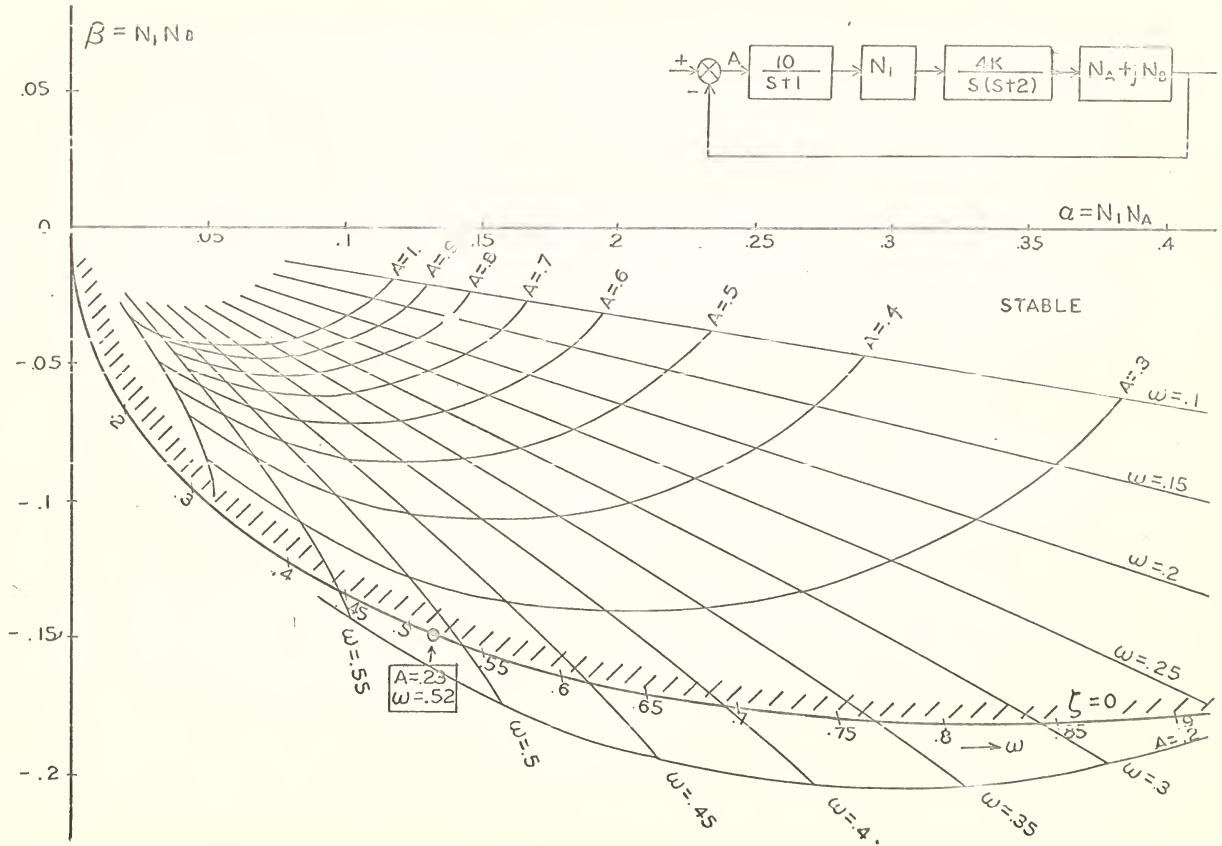

Figure 5-3. Parameter Plane Diagram for Figure 5-2, K = .15.

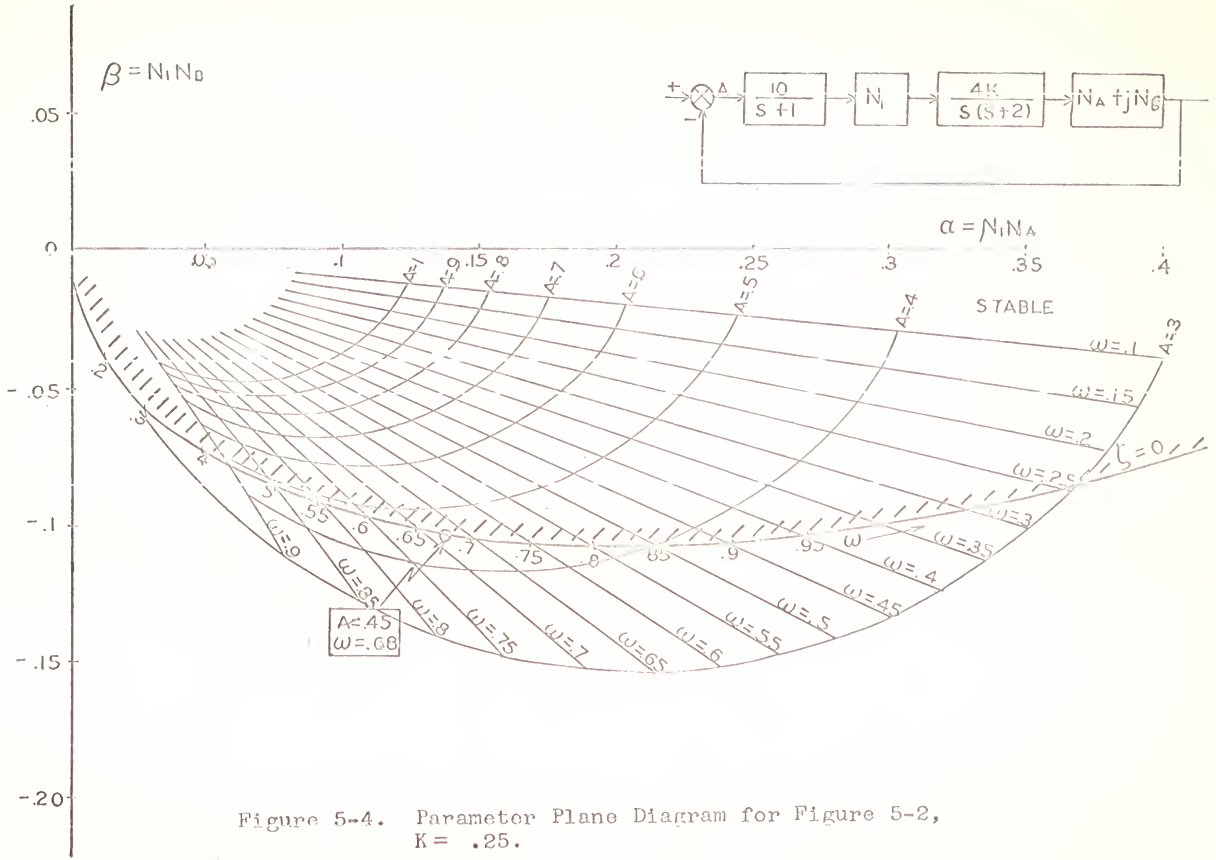

Figure 5-4. Parameter Plane Diagram for Figure 5-2, K= .25.

variations of N_1N_a and N_1N_b with respect to amplitude, A, and radian frequency, ω . The magnitude and frequency of the limit cycle is indicated adjacent to the common radian frequency intersection. Since the magnitude of the limit cycle in reference [1] was determined as the input signal to the backlash element, N_2, it was necessary to multiply the magnitude of the limit cycles indicated in Figures 5-3 and 5-4 by $|G_1(j\omega)|\ N_1\ |G_2(j\omega)|$, where ω is the limit cycle frequency, to obtain the limit cycle magnitude for reference purposes. A comparison of the amplitude and frequency of the limit cycle between the parameter plane approach and the results from reference [1] for K = .15 and K = .25 are tabulated below. The first two rows labelled "Schiring's Method" and "Analog Computer" were obtained from [1]. The results indicated in the last row were obtained from the parameter plane.

K = .15	Amplitude	ω
Schiring's Method	.7 volts	.51
Analog Computer	.8 volts	.49
Parameter Plane	.61 volts	.52

K = .25	Amplitude	ω
Schiring's Method	.9 volts	.69
Analog Computer	1.0 volts	.65
Parameter Plane	.82 volts	.68

It should be noted that excellent correlation results among the three methods. The parameter plane method also predicts a stable limit cycle because the signal amplitudes, A, are decreasing as the $\zeta = 0$ curve is approached from the stable region. This conclusion also agrees

with the theoretical and experimental results from [1].

As already indicated in section 5-1, no attempt will be made to obtain the form of the transient response since the necessarysigma-omega curves using complex coefficients are not available. However, the present example indicates for systems containing two dependent nonlinear elements that the amplitude and frequency of the limit cycle as well as the relative stability can readily be predicted with minimal effort.

CHAPTER VI

CONCLUSIONS

It has been demonstrated that systems containing two nonlinear elements belonging to three general classes can be conveniently handled on the parameter plane. When the parameter plane technique is combined with the "dynamic describing function" curve, three useful pieces of information in varying degrees of utility can be obtained for predicting system performance.

1. The dynamic describing function curve in the parameter plane lying between $0 \leq \zeta \leq 1$ determines the system's stable region.
2. When the dynamic describing function locus crosses the $\zeta = 0$ curve, one can determine the amplitude and frequency of the limit cycle as well as whether a stable or unstable limit cycle exists.
3. From the motion of the M-point along the dynamic describing function locus the transient performance can be closely determined when the following restrictions are satisfied:
   a. Second order dominancy conditions must be met.
   b. The radian frequency, ω, and the damping ratio, ζ, change slowly with time.

As in any investigative study, the analysis and synthesis of nonlinear systems on the parameter plane is far from completion. From this preliminary study, several interesting problems arose which are deemed worthy of further investigation.

A. Closed loop frequency response

As already noted the dynamic describing function curve describes the motion of the operating point during the transient period. In reference [7] the closed loop frequency response is obtained for a single nonlinear element with the aid of the Nichol's chart. A question that immediately arises is the possibility of obtaining the closed loop frequency response of a system containing two nonlinear elements from its dynamic describing function curve. The main difference is that the dynamic describing function locus considers a series of points rather than a single point at a time.

B. Transient response prediction

The graphical technique used in this thesis requires second order dominance as a necessary condition for practical application. Since the possibility of real roots increases greatly with higher order systems, a modification to the present technique which incorporates this real root effect would greatly improve the accuracy of predicting nonlinear transient performance.

C. Constant sigma-omega curves with complex coefficients

The recursion relationships used to obtain the constant sigma-omega curves made the implicit assumption that the coefficients of the characteristic equation were real. Since the coefficients become complex when hysteretic or memory type element are introduced into a nonlinear system, an immediate requirement is that the previously determined recursion relationship be modified or rederived.

CHAPTER VII

BIBLIOGRAPHY

1. Donohue, D. P., "EE 416 Project." U. S. Naval Postgraduate School, 1964.

2. MacAllister, A. J., "Transient Analysis of Nonlinear Feedback Control Systems." Ph.D. Thesis, Cornell University, 1961.

3. Nutting R. M., "Parameter Plane Techniques for Feedback Control Systems." M. S. Thesis, U. S. Naval Postgraduate School, 1965.

4. Schiring, E. E., "Effect of Saturation on the Dynamic Response of a Class of Bang-Bang Control Systems." Ph.D. Thesis, University of Pittsburgh, 1963.

5. Šiljak, D. D., "Analysis and Synthesis of Feedback Control Systems in the Parameter Plane, Part I, Linear Continuous Systems, Part III, Nonlinear Systems," IEEE Transactions on Applications and Industry, Nov. 1964.

6. Šiljak, D. D., "Analysis of Transient Oscillations in the Parameter Plane." Unpublished paper, University of Santa Clara, 1966.

7. Thaler, G. J. and Pastel, M. P., Analysis and Design of Nonlinear Feedback Control Systems. McGraw-Hill Book Co. Inc., 1962.

8. Wilson, P. L., "Use of Mitrovic's Method in Predicting Limit Cycles in Feedback Control Systems with One and Two Gain Variable Nonlinearities." M. S. Thesis, U. S. Naval Postgraduate School, 1964.

9. Yockey, H. M. and Thaler, G. J., "Analysis of a Control System with Two Nonlinearities." Unpublished paper, U. S. Naval Postgraduate School, 1965.

APPENDIX A

GRAPHICAL METHOD FOR DETERMINING THE TRANSIENT RESPONSE

A graphical technique, developed by Šiljak [6], was used for determining the transient response of a system from its dynamic describing function curve. This technique, which is accurate for second order dominance conditions, considers the amplitude of the initial conditions along the dynamic describing function curve as forming the envelope of the transient response. At each M-point the graphical value of ζ and ω from the zeta-omega curves or σ and ω from the sigma-omega curves are read. The zero signal crossings are determined from the phase relationship $\phi = \int \omega \, dt$. For an initial condition input the first zero crossing is assumed to occur in $\pi/2$ radians and subsequent zero crossings in multiples of π radians. The following example assumes an initial condition, A = 3 volts, for the describing function curve appearing in Figures 4-2 and 4-3.

A-1 Transient response from zeta-omega curves

The system transient response can be determined for the dynamic describing function curve on the zeta-omega curves using the following method. Initially, a curve of A vs ζ, Figure A-1, and A vs ω_n, Figure A-2 are plotted using the amplitude values indicated alongside the dynamic describing function curve in Figure 4-2, and the values of ζ and ω_n passing through these points. At each point the values of ω_n are obtained from the relationship $\omega = \omega_n \sqrt{1 - \zeta^2}$

From these curves values of A, ζ, and ω_n are tabulated in Table 2 incrementally from 3 volts.

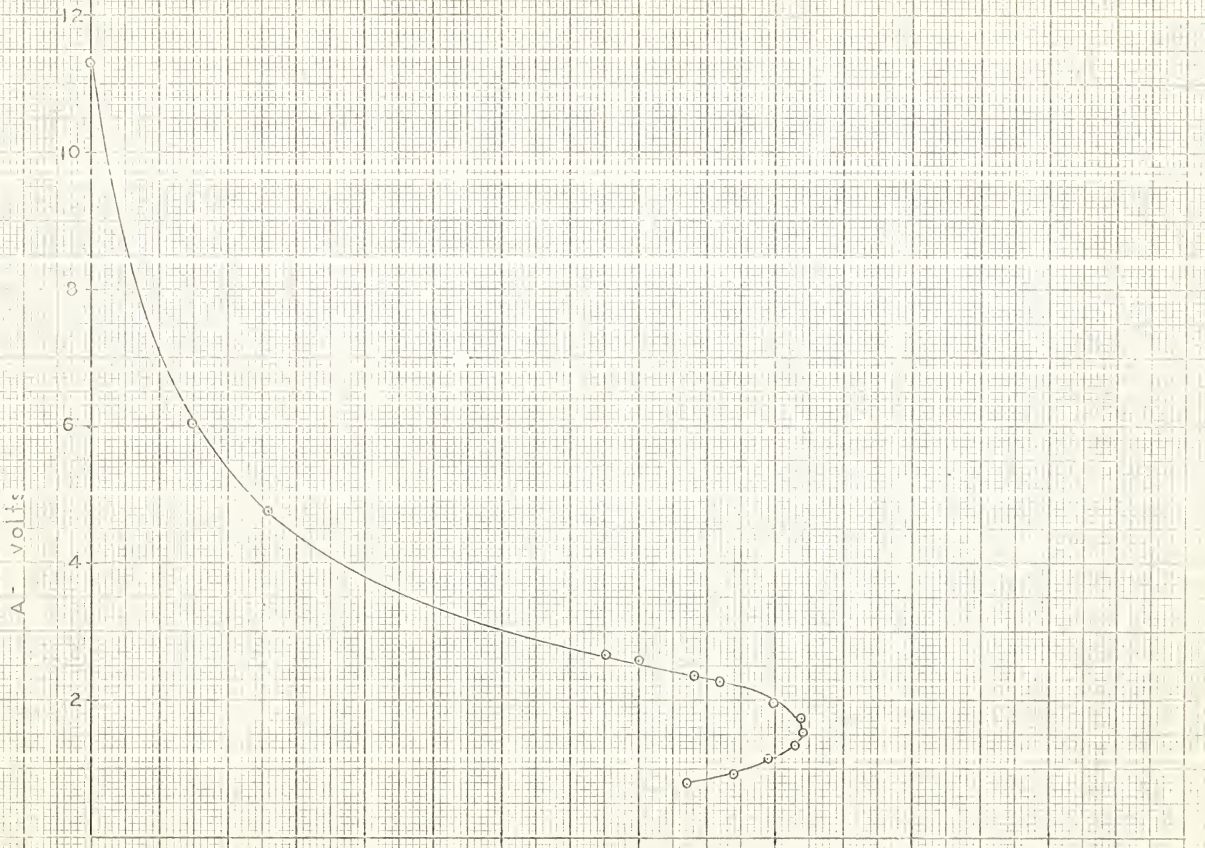

Figure A-1. A vs ζ.

Figure A-2. A vs ω_h.

Table 2. Data for Calculating Transient Responses from Zeta-Omega Curves.

	A	ζ	ω_n	$\zeta\omega_n$	τ	ω	t
A0	3.0	.3	1.22	.366	2.73	1.07	0
A1	2.5	.4	1.29	.516	1.94	1.08	.45
A2	2.0	.5	1.5	.75	1.33	1.3	.85
A3	1.5	.52	1.76	.915	1.09	1.5	1.15
A4	1.0	.475	2.01	.955	1.05	1.77	1.5
A5	.8	.435	2.11	.918	1.09	.9	1.65
A6	0.0						2.36

The reciprocal of $\zeta\omega_n$ gives the incremental exponential time decay, τ. Starting with A0 = 3 volts, the first exponential decay, approximated by τ = 2.73, is assumed to extend along a short portion of the straight line until A1 = 2.5 volts. Here the procedure is repeated for point A1 using a new τ = 1.94. When the response reaches zero or a steady state value, the plot is terminated as in Figure A-3. At each point the time is read from the abscissa and tabulated in Table A-1. Converting ω_n to ω, a plot of ω vs. time is made as in Figure A-4. By graphical integration the zero crossings at $\frac{\pi\tau}{2}$, $\pi\tau$, $2\pi\tau$, etc. are determined.

The final plot uses the amplitude envelope determined from Figure 4-3 and the zero crossings from Figure A-4, to sketch the transient response shown in Figure A-5.

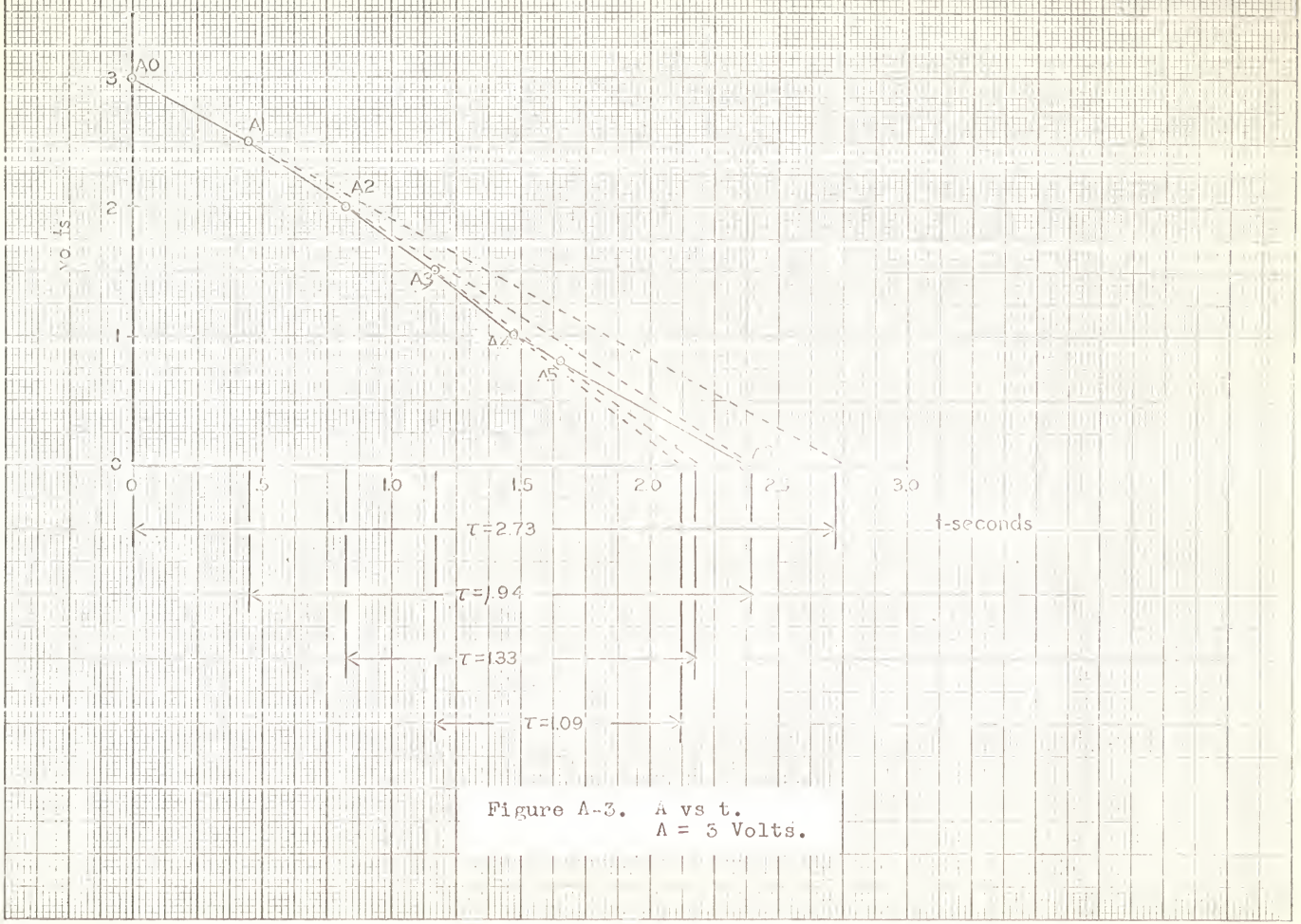

Figure A-3. A vs t.
A = 3 Volts.

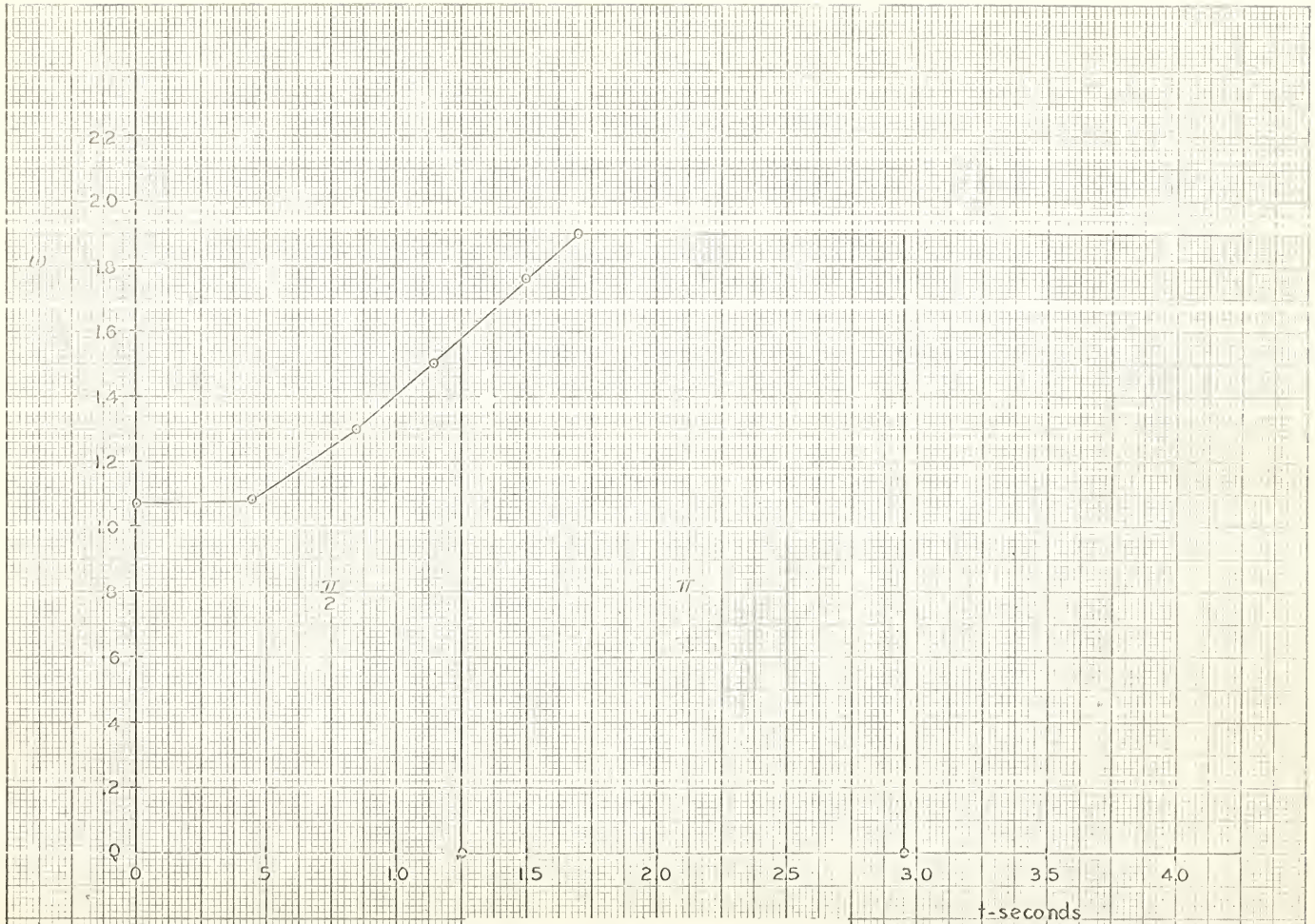
2.2
2.0
1.8
1.6
1.4
1.2
1.0
.8
.6
.4
.2
0
0
.5
1.0
1.5
2.0
2.5
3.0
3.5
4.0
t-seconds
π/2
π

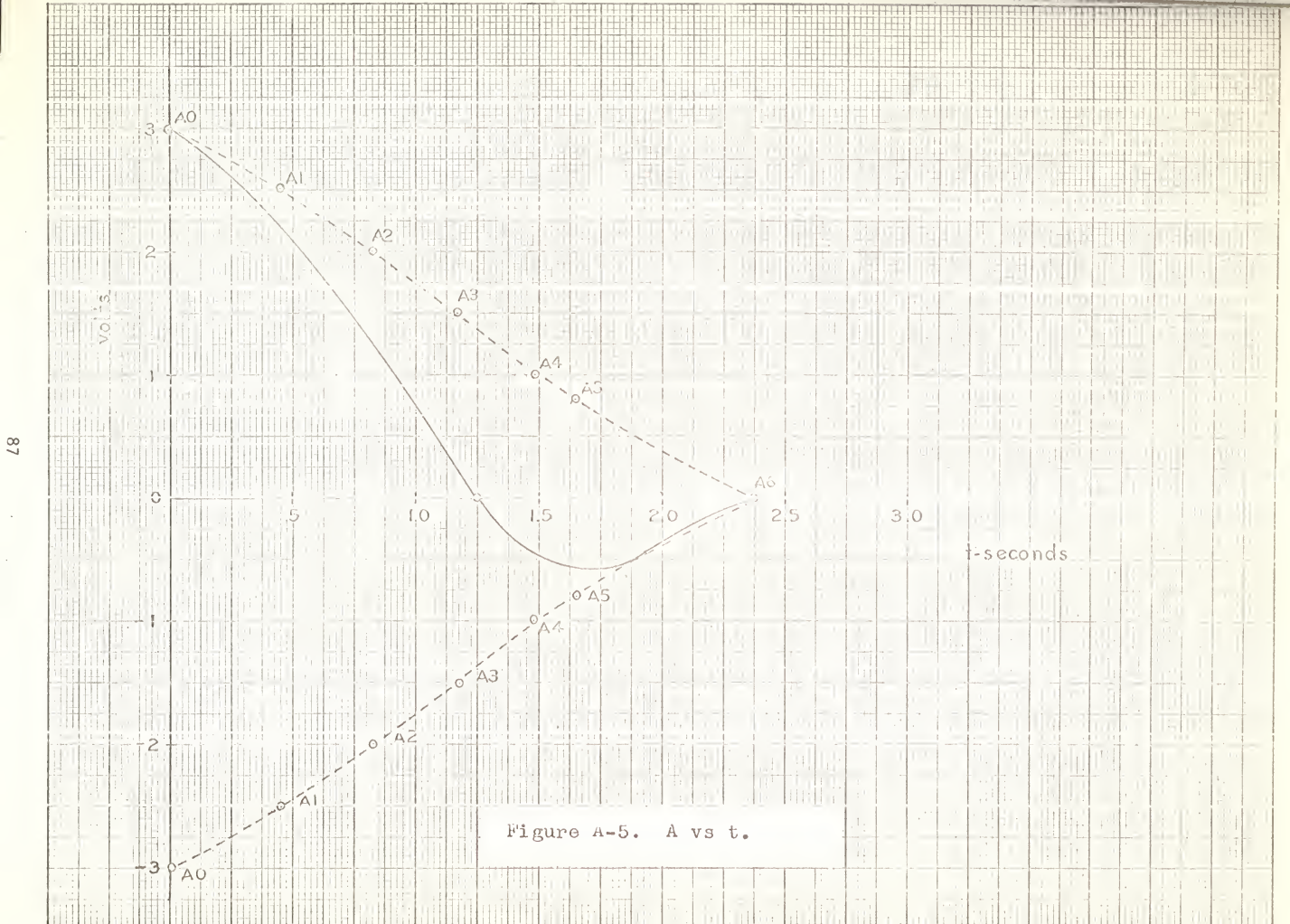

Figure A-5. A vs t.

A-2 Transient response from sigma-omega curves

When sigma-omega curves are available, the transient response can be determined more rapidly because the conversion of ω to ω_n and vice versa are avoided by the simple expedient of using constant sigma curves where $\zeta\omega_n = \sigma$ vice constant zeta curves. The previous example is reworked using the corresponding sigma-omega curves appearing in Figure 4-3. The indicated values of A, and the values of sigma and omega passing through these points are used to plot curves of A vs σ and A vs ω which appear in Figures A-6 and A-7 respectively. These curves are used to tabulate the following table for values of A selected in one-half volt increments from three volts.

Table 3. Data for Calculating Transient Response from Sigma-Omega Curves.

	A	σ	τ	ω	t
A0	3.0	.35	2.86	1.18	.0
A1	2.5	.54	1.85	1.2	.475
A2	2.0	.75	1.33	1.3	.85
A3	1.5	.92	1.09	1.5	1.175
A4	1.0	.95	1.05	1.8	1.52
A5	.5	.9	1.11	1.98	2.05
A6	.0				3.16

The values of sigma and omega are read from their respective charts. The exponential decay is now the reciprocal of sigma and is denoted by the column marked τ. Commencing with A = 3 volts, the envelope is assumed to exist along the tangential line terminated by τ = 2.86 until A = 2.5 volts is reached. Time is read along the x-axis and the

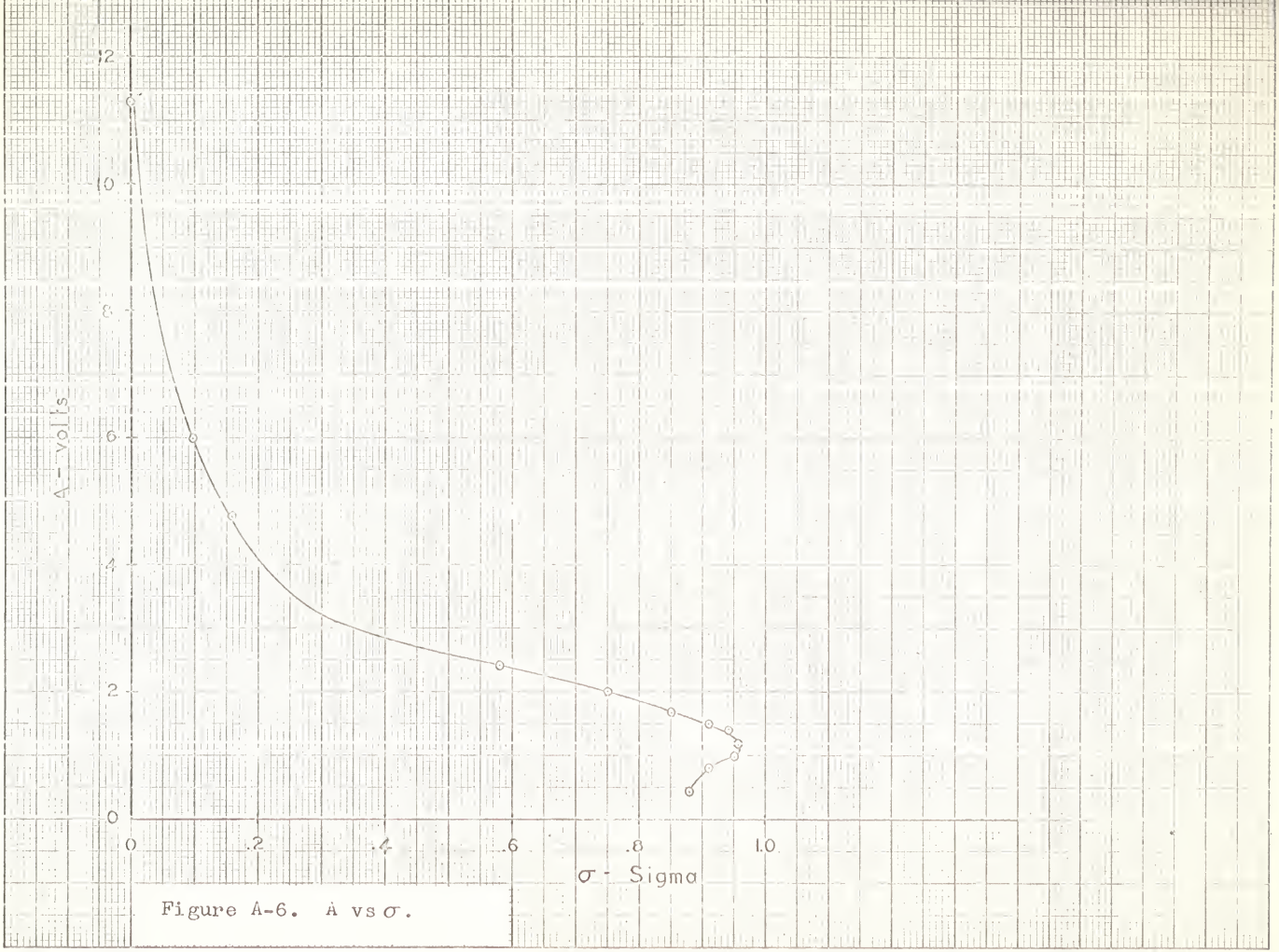

Figure A-6. A vs σ.

Figure A-7 A vs ω

Figure A-8. A vs t.
A = 3 Volts.

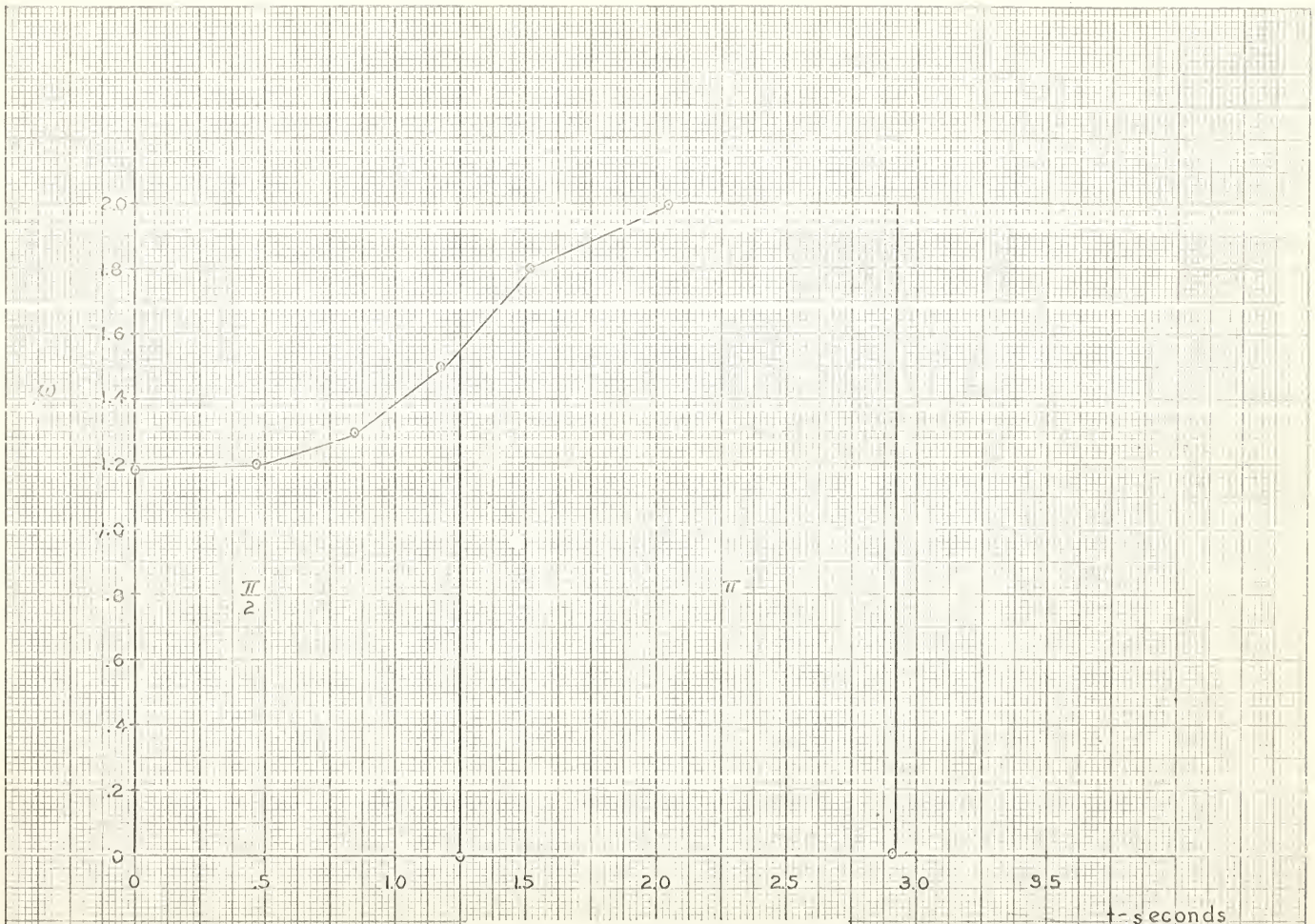

Figure A-9. ω vs t.

Figure A-10. A vs t.

procedure repeated for the remaining points as shown in Figure A-8. To obtain the zero crossings a plot of ω vs t is made (Figure A-9), and by graphical integration the zero crossings are determined. The overall transient response appearing in Figure A-10 is a composite plot of the signal envelope determined in Figure A-8 and the zero crossings in Figure A-9.

A visual comparison of the two transient responses, namely, Figures A-5 and A-10 shows that the calculated transient responses agree closely. There is a small difference in the terminal end point of the plots but this is an insignificant matter. The important point is that both methods can predict the form of the transient response - but accurately only under second order dominancy conditions. In addition, the use of sigma-omega curves increases the rapidity of this graphical technique because needless conversions are eliminated.

APPENDIX B

DIGITAL COMPUTER PROGRAM FOR PLOTTING CONSTANT ZETA-SIGMA-OMEGA CURVES

A digital computer program was written in FORTRAN 60 for use on the CDC 1604 computer to plot the curves of constant zeta, sigma, or omega used in this thesis. The comment cards at the beginning of the program indicate how to use the computer program.

```
..JOB0413F, PELLEGRINI C A
      PROGRAM PARAM C
C     THIS PROGRAM IS APPLICABLE TO POLYNOMIALS WHOSE COEFFICIENTS ARE
C     OF THE FORM (B*ALPHA + C*BETA + D) WHERE ALPHA AND BETA ARE
C     VARIABLE PARAMETERS AND B, C, AND D ARE CONSTANTS.
C     THIS PROGRAM WILL PLOT ON ONE 9 INCH BY 15 INCH GRAPH,PARAMETER
C     PLANE CURVES OF THE FOLLOWING TYPE. CONSTANT ZETA CURVES AS A
C     FUNCTION OF OMEGA(N),(THE STARTING VALUE OF OMEGA AND THE NUMBER
C     OF DECADES THAT OMEGA WILL SPAN WILL BE SPECIFIED IN THE DATA
C     CARDS), CONSTANT SIGMA CURVES AS A FUNCTION OF OMEGA, AND CONSTANT
C     OMEGA LINES AS A FUNCTION OF SIGMA. THE VALUES OF ZETA FOR THE
C     CONSTANT ZETA CURVES, THE VALUES OF SIGMA FOR THE CONSTANT SIGMA
C     CURVES, AND THE VALUES OF OMEGA FOR THE CONSTANT OMEGA CURVES MAY
C    ,BE SPECIFIED IN THE DATA CARDS. IF HOWEVER NO CURVES OF A CERTAIN
C     TYPE ARE DESIRED PLACE A ZERO IN THE APPROPRIATE COLUMN CORRESPOND
C     ING TO THE NUMBER OF CURVES. IN THIS CASE SUBMIT A BLANK CARD FOR
C     THE CURVE VALUES.
C     ALL CURVES ARE PLOTTED ON THE SAME GRAPH.
C     TH X-AXIS VARIABLE IS ALPHA,AND THE Y-AXIS VARIABLE IS BETA.
C     THE FOLLOWING SYMBOLS ARE PERTINENT TO THE PROGRAM.
C     ND-THE NUMBER OF DECADES SPANNED BY OMEGA FOR THE CONSTANT ZETA
C     CURVES AND THE CONSTANT SIGMA CURVES.
C     NO-THE ORDER OF THE EQUATION, NZ, NS, AND NW -THE NUMBER OF CON-
C     STANT ZETA,SIGMA,AND OMEGA CURVES RESPECTIVELY, IXUP-DISTANCE IN
C     INCHES OF THE X-AXIS FROM THE BOTTOM OF THE GRAPH, IYRIGHT- THE
C     DISTANCE IN INCHES OF THE Y-AXIS FROM THE LEFT SIDE OF THE GRAPH,
C     LABZ, LABS, LABW - THE LABELS FOR THE CONSTANT ZETA,SIGMA, AND OMEGA
C     CURVES, WN - THE STARTING VALUE OF OMEGA FOR THE CONSTANT ZETA AND
C     CONSTANT SIGMA CURVES, BJ,CJ,DJ, - ALPA,BETA, AND CONSTANT
C     COEFFICIENTS RESPECTIVELY.
C     THE DATA CARDS ARE SUBMITTED IN THE FOLLOWING MANNER.
C     CARD 1 THE FIRST LINE OF THE GRAPH TITLE (IN COLUMNS 1-48)
C     CARD 2 THE SECOND LINE OF THE GRAPH TITLE (IN COLUMNS 1-48)
C     CARD 3 IN 8I10 FORMAT ENTER FROM LEFT TO RIGHT
C       ND        NO        NZ        NS        NW      IXUP   IYRIGHT
C     CARD 4 IN COLUMN 10 ENTER A 1 IF PRINTOUT IS DESIRED. LEAVE BLANK
C     IF NO PRINTOUT IS DESIRED.
```

```
C      CARD 5 LABZ(20A4 FORMAT), LEAVE BLANK IF NZ=0
C      CARD 6 LABS(20A4 FORMAT), LEAVE BLANK IF NS=0
C      CARD 7 LABW(20A4 FORMAT), LEAVE BLANK IF NW=0
C      CARD 8 VALUES OF ZETA FOR CONSTANT ZETA CURVES. (8E10.5 FORMAT)
C      CARD 9 VALUES OF SIGMA FOR CONSTANT SIGMA CURVES (8E10.5 FORMAT)
C      CARD 10 VALUES OF OMEGA FOR CONSTANT OMEGA CURVES (8E10.5 FORMAT)
C      CARD 11 CONSTANT COEFFICIENTS IN ASCENDING ORDER (8E10.5 FORMAT)
C      CARD 12 ALPHA COEFFICIENTS IN ASCENDING ORDER (8E10.5 FORMAT)
C      CARD 13 BETA COEFFICIENTS IN ASCENDING ORDER (8E10.5 FORMAT)
C      CARD 14 WN (F10.5 FORMAT)
C      CARD 15 XSCALE (F10.5 FORMAT, USE 1 SIGNIFICANT FIGURE)
C      CARD 16 YSCALE (E10.5 FORMAT, USE 1 SIGNIFICANT FIGURE)
       DIMENSION A(350),B(350),ITITLE(12),ZETA(100),LABZ(100),SIGMA(100)
      1,LABS(100),W(100),LABW(100),BJ(350),CJ(350),DJ(350),AG(350),
      2 BG(350)
  250 FORMAT(1H1,17HTHE INPUT DATA IS,////)
 1485 CONTINUE
       PRINT 250
  200 FORMAT (6A8)
       READ 200,(ITITLE(I),I=1,5)
       READ 200,(ITITLE(I),I=7,12)
       PRINT 200,(ITITLE(I),I=1,6)
       PRINT 200,(ITITLE(I),I=7,12)
  251 FORMAT(//,8X, 2HND,8X, 2HNO, 8X, 2HNZ, 8X, 2HNS,8X, 2HNW, 6X,
      14HIXUP, 3X, 7HIYRIGHT,//)
       PRINT 251
  203 FORMAT(8I10)
       READ 203,ND,NO,NZ,NS,NW,IXUP,IYRIGHT
       NC=NO+1
       PRINT 203,ND,NO,NZ,NS,NW,IXUP,IYRIGHT
  463 FORMAT (//,4X,6HIPRINT,//)
       PRINT 463
  464 FORMAT (I10)
       READ 464, IPRINT
       PRINT 464,IPRINT
       AIXUP = IXUP
```

```
      AIYRGHT=IYRIGHT
  252 FORMAT (//, 4HLABZ. //)
      PRINT 252
  205 FORMAT(20A4)
      READ 205,(LABZ(M),M=1,NZ)
      PRINT 205,(LABZ(M),M=1,NZ)
  207 FORMAT (//////,4HLABS,//)
      PRINT 207
      READ 205,(LABS(M),M=1,NS)
      PRINT 205,(LABS(M),M=1,NS)
  208 FORMAT(//////, 4HLABW,//)
      PRINT 208
      READ 205,(LABW(M),M=1,NW)
      PRINT 205,(LABW(M),M=1,NW)
  206 FORMAT(8E10.5)
  210 FORMAT(//////,4HZETA,//)
      PRINT 210
      READ 206,(ZETA(M),M=1,NZ)
      PRINT 206, (ZETA(M),M=1,NZ)
  872 FORMAT(//////,5HSIGMA,//)
      PRINT 872
      READ 206,(SIGMA(M),M=1,NS)
      PRINT 206,(SIGMA(M),M=1,NS)
  212 FORMAT (//////, 1HW,//)
      PRINT 212
      READ 206, (W(M),M=1,NW)
      PRINT 206,(W(M),M=1,NW)
  214 FORMAT(//////, 37HCONSTANT COEFFICIENTS ASCENDING ORDER,//)
      PRINT 214
      READ 206,(DJ(N),N=1,NC)
      PRINT 206,(DJ(N),N=1,NC)
  215 FORMAT(//////,34HALPHA COEFFICIENTS ASCENDING ORDER,//)
      PRINT 215
      READ 206,(BJ(N),N=1,NC)
      PRINT 206,(BJ(N),N=1,NC)
  216 FORMAT(//////,33HBETA COEFFICIENTS ASCENDING ORDER,//)
      PRINT 216
```

```
      READ 206,(CJ(N),N=1,NC)
      PRINT 206,(CJ(N),N=1,NC)
  217 FORMAT (//////,22HINITIAL VALUE OF OMEGA,//)
      PRINT 217
  199 FORMAT(E10.5)
      READ 199,W0
      PRINT 199, W0
  218 FORMAT(//////, 6HXSCALE,//)
      PRINT 218
      READ 199,XSCALE
      PRINT 199,XSCALE
  418 FORMAT(//////,6HYSCALE,//)
      PRINT 418
      READ 199,YSCALE
      PRINT 199,YSCALE
      ROG=.5+AIYRGHT
      DAV=.5+AIXUP
      AROG=-ROG*XSCALE
      ADAV=-DAV*YSCALE
      ROGE=9.5-AIYRGHT
      DAVE=15.5-AIXUP
      AROGE=ROGE*XSCALE
      ADAVE=DAVE*YSCALE
      FRAN=-AIYRGHT*XSCALE
      CHEK=-AIXUP*YSCALE
      GO TO (61,62,63,64,65,66,67,68,69,70),ND
   61 G=1.0076
      GO TO 41
   62 G=1.016
      GO TO 41
   63 G=1.0245
      GO TO 41
   64 G=1.0312
      GO TO 41
   65 G=1.0394
      GO TO 41
   66 G=1.0483
```

```
      GO TO 41
   67 G=1.0568
      GO TO 41
   68 G=1.0633
      GO TO 41
   69 G=1.071
      GO TO 41
   70 G=1.078
   41 CONTINUE
      AG(1)=0.0
      BG(1)=0.0
      AG(2) = XSCALE
      BG(2)=0.0
      LABEL=4H
      CALL DRAW (2,AG,BG,1,0,LABEL,ITITLE,XSCALE,YSCALE,IXUP,IYRIGHT,
     12,2,9,15,0,LAST)
      IF(NZ) 42,42,601
  601 IF (IPRINT) 448, 448, 221
  221 FORMAT (1H1,//////, 20HCONSTANT ZETA CURVES,//)
      PRINT 221
  222 FORMAT(//,15X,5HALPHA,16X,4HBETA,15X,5HOMEGA,16X,4HZETA,//)
      PRINT 222
  448 MOD=2
      DO 22 M=1,NZ
      J=0
      JG=
      WNA=W0
      DO 7 L=1,300
      D1=0.0
      D2=0.0
      C1=0.0
      C2=0.0
      B1=0.0
      B2=0.0
      DO 18 N=1,NC
      K=N-1
      IF(K)2,3,2
```

```
    3 U=0.0
      U1=-1.0
    2 U2=2.0*ZETA(M)*U-U1
      D1=(-1.0)**K*DJ(N)*WNA**K*U1+D1
      D2=(-1.0)**K*DJ(N)*WNA**K*U+D2
      C1=(-1.0)**K*CJ(N)*WNA**K*U1+C1
      C2=(-1.0)**K*CJ(N)*WNA**K*U+C2
      B1=(-1.0)**K*BJ(N)*WNA**K*U1+B1
      B2=(-1.0)**K*BJ(N)*WNA**K*U+B2
      U1=U
   18 U=U2
      Z=1.0E-60
      IF(ABSF(B1*C2-B2*C1)-Z)35,35,39
   35 GO TO 7
   39 J=J+1
      A(J)=(C1*D2-C2*D1)/(B1*C2-B2*C1)
      B(J)=(B2*D1-B1*D2)/(B1*C2-B2*C1)
      IF(IPRINT)449,449,1002
 1003 FORMAT(4E20.5)
 1002 PRINT 1003,A(J),B(J),WNA,ZETA(M)
  449 IF(FRAN-A(J)) 104,104,7
  104 IF(A(J)-AROGE)114,114,7
  114 IF(CHEK-B(J)) 106,106,7
  106 IF(B(J)-ADAVE)107,107,7
  107 JG=JG+1
      AG(JG)=A(J)
      BG(JG)=B(J)
    7 WNA=G*WNA
      CALL DRAW(JG,AG,BG,MOD,0,LABZ(M),ITITLE,XSCALE,YSCALE,IXUP,
     1IYRIGHT,2,2,9,15,0,LAST)
   22  CONTINUE
    42 IF(NS)704,704,705
  705 IF(IPRINT)446,446,220
  220 FORMAT(1H1,//////,21HCONSTANT SIGMA CURVES,//)
      PRINT 220
  527 FORMAT(//,15X,5HALPHA,16X,4HBETA,15X,5HOMEGA,16X, 5HSIGMA,//)
      PRINT 527
```

```
446 MOD=2
    DO 5 M=1,NS
    J=0
    JG=
    WNA=W0
    DO 49 L=1,300
    D1=DJ(1)*1.0-DJ(2)*SIGMA(M)
    D2=-DJ(1)*0.0+DJ(2)*WNA
    C1=CJ(1)*1.0-CJ(2)*SIGMA(M)
    C2=-CJ(1)*0.0+CJ(2)*WNA
    B1=BJ(1)*1.0-BJ(2)*SIGMA(M)
    B2=-BJ(1)*0.0+BJ(2)*WNA
    X0=1.0
    X1=SIGMA(M)
    Y0=0.0
    Y1=WNA
    DO 10 N=3,NC
    K=N-2
    X2=2.0*SIGMA(M)*X1-(SIGMA(M)*SIGMA(M)+WNA*WNA)*X0
    Y2=2.0*SIGMA(M)*Y1-(SIGMA(M)*SIGMA(M)+WNA*WNA)*Y0
    D1=(-1.0)**(K+1)*DJ(N)*X2+D1
    D2=(-1.0)**K*DJ(N)*Y2+D2
    C1=(-1.0)**(K+1)*CJ(N)*X2+C1
    C2=(-1.0)**K*CJ(N)*Y2+C2
    B1=(-1.0)**(K+1)*BJ(N)*X2+B1
    B2=(-1.0)**K*BJ(N)*Y2+B2
    X0=X1
    X1=X2
    Y0=Y1
 10 Y1=Y2
    Z=1.0E-60
    IF(ABSF(B1*C2-B2*C1)-Z)11,11,12
 11 GO TO 49
 12 J=J+1
    A(J)=(C1*D2-C2*D1)/(B1*C2-B2*C1)
    B(J)=(B2*D1-B1*D2)/(B1*C2-B2*C1)
    IF(IPRINT)447,447,2000
```

```
1001 FORMAT(5E20.5)
2000 PRINT 1001,A(J),B(J),WNA,SIGMA(M)
 447 IF(FRAN-A(J))777,777,49
 777 IF(A(J)-AROGE)778,778,49
 778 IF(CHEK-B(J)) 779,779,49
 779 IF(B(J)-ADAVE)800,800,49
 800 JG=JG+1
     AG(JG)=A(J)
     BG(JG)=B(J)
  49 WNA=G*WNA
     CALL DRAW (JG,AG,BG,MOD,0,LABS(M),ITITLE,XSCALE,YSCALE,IXUP,
    1IYRIGHT,2,2,9,15.0,LAST)
   5 CONTINUE
 704 IF(NW)1006,1006,702
 702 IF(IPRINT)459,459,223
 223 FORMAT(1H1,21HCONSTANT OMEGA CURVES,//)
     PRINT 223
 224 FORMAT (15X,5HALPHA,16X,4HBETA,15X,5HSIGMA,15X, 5HOMEGA,//)
     PRINT 224
 459 DO 24 M=1,NW
     J=0
     JG=
     SIGMI=0.0
     DO 25 L=1,300
     D1=DJ(1)*1.0-DJ(2)*SIGMI
     D2=-DJ(1)*0.0+DJ(2)*W(M)
     C1=CJ(1)*1.0-CJ(2)*SIGMI
     C2=-CJ(1)*0.0+CJ(2)*W(M)
     B1=BJ(1)*1.0-BJ(2)*SIGMI
     B2=-BJ(1)*0.0+BJ(2)*W(M)
     X0-1.0
     X1=SIGMI
     Y0=0.0
     Y1=W(M)
     DO 26 N=3,NC
     K=N-2
     X2=2.0*SIGMI*X1-(SIGMI*SIGMI+W(M)*W(M))*X0
```

```
      Y2=2.0*SIGMI*Y1-(SIGMI*SIGMI+W(M)*W(M))*Y0
      D1=(-1.0)**(K+1)*DJ(N)*X2+D1
      D2=(-1.0)**K*DJ(N)*Y2+D2
      C1=(-1.0)**(K+1)*CJ(N)*X2+C1
      C2=(-1.0)**K*CJ(N)*Y2+C2
      B1=(-1.0)**(K+1)*BJ(N)*X2+B1
      B2=(-1.0)**K*BJ(N)*Y2+B2
      X0=X1
      X1=X2
      Y0=Y1
   26 Y1=Y2
      IF(ABSF(B1*C2-B2*C1)-Z)25,25,30
   30 J=J+1
      A(J)=(C1*D2-C2*D1)/(B1*C2-B2*C1)
      B(J)=(B2*D1-B1*D2)/(B1*C2-B2*C1)
      IF(IPRINT)460,460,461
  461 PRINT 1001,A(J),B(J),SIGMI,W(M)
  460 IF(FRAN-A(J))100,100,25
  100 IF(A(J)-AROGE)101,101,25
  101 IF(CHEK-B(J))102,102,25
  102 IF(B(J)-ADAVE)103,103,25
  103 JG=JG+1
      AG(JG)=A(J)
      BG(JG)=B(J)
   25 SIGMI=SIGMI+.01
      CALL DRAW(JG,AG,BG,MOD,0,LABW(M),ITITLE,XSCALE,YSCALE,IXUP,
     1IYRIGHT,2,2,9,15,0,LAST)
   24 CONTINUE
 1006 AG(1)=0.0
      BG(1)=0.0
      AG(2)=XSCALE
      BG(2)=0.0
      LABEL=4H
      CALL DRAW(2,AG,BG,3,0,LABEL,ITITLE,XSCALE,YSCALE,IXUP,IYRIGHT,
     12,2,9,15,0,LAST)
      GO TO 1485
      END
      END
```

```
C A PELLEGRINI  ZETA-SIGMA-OMEGA CURVES
S**4 + 7S**3 + 14S**2 + (8+20N2)S + 20N1 = 0
          3          4         10          8         11          0          0
          1
Z0. Z.1 Z.2 Z.3 Z.4 Z.5 Z.6 Z.7 Z.8 Z.9
S0. S.1 S.2 S.3 S.4 S.5 S.6 S.7
61. W1.1W1.2W1.3W1.4W1.5W1.6W1.7W1.8W1.9W2.
 .0         .1         .2         .3         .4         .5         .6         .7
.8         .9
 .0         .1         .2         .3         .4         .5         .6         .7
1.0        1.1        1.2        1.3        1.4        1.5        1.6        1.7
1.8        1.9        2.0
 .0        8.0       14.0        7.0        1.0
20.0
          20.0
.1
.1
```

INITIAL DISTRIBUTION LIST

		No. Copies
1.	Defense Documentation Center Cameron Station Alexandria, Virginia 22314	20
2.	Library U. S. Naval Postgraduate School, Monterey, Calif.	2
3.	Chief, Bureau of Ships Code Department of the Navy Washington, D. C. 20360	1
4.	Prof. G. J. Thaler Department of Electrical Engineering U. S. Naval Postgraduate School Monterey, Calif.	10
5.	LT Charles A. Pellegrini 37 Work Avenue Monterey, California	1
6.	Prof. D. D. Šiljak Department of Electrical Engineering University of Santa Clara Santa Clara, Calif. 95053	1
7.	Prof. Toyomi Ohata Electrical Department, Defense Academy Obaradai, Yokosuka, Japan	1
8.	LT H. H. Choe Electrical Department, ROKN Naval Academy Chinhae, Korea	1
9.	LT C. H. Hyon Electrical Department, ROKN Naval Academy Chinhae, Korea	1
10.	Dr. K. W. Han Institute of Electronics National Chiao-Tung University Hsinchu, Taiwan	1

11. Dr. S. H. Liu — 1
P. O. Box 1
Shih-yi-Fen
Lungtan, Taiwan

12. Mr. R. Kogge — 1
Code LF
U. S. Naval Ordnance Laboratory
White Oaks, Silver Springs, Maryland 20910

13. CDR R. L. Ashford — 1
U. S. Naval Ordnance Laboratory
White Oaks, Silver Springs, Maryland 20910

14. LT Floyd Hollister — 1
U. S. Naval Electronics Laboratory
San Diego, California 92152

15. LT A. R. Miller — 1
U. S. Naval Mine Defense Laboratory
Panama City, Florida 32402

16. LT H. M. Yockey — 1
U.S.S. SIRAGO (SS-485)
% FPO
New York, N. Y. 09501

17. Dr. Z. Slawsky — 1
U. S. Naval Ordnance Laboratory
White Oaks, Silver Springs, Maryland 20910

18. Mr. Walt Blumburg — 1
U. S. Naval Marine Engineering
Annapolis, Maryland 21402

19. Mr. Seltzer — 1
Code R - ASTR - NG
NASA George Marshall Space Flight Center
Huntsville, Alabama 35812

20. Mr. D. R. Towill — 1
Welsh College of Advanced Technology
Cathays Park, Cardiff, Wales.

DOCUMENT CONTROL DATA - R&D

(Security classification of title, body of abstract and indexing annotation must be entered when the overall report is classified)

1. ORIGINATING ACTIVITY *(Corporate author)*
U. S. Naval Postgraduate School
Monterey, California

2a. REPORT SECURITY CLASSIFICATION
Unclassified

2b. GROUP

3. REPORT TITLE
An Investigation of Nonlinear System Performance on the Parameter Plane

4. DESCRIPTIVE NOTES *(Type of report and inclusive dates)*
M. S. Thesis - Engineering Electronics - 1966

5. AUTHOR(S) *(Last name, first name, initial)*
Pellegrini, Charles, A., Lieutenant, U. S. Navy

6. REPORT DATE	7a. TOTAL NO. OF PAGES	7b. NO. OF REFS
May 1966	118	9

8a. CONTRACT OR GRANT NO.	9a. ORIGINATOR'S REPORT NUMBER(S)
b. PROJECT NO.	
c.	9b. OTHER REPORT NO(S) *(Any other numbers that may be assigned this report)*
d.	

10. AVAILABILITY/LIMITATION NOTICES
Foreign announcement and dissemination of this report by DDC is not authorized.

11. SUPPLEMENTARY NOTES	12. SPONSORING MILITARY ACTIVITY
	Bureau of Ships

13. ABSTRACT

Control systems containing two nonlinear elements are separated into three broad classes which are dependent upon the location of an initial signal excitation with respect to the two nonlinear elements. The nonlinear elements are considered as the α and β variables of the parameter plane which defines the region containing the roots of the system characteristic equation. A "dynamic describing function" curve, which determines the locus of the M or operating point for initial condition input signals, is plotted on the parameter plane. Additionally, the transient response is graphically determined for conditions of second order dominance. The theoretical results are compared with actual analog computer simulation.

DD FORM 1 JAN 64 1473

Unclassified

14. KEY WORDS	LINK A		LINK B		LINK C	
	ROLE	WT	ROLE	WT	ROLE	WT
Parameter Plane Nonlinear Control System Performance						

INSTRUCTIONS

1. ORIGINATING ACTIVITY: Enter the name and address of the contractor, subcontractor, grantee, Department of Defense activity or other organization *(corporate author)* issuing the report.

2a. REPORT SECURITY CLASSIFICATION: Enter the overall security classification of the report. Indicate whether "Restricted Data" is included. Marking is to be in accordance with appropriate security regulations.

2b. GROUP: Automatic downgrading is specified in DoD Directive 5200.10 and Armed Forces Industrial Manual. Enter the group number. Also, when applicable, show that optional markings have been used for Group 3 and Group 4 as authorized.

3. REPORT TITLE: Enter the complete report title in all capital letters. Titles in all cases should be unclassified. If a meaningful title cannot be selected without classification, show title classification in all capitals in parenthesis immediately following the title.

4. DESCRIPTIVE NOTES: If appropriate, enter the type of report, e.g., interim, progress, summary, annual, or final. Give the inclusive dates when a specific reporting period is covered.

5. AUTHOR(S): Enter the name(s) of author(s) as shown on or in the report. Enter last name, first name, middle initial. If military, show rank and branch of service. The name of the principal author is an absolute minimum requirement.

6. REPORT DATE: Enter the date of the report as day, month, year; or month, year. If more than one date appears on the report, use date of publication.

7a. TOTAL NUMBER OF PAGES: The total page count should follow normal pagination procedures, i.e., enter the number of pages containing information.

7b. NUMBER OF REFERENCES: Enter the total number of references cited in the report.

8a. CONTRACT OR GRANT NUMBER: If appropriate, enter the applicable number of the contract or grant under which the report was written.

8b, 8c, & 8d. PROJECT NUMBER: Enter the appropriate military department identification, such as project number, subproject number, system numbers, task number, etc.

9a. ORIGINATOR'S REPORT NUMBER(S): Enter the official report number by which the document will be identified and controlled by the originating activity. This number must be unique to this report.

9b. OTHER REPORT NUMBER(S): If the report has been assigned any other report numbers *(either by the originator or by the sponsor)*, also enter this number(s).

10. AVAILABILITY/LIMITATION NOTICES: Enter any limitations on further dissemination of the report, other than those imposed by security classification, using standard statements such as:

(1) "Qualified requesters may obtain copies of this report from DDC."

(2) "Foreign announcement and dissemination of this report by DDC is not authorized."

(3) "U. S. Government agencies may obtain copies of this report directly from DDC. Other qualified DDC users shall request through

_____."

(4) "U. S. military agencies may obtain copies of this report directly from DDC. Other qualified users shall request through

_____."

(5) "All distribution of this report is controlled. Qualified DDC users shall request through

_____."

If the report has been furnished to the Office of Technical Services, Department of Commerce, for sale to the public, indicate this fact and enter the price, if known.

11. SUPPLEMENTARY NOTES: Use for additional explanatory notes.

12. SPONSORING MILITARY ACTIVITY: Enter the name of the departmental project office or laboratory sponsoring *(paying for)* the research and development. Include address.

13. ABSTRACT: Enter an abstract giving a brief and factual summary of the document indicative of the report, even though it may also appear elsewhere in the body of the technical report. If additional space is required, a continuation sheet shall be attached.

It is highly desirable that the abstract of classified reports be unclassified. Each paragraph of the abstract shall end with an indication of the military security classification of the information in the paragraph, represented as *(TS)*, *(S)*, *(C)*, or *(U)*.

There is no limitation on the length of the abstract. However, the suggested length is from 150 to 225 words.

14. KEY WORDS: Key words are technically meaningful terms or short phrases that characterize a report and may be used as index entries for cataloging the report. Key words must be selected so that no security classification is required. Identifiers, such as equipment model designation, trade name, military project code name, geographic location, may be used as key words but will be followed by an indication of technical context. The assignment of links, roles, and weights is optional.

DD FORM 1 JAN 64 1473 (BACK)

thesP3275
DUDLEY KNOX LIBRARY
3 2768 00416397 2
DUDLEY KNOX LIBRARY